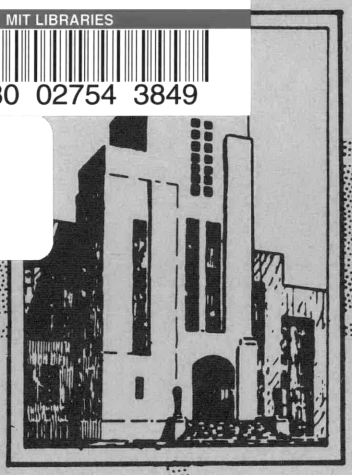

DEPARTMENT OF THE NAVY
DAVID TAYLOR MODEL BASIN

HYDROMECHANICS

○

AERODYNAMICS

○

STRUCTURAL MECHANICS

○

APPLIED MATHEMATICS

COMPARISON OF THEORY AND EXPERIMENT FOR SLAMMING OF A DUTCH DESTROYER

by

Ralph C. Leibowitz

STRUCTURAL MECHANICS LABORATORY
RESEARCH AND DEVELOPMENT REPORT

June 1962

Report 1511

COMPARISON OF THEORY AND EXPERIMENT FOR SLAMMING OF A DUTCH DESTROYER

by

Ralph C. Leibowitz

June 1962

Report 1511

TABLE OF CONTENTS

LIST OF FIGURES

LIST OF TABLES

NOTATION*

A	Cross-sectional area; ft^2
B	Breadth of ship; ft
(C_V), $(C_V)_{y'}$	Added mass coefficient; added mass coefficient for draft y'
c	Damping constant per unit velocity per unit length; ton-sec/ft^2
c, c', c''	Half breadth of ship at immersion y', y, and y''', respectively; ft
D	Still-water draft; ft
d	Draft used in computation of m (Table 5); ft
E	Modulus of elasticity in tension and compression; ton/ft^2
EI	Flexural rigidity of hull; ton-ft^2
F; $\frac{dF}{d\xi}$	Total upward rigid-body force per unit length on hull; kips/ft (1000 lb/ft)
F_b	Smith-corrected buoyancy force per unit length; kips/ft
$f(\theta)$	Equals $\frac{-d\xi}{dt} = (U - u \cos \theta_s) = 28.71 + 4.065 \cos \theta$; ft/sec
G	Modulus of elasticity in shear; ton/ft^2
g	Vertical acceleration of hull due to gravity; ft/sec^2
h	Wave height; ft
h'	y-coordinate of ground; wave height; ft
I	Sectional area moment of inertia; ft^4
$I_{\mu z}$	Mass polar moment of inertia per unit length of section of hull Δx long taken about a horizontal axis through its cg (including allowance for virtual mass of surrounding water); $ton\text{-}sec^2$
i	$\sqrt{-1}$
K	Shear flexibility factor; $\frac{\Gamma\left(\frac{1}{2}+\frac{\beta}{\pi}\right)\Gamma\left(1-\frac{\beta}{\pi}\right)\cos\beta}{\sqrt{\pi}}$; $\frac{t}{\Delta t}$
KAG	Shear rigidity of hull; tons
k	Wave number; 1/ft

*The ft-lb (ton)-sec system of units is used throughout this report except for units of stress.

l	Length of ship; ft
M	Bending moment on hull; ft-ton
M_n^{m+1}	Value of M at position $x_0 + n\Delta x$ at time $t_0 + (m+1)\Delta t$ $\begin{cases} n = 0, 1, 2, \ldots \\ m = 0, 1, 2, \ldots \end{cases}$, ft-ton
m	Hydrodynamic added mass per unit length; slugs/ft = lb-sec^2/ft^2; also $\frac{\text{ton-sec}^2}{\text{ft}^2}$
m_s	Ship mass per unit length; slugs/ft; also $\frac{\text{ton-sec}^2}{\text{ft}^2}$
$n,\ n + \frac{1}{2}$	Station and midstation numbers respectively, for ship where stations run 0 (stern), 1, ... $N-1$, N (bow) and midstations run $\frac{1}{2}$, $1\frac{1}{2}$, ... $N - \frac{1}{2}$; N is also distance along normal to surface; ft
P	Equals F per unit length; ton/ft
$\overline{P}(x, t)$	Total force per unit length acting upon the ship hull, ton/ft
p	Pressure; lb/ft^2
$\overline{q}_s(\xi)$	Velocity of point on ship in flow plane; ft/sec
$\overline{q}_w(x)$	Velocity vector of particle at surface; ft/sec
T	Period of encounter; sec
$t,\ t_0,\ t_n$	Time, initial time, and regular values of time, respectively; sec
t_1	Pulse duration; sec
t_2	Total time during which response is to be calculated; sec
U	Uniform forward velocity of ship along its heading; ft/sec
U'	Gravity potential per unit of volume taken at surface; lb/ft^2
u	In general, the horizontal component of particle velocity at any depth in the undisturbed fluid; ft/sec
V	Vertical shearing force acting on hull; ton
V_a	Apparent velocity of ship; ft/sec
$V_s,\ (V_s)_n$	Surface velocity and normal component of surface velocity; ft/sec

V_w	Velocity of wave propagation; ft/sec
v, $\dot{v}$	In general, the vertical component of particle velocity and acceleration respectively at any depth; ft/sec and ft/sec^2, respectively
v_n	Normal component of particle velocity v at the surface; ft/sec
W	Weight of hull per unit length; tons/ft
x	Abscissa or axis of abscissas in a rectangular coordinate system; a coordinate indicating distance from wave crest of point on ship; horizontal displacement of particle at time t; particle coordinate of particle at rest; longitudinal distance measured from stern of ship; ft
x'	Coordinate of particle disturbed by wave motion; ft
x_0	Initial position; ft
x_n	x-coordinate of station n; $x_0 + n\Delta x$; ft
y	Ordinate or axis of ordinate in a rectangular coordinate system; immersion; particle coordinate of a particle at rest; ft
$\overline{y}$	Lateral deflection of hull; ft
$\dot{y}$	Immersion velocity; ft/sec
y'	Draft for increasing immersion; coordinate of particle disturbed by wave motion; ft; other meanings used for computational purposes are given in Appendix B
y''	Draft; ft; see Appendix B
y'''	Draft for decreasing immersion; ft
y_h, $\dot{y}_h$	Displacement and vertical velocity of keel, respectively, due to heave; ft and ft/sec, respectively
$y^m_{n+\frac{1}{2}}$	Value of y at position $x_0 + \left(n + \frac{1}{2}\right)\Delta x$ at times $t_0 + m\Delta t$ $\begin{cases} n = 0, 1, 2, \ldots \\ m = 0, 1, 2, \ldots \end{cases}$; ft
y_p, $\dot{y}_p$	Displacement and vertical velocity of keel, respectively, due to pitch; ft and ft/sec, respectively
$\dot{y}_r$	Downward relative velocity of hull with respect to fluid undisturbed by ship (not wave); ft/sec
y_w	Elevation of wave surface above mean water level; ft
β	Deadrise angle; deg
γ, $\dot{\gamma}$	Rotation and angular velocity respectively of transverse sections with respect to a horizontal axis; radians and radians/sec, respectively

ΔM, ΔV, Δy, $\Delta \gamma$	Increments in M, V, y, and γ, respectively; ft-ton, ton, ft and radians, respectively
Δt	Time interval or increment; sec
Δx	Length of element, $\frac{l}{20}$; increment of length; ft
δt	Time interval of tabular listings of response; sec
ζ	Distance of station n forward of position of heave meter; ft
η, $\dot{\eta}$	Vertical displacement from rest condition and associated vertical velocity of particle at arbitrary depth y; ft and ft/sec, respectively; section area coefficient (dimensionless)
θ	$\frac{2\pi x}{\lambda}$ radians
θ_n	Value of θ at any station n $\left(\text{equal to } 0.1366 \frac{t}{0.1096} + 0.2732n - 2.732\right)$; radians
θ_s	Ship's heading; deg
λ	Wave length; ft
μ	Mass per unit length of hull (including allowance for virtual mass) ton-sec^2/ft^2
ξ, $\dot{\xi}$	ξ is distance of any station n along keel forward of midlength; horizontal displacement from rest condition and associated horizontal velocity of a particle at arbitrary depth y; ft and ft/sec, respectively
ξ_n	Value of ξ at station n; ft
ρ	Density of sea water; lb-sec^2/ft^4
τ	Period; sec
ϕ	Velocity potential; ft^2/sec
ψ, $\dot{\psi}$	Pitch angle and angular velocity, respectively; radians or deg and deg/sec, respectively
ω	Angular velocity; radians/sec

PAGES (S) MISSING FROM ORIGINAL

ABSTRACT

This report presents a theoretical analysis and computation of the "slamming" (hydrodynamic) forces* acting on a ship, based upon an experimental knowledge of the ship's rigid-body motions relative to the wave. These forces are considered to be due to the time rate of change of fluid momentum and to buoyancy forces incident to immersion of the hull. In addition, a computation is made of the transient elastic response and associated hull girder stresses of the ship due to the total force exerted by the fluid on the ship. A comparison between the theoretical and measured stresses shows good agreement.

1. INTRODUCTION

Prior investigation has shown that large "whipping stresses" and motions occur in certain ships subject to "slam"* by hydrodynamic forces.[1] The analysis in Reference 1 indicates that the magnitude of these stresses and motions is related to the immersion of the bow flare, whereas the empirical evidence indicates that for rough seas the magnitudes of the whipping stresses, for a ship of given length, are larger for ships with bow flare. For certain ships bow flare may be the most significant single source of hull girder stresses. Therefore, large magnitudes of slam may cause serious structural damage while small magnitudes of slam, occurring frequently, may weaken the hull through fatigue. Avoidance of such deleterious effects by reduction of speed imposes a serious restraint upon the ship designer wishing to extend the operating speed range.

These facts suggest, as a worthwhile objective, the undertaking of an analytical investigation, the results of which can be used to predict the effects of the bow flare on the whipping of ships. A well-devised theory could lead to an improvement in ship forms designed for high speed from a knowledge of the slamming stresses on the bow predicted prior to construction of the bow. The theory could also lead to an improvement of existing ship form designs.

Accordingly, based upon an *experimental* knowledge of a ship's rigid-body motions relative to the wave, this report presents a *theoretical* analysis and computation of the "slamming"(hydrodynamic) forces—associated with *rigid-body* motions only—acting on a ship and an evaluation of the transient stresses** of the ship due to the sum of the hydrodynamic and

---

*In this report, slamming is defined as a rapidly applied hydrodynamic force at the bow, and perhaps other locations on a ship, created by the ship's forward motion through opposing seas. This force varies with time in a complex manner and causes vibration of the ship's structure. It should be clear that we refer here to the time-varying equivalent or integrated load force on each cross section rather than the detailed load distribution around the cross section.

[1]References are listed on page 90.

**The stress due to slam is superposed on the still-water bending stress. No allowance is made for the different damping in each mode.

Smith-corrected buoyancy forces; for the stress computation the hydrodynamic forces are associated with *rigid-body* and *flexural* vibrations of the ship. The theoretical and measured hull girder stresses are compared. The analysis comprehends the period which includes the immersion and subsequent emergence of the bow flare.

The computation made in this report for the Dutch Destroyer represents the first attempt to reconcile detailed computation procedures with experimental results for full-scale ships.

2. BACKGROUND

The severity of hull girder stresses incident to bow immersion was strikingly demonstrated by observations and analyses of strains measured on USS ESSEX (CVA 9) during a storm passage around Cape Horn; see Reference 1. Heretofore most of the literature on slamming has been concerned with bottom impact. A method for calculating the time-varying hydrodynamic forces, at various ship sections, incident to bow immersion is given in References 2 and 3; this method is the first step in an attempt to explain the mechanism generating the observed extreme whipping of the ESSEX and the Dutch Destroyer, respectively. The total procedure for computing the slamming force, response to slam, and the comparison of theoretical and experimental results, which substantiates the validity of the theorized generating mechanism is given in this present report.

3. THEORETICAL ANALYSIS OF PROBLEM

An analysis of the problem will be made prior to formulating a method for attacking the problem.

3.1 MECHANISM OF FORCE GENERATION

When a ship moves through a sea disturbed by waves, it assumes rigid-body as well as elastic, flexural vibrations. The pressure at a point of the hull acquires an appreciable variation with time, and the integrated pressures over the surface of the hull constitute longitudinally distributed time-variant fluid forces which are the cause of the oscillatory response of the ship to waves. The frequency ranges of the rigid-body motion and flexural vibrations are quite distinct so that, although the rigid-body motions might be considered as fundamental modes of vibratory response, it is more convenient to treat them independently.[2,4,5]

All the forces exerted by the fluid on the ship may be considered to be external forces. These forces are due to the interaction of the rigid-body and flexural vibratory motions of the ship and the total time-varying hydrodynamic mass (i.e., virtual or added mass) at any section along the ship.[5,6,7*] For convenience in computation, that part of the total time-varying hydrodynamic mass for each ship section associated with flexural vibrations may be added to the

*A mathematical description of the relationship between these forces and the total motion of the ship is presented in Appendix F.

corresponding ship mass,[5] thereby removing the consideration of external vibratory forces on the ship. The remaining fluid pressure-exciting forces are then rigid-body forces determined by the characteristics of the seawaves and by the rigid-body response, both of which are defined by the recorded observations.

The theory of the computation of forces due to the rigid-body motions of a ship in waves is discussed in Appendix A. The theory is based on the cross-flow hypothesis similar to that used by Munk[8] for airships and subsequently adopted for studies of seaplane landing impact forces[9] and more recently for ship motion studies.[10,11] Thus the relative vertical flow in a plane normal to the baseline of the ship is considered to account for the vertical force imposed on the ship (in addition to the static buoyancy force with Smith correction for the pressure gradient in the wave.) It is assumed that this flow is irrotational and can therefore be described by its velocity potential. In such a flow the principal hydrodynamic force results from nonuniform motion and is associated with hydrodynamic added mass.

It is shown in Appendix A that the upward force per unit length on the hull at any transverse section ξ ft forward of amidship is (see Figures 1 and 2):

$$\frac{dF}{d\xi} = \frac{\partial}{\partial t}(m\dot{y}_r) - (U - u\cos\theta_s)\frac{\partial}{\partial \xi}(m\dot{y}_r) + (g+\dot{v})\rho A \qquad [1]$$

where

$$\dot{y}_r = v - \dot{y}_h - \dot{y}_p + (U - u\cos\theta_s)\psi \qquad [2]$$

The term $\rho g A$ is the buoyancy force per unit length in still water and $\dot{v}\rho A$ represents the Smith correction to the buoyancy force per unit length (at the surface) induced by the vertical acceleration of the fluid undisturbed by the ship (not wave) in a lamina;

m is the hydrodynamic added mass per unit length in slugs per foot;

$\dot{y}_r$ is the downward relative velocity of the hull with respect to the fluid undisturbed by the ship (not wave) in feet per second;

$\dot{y}_h$ is the vertical velocity due to heave in feet per second;

$\dot{y}_p$ is the vertical velocity due to pitch in feet per second;

U is the uniform forward velocity of the ship along its heading in feet per second;

u is the horizontal component of fluid particle velocity normal to the wave crests; in Equations [1] and [2] the particle velocity is taken at the surface in feet per second;

θ_s is the ship's heading (angle the ship makes with the normal to the wave crests) in degrees;

ψ is the pitch angle in radians;

g is the vertical acceleration of the hull due to gravity in feet per second squared;

v is the vertical velocity of the undisturbed fluid; this is equal to the vertical component of particle velocity at the surface in feet per second;

ρ is the density of sea water; 64.0 pounds per foot cubed;

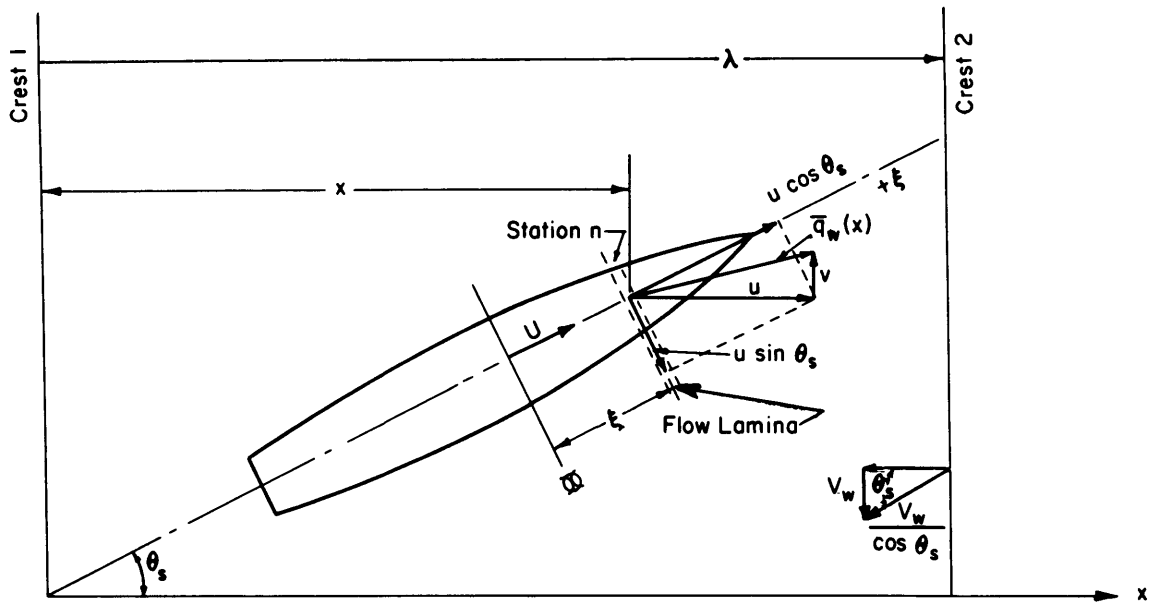

Figure 1 – Motion of Ship in an Oblique Sea

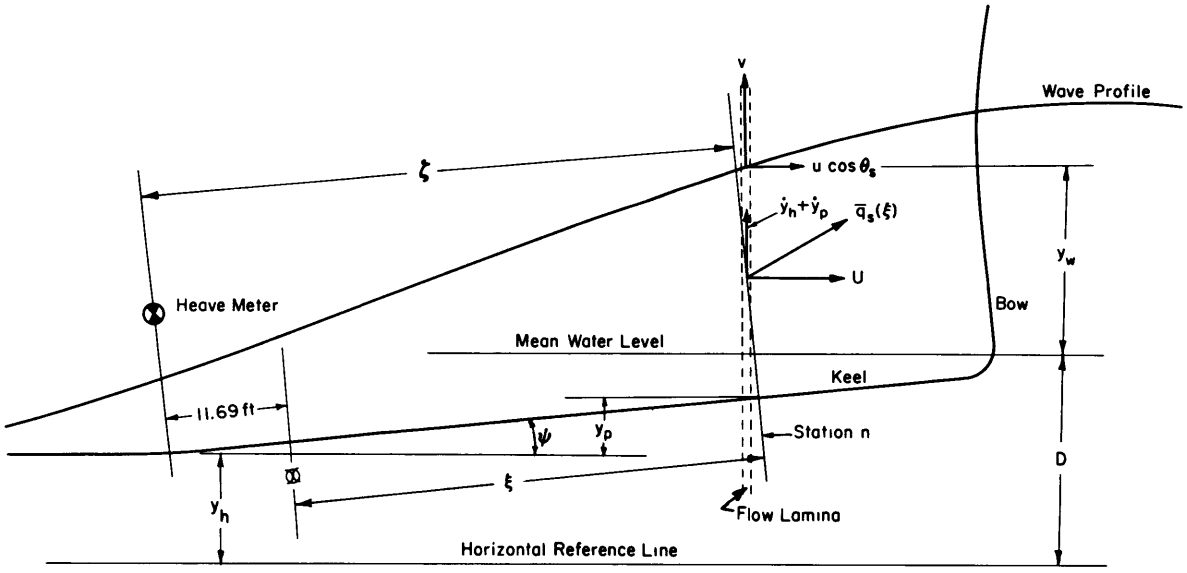

Figure 2 – View of Ship's Center Plane Showing Immersion and Velocity Components

A is the cross section area in feet squared;

F is the upward force on the hull in kips (1000 pounds);

ξ is the distance of any station n along the keel forward of the midlength in feet; and

t is the time in seconds.

3.2 HYDRODYNAMIC ADDED MASS

Since the ship is on the surface, and the immersion at any transverse section is changing continually with time and at any fixed time is changing continually with ξ, the mass is also varying and cannot be considered constant during the indicated differentiation; see Equation [1]. In fact, the rapid increase in beam at the waterline and, hence, of added mass when the flared bow enters the water is responsible for the biggest part of the force exerted on the ship at the forward sections.

It should be observed that the motions studied here are more extreme than those usually considered, so that a very substantial rise of the water surface is to be considered. The hydrodynamic added mass m depends on the shape and size of the immersed section. The method of computation, based upon Szebehely's[12] and Prohaska's[13] procedure for finding the added mass, is given in Appendix B. It is necessary, therefore, to compute the immersion at any station.

3.3 IMMERSION

From Figure 2 it is evident that the immersion at any station* is

$$y = D + y_w - y_h - y_p \qquad [3]$$

where y is the immersion in feet,

D is the draft in still water; 13.09 feet,

y_w is the elevation of the wave surface above the mean water level in feet,

y_h is the elevation of the keel due to heaving in feet, and

y_p is the elevation of the keel due to pitching in feet.

Note that the relative velocity $\dot{y}_r \neq \dot{y} = \dot{y}_w - \dot{y}_h - \dot{y}_p$, the immersion velocity (see Appendix A).

*The ship is divided into 20 sections of equal length; the locations of the ends of the sections, called stations, are denoted by $n = 0, 1, \ldots N$ starting from the stern, and their midstations, by $n = \frac{1}{2}, 1\frac{1}{2} \ldots 19\frac{1}{2}$.

4. METHOD OF ATTACK

Based upon the theory given in Section 3, the following procedure is used to compute the rigid-body forces per unit length on a ship and the bending moments and stresses of the ship for the period of one wave passage; i.e., for an arbitrary transient excitation.*

a. An evaluation is made of the time histories of the horizontal component of particle velocity u and of the relative ship to wave (1) position y and (2) velocity $\dot{y}_r$ at each section of the ship. Forward velocity U and ship's heading θ_s are known.

b. An evaluation is then made, from a knowledge of the ship to wave position y, of the time history of the virtual mass per unit length m associated with rigid-body motions at each section of the ship.

c. The time history of the hydrodynamic forces per unit length, associated with rigid-body motions, at each section of the ship are evaluated from a knowledge of m, $\dot{y}_r$, U, u, and θ_s. The total time-varying rigid-body force per unit length at any section is the sum of the Smith-corrected buoyancy and hydrodynamic (unsteady) forces per unit length; see Equation [1].

d. An evaluation is made of the ship parameters[5] to obtain a lumped parameter representation of each section of the ship for use in finite difference equations.[14] The total time-varying rigid-body forces per unit length at all ship sections found in Item c *plus the time-varying elastic forces per unit length* are used in these equations. The solution of the finite difference equations by a digital computer represents the total motion (i.e., response) and associated moments and stresses of the ship due to slam.

e. The stresses are computed.

f. A comparison is made of the theoretical and observed stresses.

5. RESULTS

5.1 CALCULATION OF THE FORCES

The photographs of Figure 3 and the experimental data of Figure 4 were used in the computations made to determine the total force per unit length along the keel at regular time intervals for Stations 0 through 20, inclusive.

For convenience in computation of the components of this force, a time scale was adopted which started from zero at the beginning of the computation. The zero of "computation" time was taken at the instant when a wave crest is amidships. From an analysis of the wave profile given in Appendix C, it was established that the wave crest is amidships when $t = 8.18$ sec on the scale of time given in Figures 3 and 4.

*When a ship is subjected to slam, the deflection of a loaded ship section is permitted by the elasticity of the adjacent structure. The impulse of the impact force is first absorbed by the momentum of the masses in its immediate vicinity. After the impact impulse is expended, the structure is left in a strained state, and interplay of elastic and inertial forces produce a state of vibration.

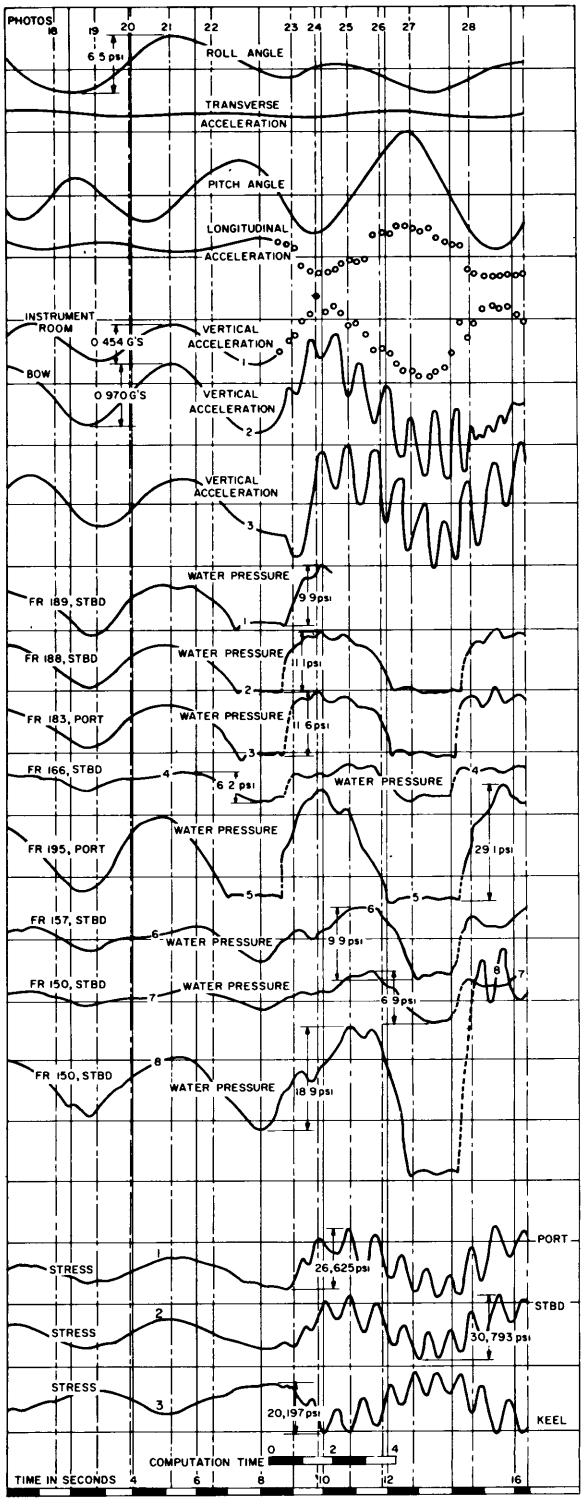

Figure 4 – Ship Records for Period of Time Comprehending Time Period of Photographs of Figure 3

To compute the force, the components of immersion are considered first; see Equation [3].

5.1.1 Immersion y

The draft D in still water was taken as 13.09 ft.

The contribution y_w of the wave to the immersion at each station was obtained by establishing the wave geometry, wave kinematics, and location of each station on the wave at each instant of time for which the computations are made, as discussed in Appendixes C, D, and E, respectively. The function y_w is tabulated* in Column 6 of Table 1 for values of θ, corresponding to regular time intervals (integer multiples of 0.1096 sec), required in computations carried out in Table 2. In Appendix D it is shown that

$$y_w = 7 \cos \theta \qquad [4]$$

where, from Appendix E, the value of θ at any station n is

$$\theta = \theta_n = 0.1366 \frac{t}{0.1096} + 0.2732n - 2.732 \qquad [5]$$

The method of determining the time history of the faired heave displacement y_h (Figure 5) from a double integration of the heave acceleration record (Figure 4) is discussed in Appendix C. Values of y_h taken from Figure 5 at regular time intervals are tabulated in Column 11 of Table 1.

The pitch displacement at each station was obtained from the equation

$$y_p = \frac{\pi}{180} \zeta\psi \qquad [6]$$

where $\zeta = \xi + 11.69$ ft is the distance of Station n forward of the position of the heave meter (see Figure 2) and ψ is the pitch angle in degrees. The pitch angle ψ recorded during the trials (Figure 4) is replotted in Figure 6 against the "computation" time. Values of ψ, taken from Figure 6 at regular time intervals are tabulated in Column 9 of Table 1. From these values of ψ, the pitch displacement y_p is computed and is tabulated in Column 10 of Table 1.

The immersion y was then computed and tabulated in Column 12 of Table 1.

---

*The tables in which the computations have been carried out for each station are too extensive for reproduction in this report. Only sample computations for Station 20 (the bow) are given. The complete data are available in the files of the Ship Dynamics Division of the Structural Mechanics Laboratory at the David Taylor Model Basin.

TABLE 1

Computation Data for Immersion, Particle Velocity, Hydrodynamic Added Mass, and Buoyancy Force at Station 20

t sec	$0.1366\frac{t}{0.1096}$	θ radians	$\cos\theta$	$\sin\theta$	y_w ft	$v=\dot{y}_w$ ft/sec	u ft/sec	ψ deg	y_p ft	y_h ft	y ft	m slugs/ft	F_b kips/ft
0	0	2.7320	−0.91728	0.39824	−6.421	−2.289	5.272	1.70	5.83	6.02	− 5.181	0.0	0.00
0.1096	0.1366	2.8686	−0.96308	0.26923	−6.742	− 1.547	5.535	1.20	4.12	6.02	− 3.792		
0.2192	0.2732	3.0052	−0.99135	0.13121	−6.939	−0.754	5.697	0.70	2.40	6.00	− 2.249		
0.3288	0.4098	3.1418	− 1.00000	0.0000	−7.000	0.000	5.747	0.10	0.34	5.75	0		
0.4384	0.5464	3.2784	−0.99044	−0.13797	−6.933	0.793	5.692	−0.60	− 2.06	5.30	2.917		
0.5480	0.6830	3.4150	−0.96149	−0.27482	−6.730	1.579	5.526	−1.25	− 4.29	4.80	5.850		
0.6576	0.8196	3.5516	−0.91775	−0.39715	−6.424	2.282	5.274	−1.90	− 6.52	4.30	8.886		
0.7672	0.9562	3.6882	−0.85336	−0.52133	−5.974	2.996	4.904	−2.45	− 8.40	3.60	11.916		
0.8768	1.0928	3.8248	−0.77857	−0.62755	−5.450	3.607	4.474	−3.05	−10.46	2.95	15.150	0.0	0.20
0.9864	1.2294	3.9614	−0.68338	−0.73006	−4.784	4.196	3.927	−3.50	−12.01	2.10	18.216	1.0	0.40
1.0960	1.3660	4.0980	−0.57482	−0.81828	−4.024	4.703	3.303	−3.82	−13.10	1.50	20.666	4.0	0.70
1.2056	1.5026	4.2346	−0.46390	−0.88589	−3.247	5.091	2.666	−4.05	−13.89	0.90	22.833	6.0	1.10
1.3152	1.6392	4.3712	−0.33574	−0.94196	−2.350	5.413	1.929	−4.17	−14.30	0.20	24.840	12.5	1.60
1.4248	1.7758	4.5078	−0.20101	−0.97959	−1.407	5.630	1.155	−4.20	−14.41	−0.50	26.593	20.0	2.20
1.5344	1.9124	4.6444	−0.07233	−0.99738	−0.506	5.732	0.416	−4.15	−14.23	−1.30	28.114	30.0	1.80
1.6440	2.0490	4.7810	0.06756	−0.99772	0.473	5.734	−0.388	−4.00	−13.72	−2.00	29.283	41.0	3.40
1.7536	2.1856	4.9176	0.20612	−0.97853	1.443	5.624	−1.185	−3.75	−12.86	−3.00	30.393	57.0	4.00
1.8632	2.3222	5.0542	0.33123	−0.94355	2.319	5.423	−1.904	−3.40	−11.66	−3.75	30.819	40.0	4.30
1.9728	2.4588	5.1908	0.45966	−0.88810	3.218	5.104	−2.642	−3.00	−10.29	−4.20	30.798	40.0	4.30
2.0824	2.5954	5.3274	0.57909	−0.81526	4.054	4.685	−3.328	−2.57	− 8.82	−4.67	30.634	37.0	4.20
2.1920	2.7320	5.4640	0.67989	−0.73332	4.759	4.214	−3.907	−2.10	− 7.20	−4.88	29.929	31.0	3.70
2.3016	2.8686	5.6006	0.77557	−0.63127	5.429	3.628	−4.457	−1.65	− 5.66	−5.00	29.179	27.0	3.40
2.4112	3.0052	5.7372	0.85607	−0.51687	5.992	2.970	−4.920	−1.10	− 3.77	−5.00	27.852	19.0	2.70
2.5208	3.1418	5.8738	0.91585	−0.40153	6.411	2.308	−5.263	−0.60	− 2.06	−4.98	26.541	15.0	2.20
2.6304	3.2784	6.0104	0.96292	−0.26980	6.740	1.551	−5.534	0.00	0	−4.83	24.660	10.0	1.60
2.7400	3.4150	6.1470	0.99114	−0.13279	6.938	0.763	−5.696	0.50	1.72	−4.50	22.808	5.0	1.10
2.8496	3.5516	6.2836	1.00000	0.0000	7.000	0.000	−5.747	0.95	3.26	−4.20	21.030	4.0	0.75
2.9592	3.6882	6.4202	0.99063	0.13657	6.934	−0.785	−5.693	1.52	5.21	−3.95	18.764	1.0	0.50
3.0688	3.8248	6.5568	0.96270	0.27058	6.739	− 1.555	−5.533	2.05	7.03	−3.59	16.389	0.0	0.30
3.1784	3.9614	6.6934	0.91712	0.39861	6.420	−2.291	−5.271	2.57	8.82	−3.22	13.910		0.10
3.2880	4.0980	6.8300	0.85409	0.52013	5.979	−2.989	−4.908	3.00	10.29	−2.80	11.579		0.00
3.3976	4.2346	6.9666	0.77568	0.63112	5.430	−3.627	−4.458	3.54	12.14	−2.30	8.680		
3.5072	4.3712	7.1032	0.68222	0.73115	4.776	−4.202	−3.921	4.02	13.79	− 1.90	5.976		
3.6168	4.5078	7.2398	0.57597	0.81747	4.032	−4.698	−3.310	4.52	15.50	− 1.35	2.972		
3.7264	4.6444	7.3764	0.45982	0.88801	3.219	−5.103	−2.643	5.00	17.15	−0.70	− 0.141		
3.8360	4.7810	7.5130	0.33424	0.94249	2.340	−5.416	− 1.921	5.50	18.87	0	− 3.440		
3.9456	4.9176	7.6496	0.20337	0.97910	1.424	−5.627	− 1.169	5.94	20.37	0.60	− 6.456		
4.0552	5.0542	7.7862	0.06774	0.99770	0.474	−5.734	−0.389	6.13	21.03	1.30	− 8.766		
4.1648	5.1908	7.9228	−0.09904	0.99508	−0.693	−5.719	0.569	6.45	22.12	2.00	−11.723		
4.2744	5.3274	8.0594	−0.20377	0.97902	−1.426	−5.626	1.171	6.56	22.50	2.50	−13.336		
4.3840	5.4640	8.1960	−0.33556	0.94202	−2.349	−5.414	1.928	6.54	22.43	3.00	−14.689		
4.4936	5.6006	8.3326	−0.46019	0.88782	−3.221	−5.102	2.645	6.35	21.78	3.70	−15.611		
4.6032	5.7372	8.4692	−0.57712	0.81666	−4.040	−4.693	3.317	6.14	21.06	4.20	−16.210		
4.7128	5.8738	8.6058	−0.68325	0.73019	−4.783	−4.196	3.927	5.80	19.89	4.67	−16.253		
4.8224	6.0104	8.7424	−0.77594	0.63081	−5.432	−3.625	4.459	5.35	18.35	5.00	−15.692		
4.9320	6.1470	8.8790	−0.85482	0.51893	−5.984	−2.982	4.913	4.80	16.46	5.43	−14.784		
5.0416	6.2836	9.0156	−0.91728	0.39824	−6.421	−2.289	5.272	4.15	14.23	5.70	−13.261		
5.1512	6.4202	9.1522	−0.96308	0.26923	−6.742	− 1.547	5.535	3.40	11.66	6.10	−11.412		
5.2608	6.5568	9.2888	−0.99135	0.13121	−6.939	−0.754	5.697	2.75	9.43	6.20	− 9.479		
5.3704	6.6934	9.4254	− 1.00000	0.0000	−7.000	0.000	5.747	2.10	7.20	6.21	− 7.320		
5.4800	6.8300	9.5620	−0.99044	−0.13797	−6.933	0.793	5.692	1.30	4.46	6.20	− 4.503		
5.5896	6.9666	9.6986	−0.96149	−0.27482	−6.730	1.580	5.526	0.80	2.74	6.15	− 2.530		
5.6992	7.1032	9.8352	−0.91775	−0.39715	−6.424	2.282	5.274	0.0	0	6.06	0.606	0.0	0.00

$y_w = 7\cos\theta$

$\theta = 0.1366\frac{t}{0.1096} + 0.2732(20) - 2.732$

$v = \dot{y}_w = -5.74\sin\theta$

$u = -5.74\cos\theta$

ψ – see Figure 6

$y_p = \frac{\pi}{180}\left(\frac{369}{2} + 11.69\right)\psi = 3.43\psi;\ \xi = \frac{369}{2}$ ft at Station 20 (the bow)

y_h – see Figure 5

$y = D + y_w - y_h - y_p;\ D = 13.09$ ft

m – see Figure 9

$F_b = \left(1 + \frac{b}{g}\right)\rho gA = (1 - 0.1466\cos\theta)\,\rho gA$

ρgA – see Figure 10

TABLE 2

Computation Data for Downward Relative Velocity $\dot{y}_r$ at Station 20

Time sec	$v = \dot{y}_w$ ft/sec	$\dot{\psi}$ deg/sec	$\dot{y}_p$ ft/sec	U ft/sec	$u \cos \theta_s$ ft/sec	0.01745 ψ deg radians	0.01745 $(U - u \cos \theta_s)\psi$ deg ft/sec	$\dot{y}_h$ ft/sec	$\dot{y}_r$ ft/sec
0.0000	−2.289	−4.19	−14.347	28.71	3.728	0.0297	0.742	−0.35	12.45
0.1096	−1.547	−4.98	−17.052		3.914	0.0209	0.518	−0.52	16.54
0.2192	−0.754	−5.53	−18.935		4.028	0.0122	0.301	−1.50	19.98
0.3288	0.000	−5.95	−20.373		4.064	0.0017	0.042	−2.39	22.81
0.4384	0.793	−6.17	−21.126		4.025	−0.0105	−0.259	−3.25	24.91
0.5480	1.579	−6.10	−20.886		3.907	−0.0218	−0.541	−4.10	26.02
0.6576	2.282	−5.80	−19.859		3.729	−0.0332	−0.829	−4.87	26.18
0.7672	2.996	−5.34	−18.284		3.468	−0.0428	−1.080	−5.61	25.81
0.8768	3.607	−4.75	−16.264		3.164	−0.0532	−1.359	−6.25	24.76
0.9864	4.196	−3.95	−13.525		2.777	−0.0611	−1.585	−6.73	22.87
1.0960	4.703	−2.75	− 9.416		2.336	−0.0667	−1.759	−7.00	19.36
1.2056	5.091	−1.76	− 6.026		1.885	−0.0707	−1.897	−7.14	16.36
1.3152	5.413	−0.72	− 2.465		1.364	−0.0728	−1.991	−7.11	13.00
1.4248	5.630	0.05	0.171		0.817	−0.0733	−2.045	−7.00	10.41
1.5344	5.732	0.80	2.739		0.294	−0.0724	−2.057	−6.76	7.70
1.6440	5.734	1.70	5.821		−0.274	−0.0698	−2.023	−6.38	4.27
1.7536	5.624	2.70	9.245		−0.838	−0.0654	−1.932	−5.80	0.25
1.8632	5.423	3.15	10.786		−1.346	−0.0593	−1.782	−5.12	− 2.03
1.9728	5.104	3.78	12.943		−1.868	−0.0524	−1.602	−4.46	− 4.98
2.0824	4.685	4.18	14.312		−2.353	−0.0448	−1.392	−3.28	− 7.74
2.1920	4.214	4.38	14.997		−2.763	−0.0366	−1.152	−2.18	− 9.76
2.3016	3.628	4.59	15.716		−3.152	−0.0288	−0.918	−1.20	−11.81
2.4112	2.970	4.70	16.093		−3.479	−0.0192	−0.618	−0.23	−13.51
2.5208	2.308	4.78	16.367		−3.721	−0.0105	−0.341	0.53	−14.93
2.6304	1.551	4.84	16.572		−3.913	0.0000	0.000	1.23	−16.25
2.7400	0.763	4.88	16.709		−4.028	0.0087	0.285	1.94	−17.60
2.8496	0.000	4.93	16.880		−4.064	0.0166	0.544	2.43	−18.77
2.9592	−0.785	4.92	16.846		−4.025	0.0265	0.867	3.01	−19.77
3.0688	−1.555	4.88	16.709		−3.912	0.0358	1.168	3.52	−20.62
3.1784	−2.291	4.80	16.435		−3.727	0.0448	1.453	4.02	−21.29
3.2880	−2.989	4.76	16.298		−3.470	0.0524	1.686	4.46	−22.06
3.3976	−3.627	4.66	15.956		−3.152	0.0618	1.969	4.88	−22.49
3.5072	−4.202	4.51	15.442		−2.773	0.0700	2.204	5.21	−22.65
3.6168	−4.698	4.30	14.723		−2.341	0.0790	2.453	5.50	−22.47
3.7264	−5.103	4.10	14.038		−1.869	0.0870	2.660	5.74	−22.22
3.8360	−5.416	3.80	13.011		−1.358	0.0960	2.887	5.93	−21.47
3.9456	−5.627	3.34	11.436		−0.827	0.1040	3.072	6.02	−20.01
4.0552	−5.734	2.71	9.279		−0.275	0.1070	3.101	5.98	−17.89
4.1648	−5.719	1.98	6.780		0.402	0.1130	3.199	5.88	−15.18
4.2744	−5.626	0.70	2.397		0.828	0.1140	3.179	5.72	−10.56
4.3840	−5.414	−0.60	− 2.054		1.363	0.1140	3.118	5.46	− 5.70
4.4936	−5.102	−1.82	− 6.232		1.870	0.1110	2.979	5.08	− 0.97
4.6032	−4.693	−2.90	− 9.930		2.345	0.1070	2.821	4.63	3.43
4.7128	−4.196	−3.90	−13.354		2.777	0.1010	2.619	4.14	7.64
4.8224	−3.625	−4.80	−16.435		3.153	0.0930	2.377	3.58	11.61
4.9320	−2.982	−5.65	−19.346		3.474	0.0840	2.120	2.98	15.50
5.0416	−2.289	−6.12	−20.955		3.728	0.0720	1.799	2.28	18.19
5.1512	−1.547	−6.38	−21.845		3.914	0.0590	1.463	1.55	20.21
5.2608	−0.754	−6.49	−22.222		4.028	0.0480	1.185	0.87	21.78
5.3704	0.000	−6.50	−22.256		4.064	0.0370	0.912	0.28	22.89
5.4800	0.793	−6.48	−22.188		4.025	0.0230	0.568	−0.42	23.97
5.5896	1.580	−6.37	−21.811	28.71	3.907	0.0140	0.347	−0.93	24.67

v $= \dot{y}_w = -5.74 \sin \theta$

$\dot{y}_p$ $= \frac{\pi}{180}\left(\frac{369}{2} + 11.69\right)\dot{\psi} = 3.425\,\dot{\psi}$

$\dot{\psi}$ – see Figure 8

$u \cos \theta_s = u \cos 45 \text{ deg} = 0.707\,u$

$\dot{y}_h$ – see Figure 7

$\dot{y}_r$ $= v - \dot{y}_h - \dot{y}_p + \frac{\pi}{180}(U - u \cos \theta_s)\psi$

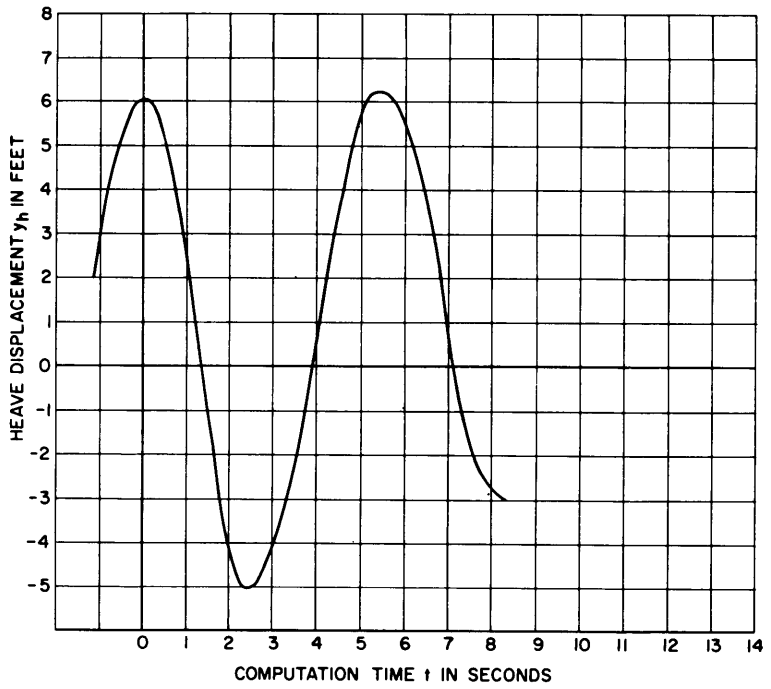

Figure 5 – Time History of Faired Heave Displacement

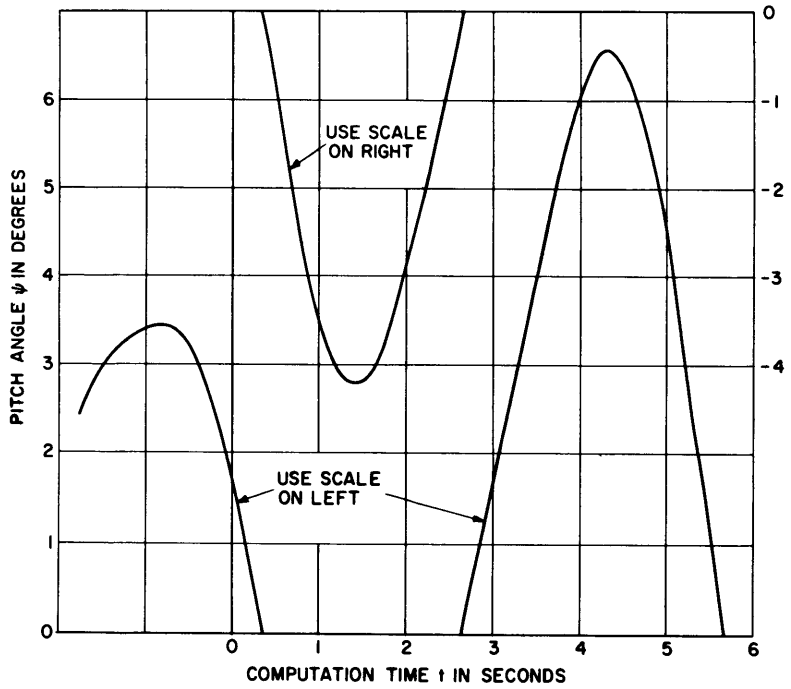

Figure 6 – Time History of Pitch Angle

5.1.2 Downward Relative Velocity $\dot{y}_r$

Next, the components of the downward relative velocity $\dot{y}_r$ are considered (see Equation [2]).

The method of determining the time history of the heave velocity $\dot{y}_h$ (Figure 7) from an

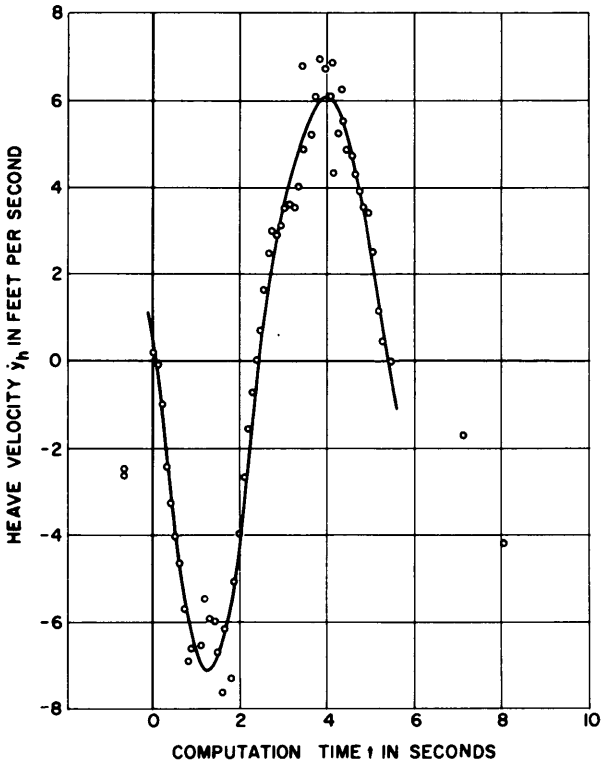

Figure 7 – Time History of Faired Heave Velocity

integration of the heave acceleration record is discussed in Appendix C. Values of $\dot{y}_h$ taken from Figure 7 at regular time intervals are tabulated in Column 9 of Table 2.

The vertical velocity due to pitching is

$$\dot{y}_p = \frac{\pi}{180}\,\zeta\dot{\psi} \qquad [7]$$

The time history of the pitch velocity $\dot{\psi}$ (Figure 8) was determined by numerical differentiation of the recorded pitch curve; see Figures 4 and 6. Values of $\dot{\psi}$ taken from Figure 8 at regular time intervals are tabulated in Column 3 of Table 2. Values of $\dot{y}_p$ are tabulated in Column 4 of Table 2.

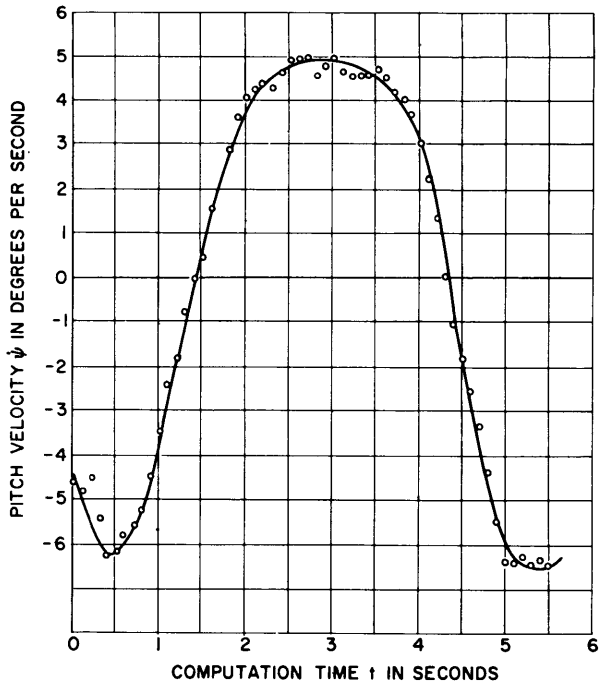

Figure 8 – Time History of Pitch Velocity

In Appendix D it is shown that the vertical and horizontal components of velocity of the wave at the surface are

$$v = -5.74 \sin \theta \text{ ft/sec} \qquad [8]$$

$$u = -5.74 \cos \theta \text{ ft/sec} \qquad [9]$$

Then from Appendix A and Equation [9], we have

$$f(\theta) = -\frac{d\xi}{dt} = (U - u \cos \theta_s) = 28.71 + 4.065 \cos \theta \qquad [10]$$

where U is 17 knots per hour (28.71 feet per second),

θ_s is 45 degrees, and

θ is related to t by Equation [5] and has values corresponding to regular time intervals.

θ is tabulated in Tables 1 and 3 for time values increasing in increments of 0.1096 sec.

Values of v are tabulated in Column 7 of Table 1 and in Column 2 of Table 2 for values of θ or t required in the computations.

Values of u are tabulated in Column 8 of Table 1.

Values of U, $u \cos \theta_s$, and $\frac{f(\theta)\psi^0}{57.3} = \frac{(U - u \cos \theta_s)\psi^0}{57.3}$ are tabulated in Columns 5, 6,

TABLE 3

Computation Data for Total Upward Force on Hull at Station 20

t sec	θ radians	F_b kips/ft	$\dot{y}_r$ ft/sec	m slugs/ft	$m\dot{y}_r$ (computed) slugs/sec	$m\dot{y}_r$ (corrected) slugs/sec	$\frac{\partial}{\partial t}\Big\vert_{\xi}(m\dot{y}_r)$ kips/ft	$\frac{\partial}{\partial \xi}\Big\vert_{t}(m\dot{y}_r)$ kips/ft	$f(\theta)$ ft/sec	$\frac{d}{dt}(m\dot{y}_r)$ kips/ft	F kips/ft
0	2.7320	0.00	12.45								
0.1096	2.8686	0.00	16.54								
0.2192	3.0052	0.00	19.98								
0.3288	3.1418	0.00	22.81								
0.4384	3.2784	0.00	24.91								
0.5480	3.4150	0.00	26.02								
0.6576	3.5516	0.00	26.18								
0.7672	3.6882	0.00	25.81								
0.8768	3.8248	0.20	24.76								0.20
0.9864	3.9614	0.40	22.87	1.0	22.88	22	0.456	−0.0352	25.93	1.369	1.769
1.0960	4.0980	0.70	19.36	4.0	77.44	72	0.438	−0.0378	26.36	1.434	2.134
1.2056	4.2346	1.10	16.36	6.0	98.16	122	0.461	−0.0508	26.83	1.824	2.924
1.3152	4.3712	1.60	13.00	12.5	162.50	172	0.445	−0.0577	27.34	2.023	3.623
1.4248	4.5076	2.20	10.41	20.0	208.20	216	0.360	−0.0602	27.87	2.038	4.238
1.5344	4.6444	1.80	7.70	30.0	231.00	239	−0.085	−0.0540	28.42	1.450	3.250
1.6440	4.7810	3.40	4.27	41.0	175.00	184	−1.017	−0.0321	28.98	−0.087	3.313
1.7536	4.9176	4.00	0.25	57.0	14.25	28	−1.522	−0.0124	29.52	−1.156	2.844
1.8632	5.0542	4.30	− 2.03	40.0	− 81.20	−135	−1.582	0.0153	30.06	−2.042	2.258
1.9728	5.1908	4.30	− 4.98	40.0	−199.20	−312	−1.568	0.0464	30.57	−2.986	1.314
2.0824	5.3274	4.20	− 7.74	37.0	−286.20	−456	−0.771	0.0702	31.04	−2.950	1.250
2.1920	5.4640	3.70	− 9.76	31.0	−302.30	−478	0.092	0.0865	31.47	−2.630	1.070
2.3016	5.6006	3.40	−11.81	27.0	−319.00	−449	0.475	0.0845	31.85	−2.216	1.184
2.4112	5.7372	2.70	−13.51	19.0	−256.30	−377	0.860	0.0796	32.17	−1.701	0.999
2.5208	5.8738	2.20	−14.93	15.0	−224.00	−272	0.872	0.0724	32.42	−1.475	0.725
2.6304	6.0104	1.60	−16.25	10.0	−162.50	−193	0.669	0.0657	32.61	−1.473	0.127
2.7400	6.1470	1.10	−17.60	5.0	− 88.00	−124	0.553	0.0634	32.72	−1.521	−0.421
2.8496	6.2836	0.75	−18.77	4.0	− 75.08	− 73	0.359	0.0528	32.76	−1.371	−0.621
2.9592	6.4202	0.50	−19.77	1.0	− 19.77	− 39	0.236	0.0374	32.72	−0.988	−0.488
3.0688	6.5568	0.30	−20.62								0.30
3.1784	6.6934	0.10	−21.29								0.10
3.2880	6.8300	0.00	−22.06								
3.3976	6.9666	0.00	−22.49								
3.5072	7.1032	0.00	−22.65								
3.6188	7.2398	0.00	−22.47								
3.7264	7.3764	0.00	−22.22								
3.8360	7.5130	0.00	−21.47								
3.9456	7.6496	0.00	−20.01								
4.0552	7.7862	0.00	−17.89								
4.1648	7.9228	0.00	−15.18								
4.2744	8.0594	0.00	−10.56								
4.3840	8.1960	0.00	− 5.70								
4.4936	8.3326	0.00	− 0.97								
4.6032	8.4692	0.00	3.43								
4.7128	8.6058	0.00	7.64								
4.8224	8.7424	0.00	11.61								
4.9320	8.8790	0.00	15.50								
5.0416	9.0156	0.00	18.19								
5.1512	9.1522	0.00	20.21								
5.2608	9.2888	0.00	21.78								
5.3704	9.4254	0.00	22.89								
5.4800	9.5620	0.00	23.97								
5.5896	9.6986	0.00	24.67								

$\theta = \frac{0.1366\,t}{0.1096} + 0.2732(20) - 2.732$

$F_b = \left(1+\frac{\dot{\phi}}{g}\right)\rho g A = (1-0.1466\cos\theta)\,\rho g A$

$\rho g A$ – see Figure 10

$\dot{y}_r$ – see Table 2

m – see Table 1

$m\dot{y}_r$ (corrected) – see Column 7 of this table

$f(\theta) = U - s\cos\theta_s = 28.75 + 4.065\cos\theta$

$\frac{d}{dt}(m\dot{y}_r) = \frac{\partial}{\partial t}\Big\vert_{\xi}(m\dot{y}_r) - f(\theta)\frac{\partial}{\partial \xi}\Big\vert_{t}(m\dot{y}_r)$

$F = F_b + \frac{d}{dt}(m\dot{y}_r)$

and 8 of Table 2, respectively, where $\frac{\psi^0}{57.3} = \psi$ radians is obtained from the tabulation in Column 7 of Table 2. ψ and θ correspond to the same time t for a particular calculation of $\dot{y}_r$. $f(\theta)$ is also tabulated in Column 10 of Table 3.

Now $\dot{y}_r = v - \dot{y}_h - \dot{y}_p + (U - u \cos \theta_s)\psi$ is computed and tabulated in Column 10 of Table 2 and Column 4 of Table 3.

5.1.3 Added Mass m

The procedure for determining the added mass per unit length m at any station as a function of the immersion is given in Appendix B. The resulting values of m are plotted in Figure 9 for the stations designated, against both y and y'' (labeled "in" and "out," respectively), the increasing and decreasing immersions or drafts, respectively. Values of m read from Figure 9 for Station 20 are tabulated in Column 13 of Table 1 and Column 5 of Table 3.

5.1.4 Force F

The product $m\dot{y}_r$ was computed and, since a numerical differentiation is to be performed, it was plotted and faired. The computed and faired values are tabulated in Columns 6 and 7, respectively, of Table 3.

The partial derivatives $\frac{\partial}{\partial t}(m\dot{y}_r)$ and $\frac{\partial}{\partial \xi}(m\dot{y}_r)$ required in Equation [1] were computed numerically by means of Stirling's formulas and Newton's interpolation formulas[15] and are tabulated in Columns 8 and 9, respectively, of Table 3. The total derivative $\frac{d}{dt}(m\dot{y}_r)$, which is the "unsteady force" (see Appendix A), is tabulated in Column 11 of Table 3.

The section areas A at various immersions were determined from the body plan of the ship by means of a planimeter. From these values of A, the function $\rho g A$ was computed and plotted in Figures 10a and 10b against the immersion. The values of $\rho g A$ were read from these figures, and by the use of the equation

$$\frac{\dot{v}}{g} = -0.1466 \cos \theta \qquad [11]$$

derived in Appendix D, the Smith-corrected buoyancy force per unit length term $F_b = \left(1 + \frac{\dot{v}}{g}\right) \rho g A$ in Equation [1] was then computed. This term is tabulated in Column 14 of Table 1 and Column 3 of Table 3. Curves of *buoyancy force* per unit length versus computation time are plotted for Stations 0 through 9 and 10 through 14 in Figures 11a and 11b, respectively.

The total rigid-body force per unit length F corresponding to Equation [1] is tabulated in Column 12 of Table 3 in units of kips per foot of length along the keel, and is plotted for Stations 15 through 20 and Stations 1, 3, 6, 10, and 13 in Figures 12a and 12b, respectively. For comparison, the *buoyancy* force per unit length for Station 15 is also plotted in Figure 12a.

(Text continued on page 24.)

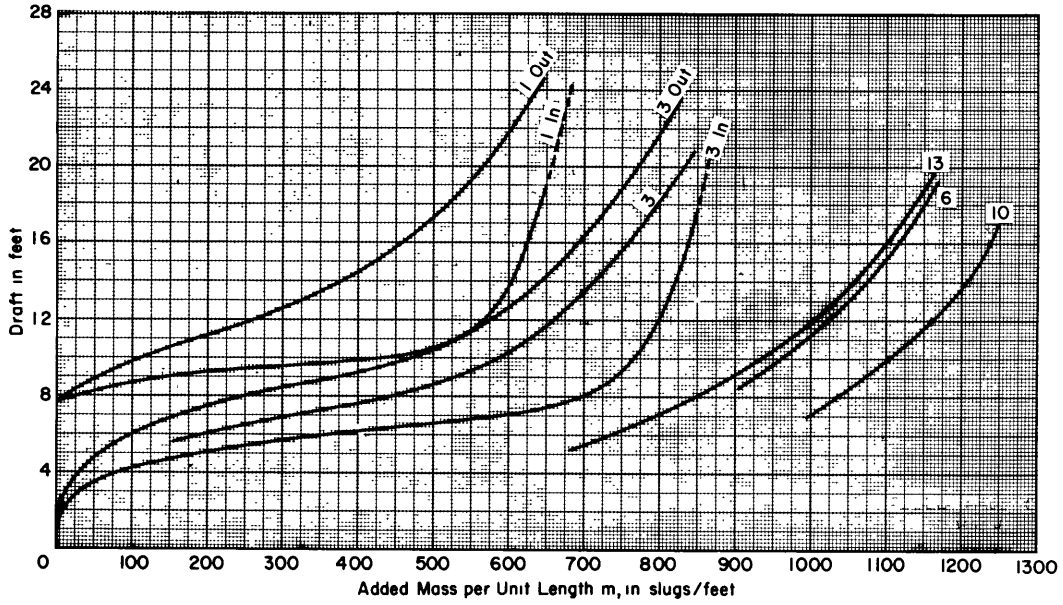

Figure 9a

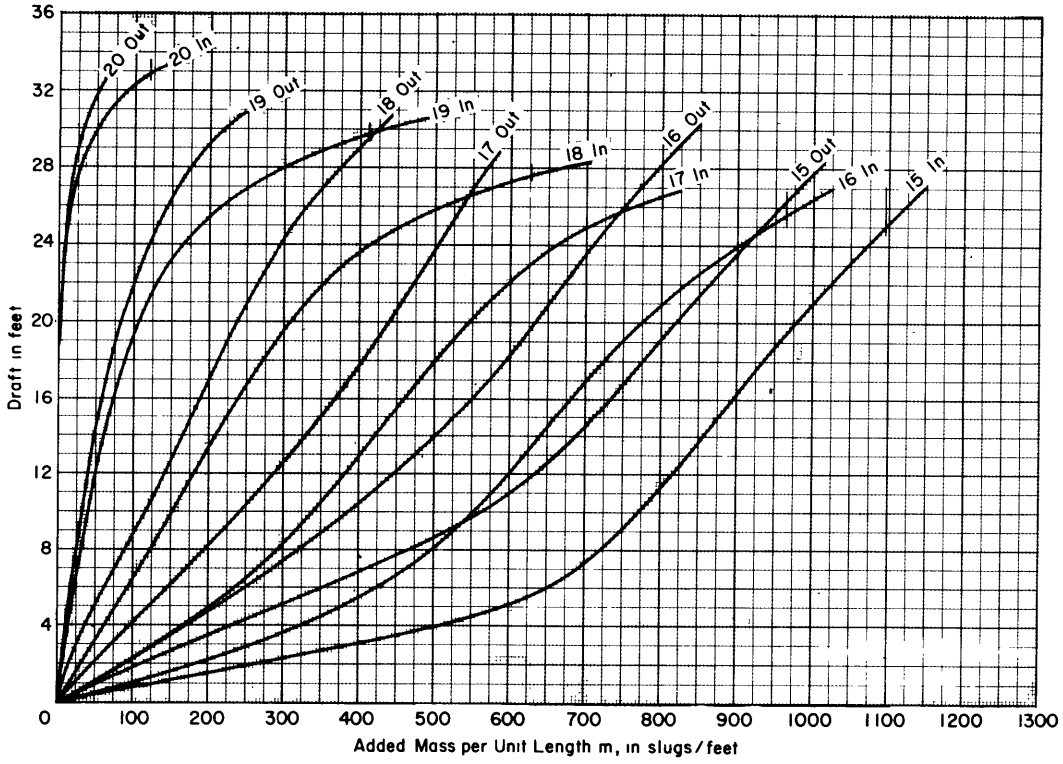

Figure 9b

Figure 9 – Curves of Added Mass as a Function of Immersion

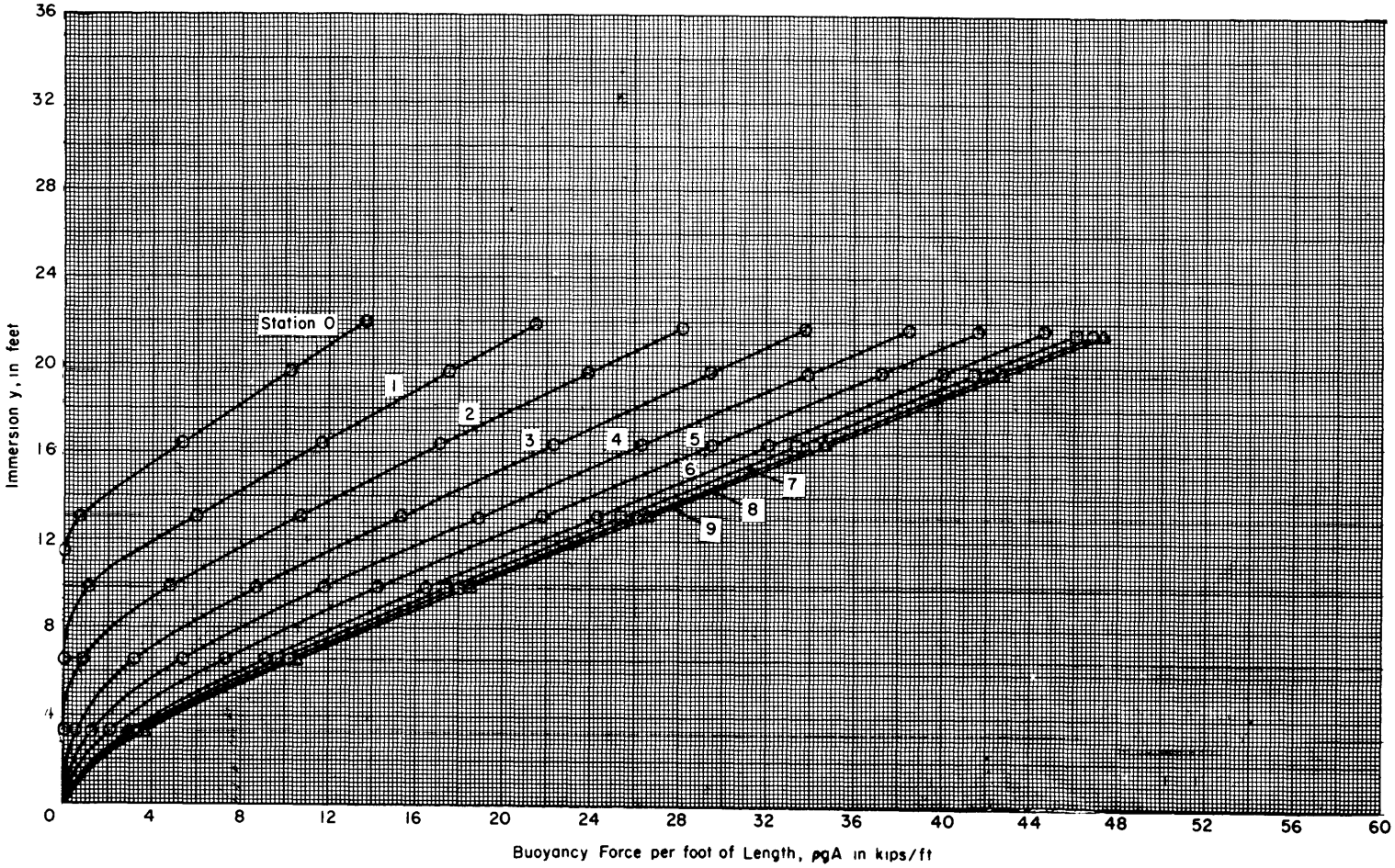
Immersion y, in feet
Buoyancy Force per foot of Length, ρgA in kips/ft
Station 0
1
2
3
4
5
6
7
8
9
0
4
8
12
16
20
24
28
32
36
40
44
48
52
56
60

Figure 10a

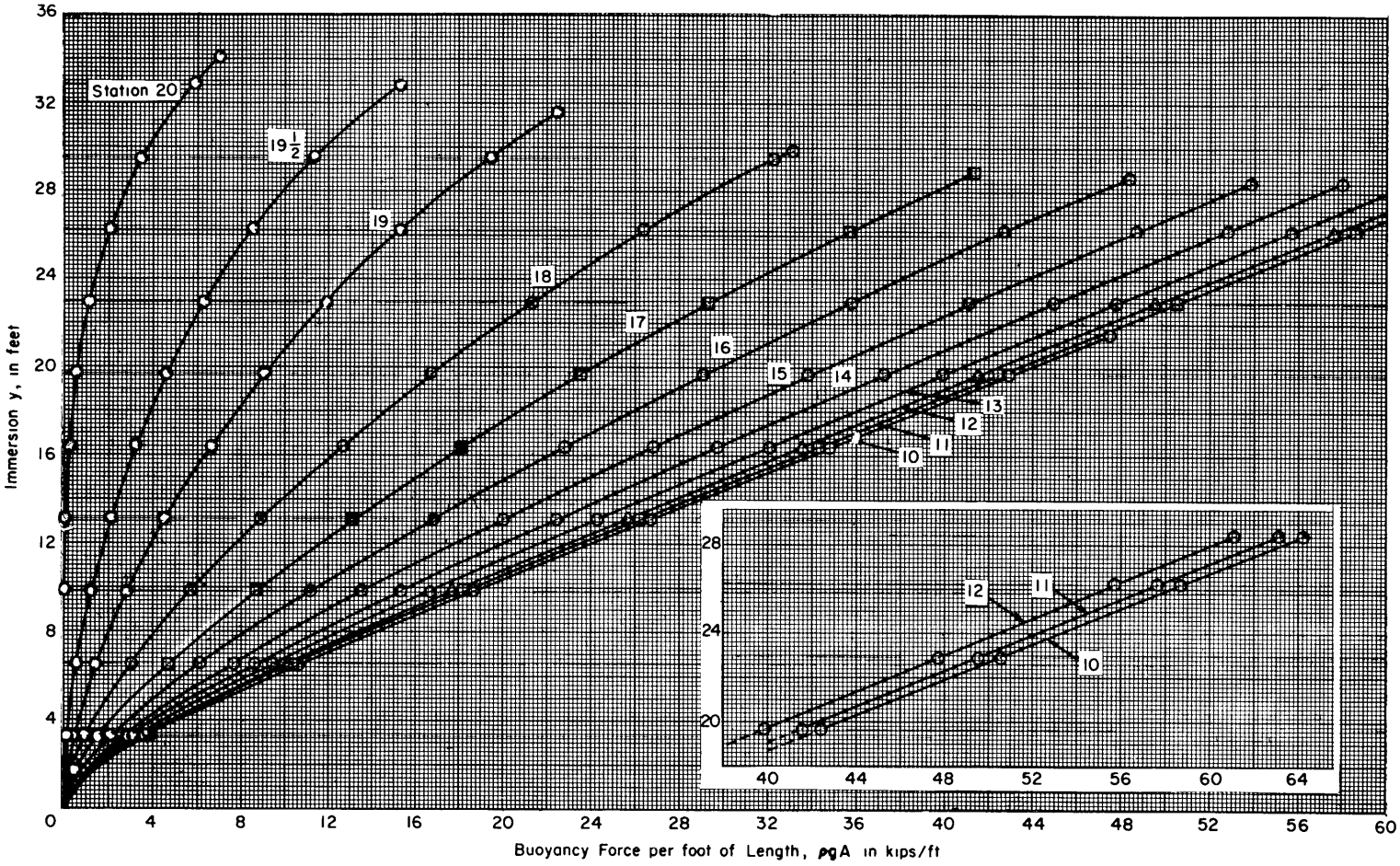

Figure 10b

Figure 10 – Curves of Buoyancy Force as a Function of Immersion

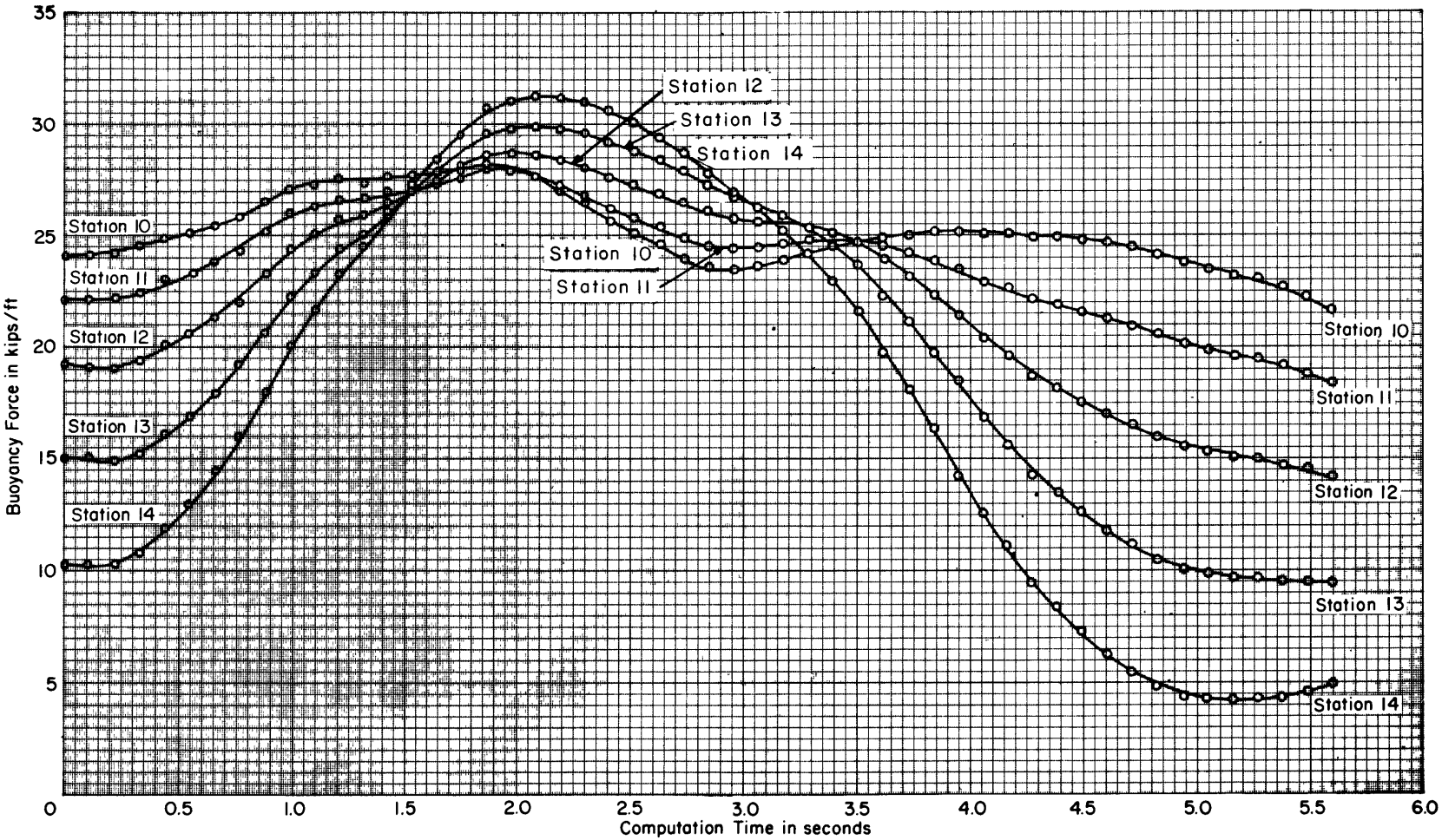

Figure 11a — Stations 10 to 14 Inclusive

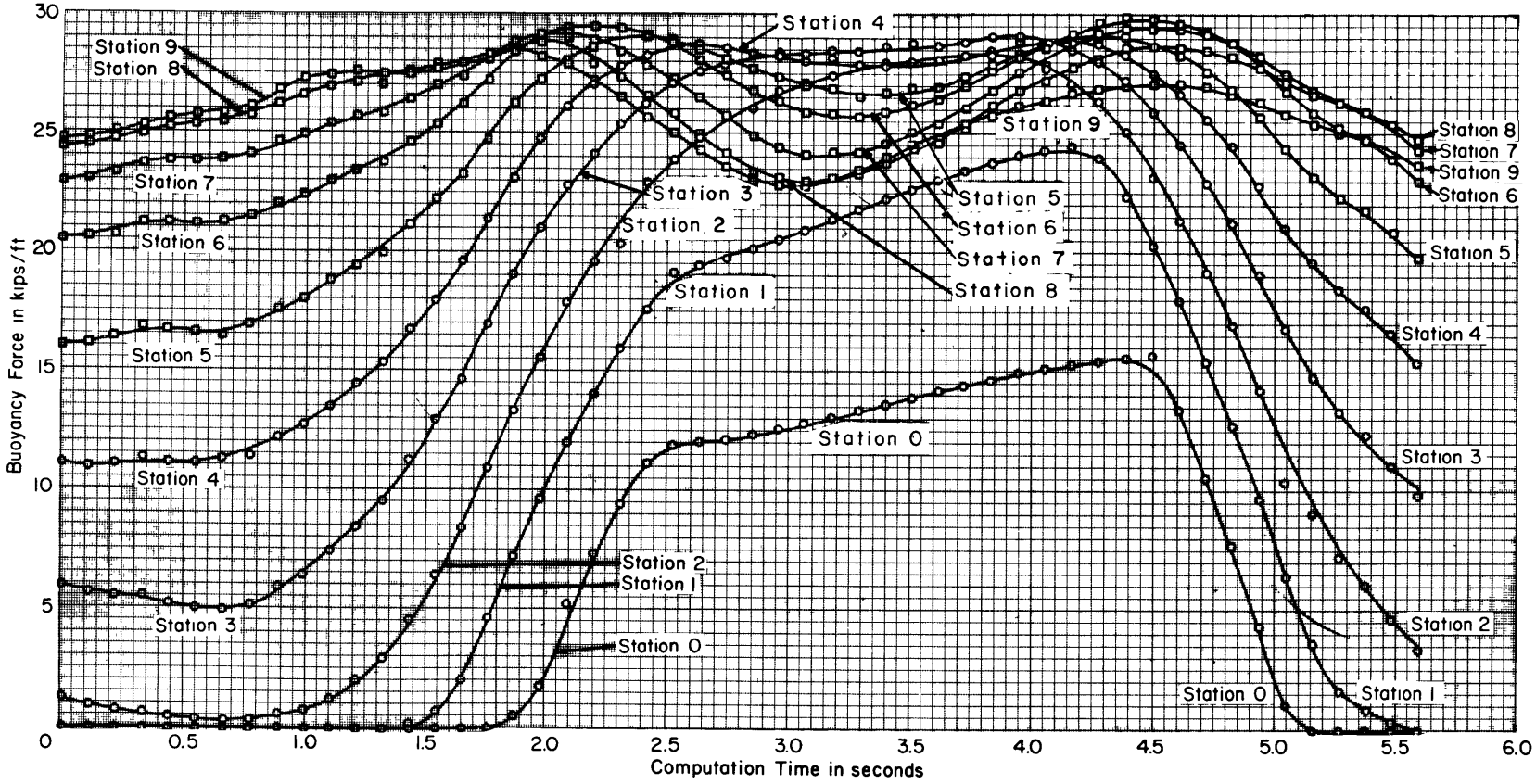

Figure 11b — Stations 0 to 9 Inclusive

Figure 11 – Time History of Smith-Corrected Buoyancy Force

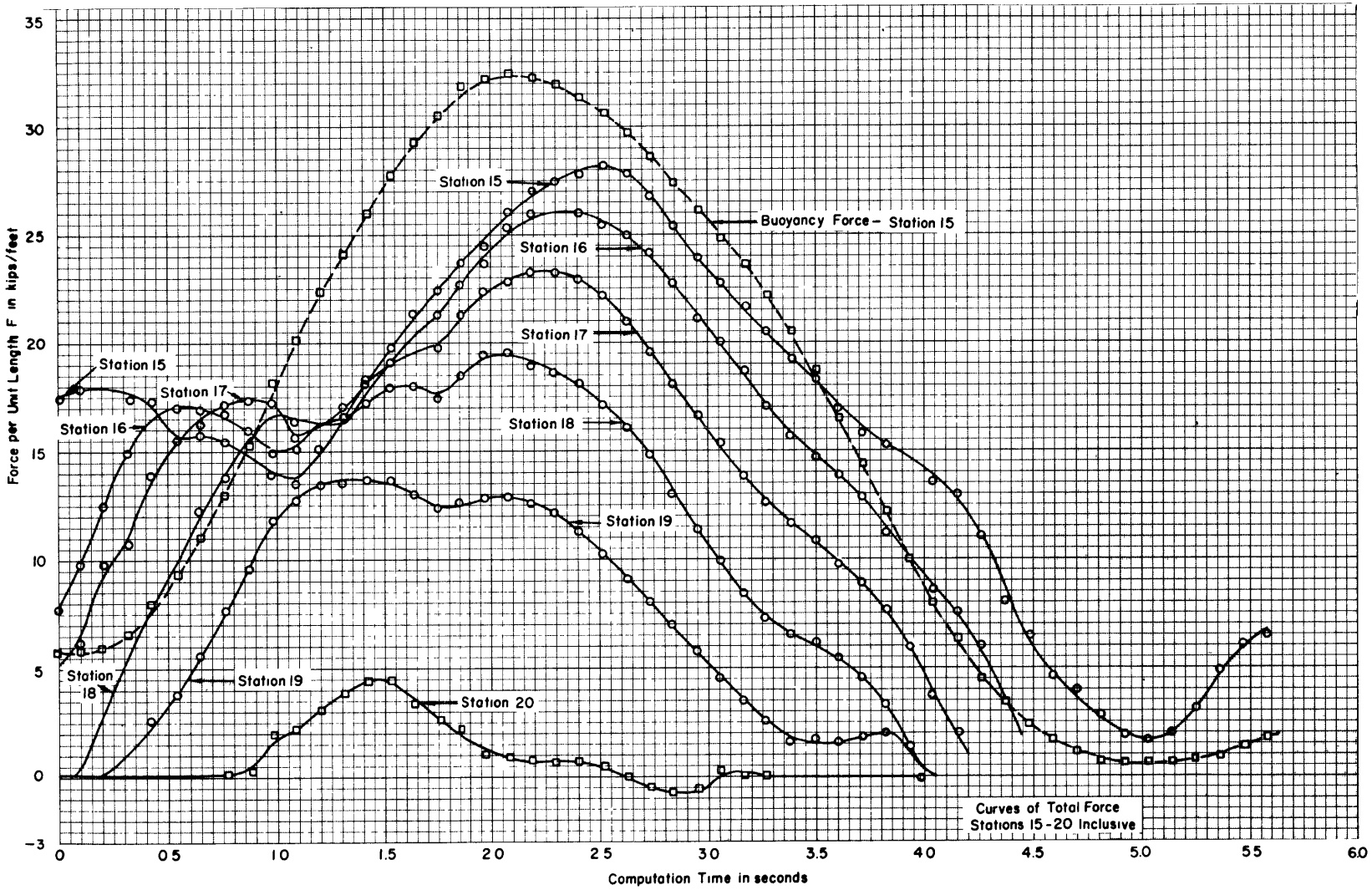
Force per Unit Length F in kips/feet
Computation Time in seconds
Station 15
Station 16
Station 17
Station 18
Station 19
Station 20
Buoyancy Force – Station 15
Curves of Total Force
Stations 15-20 Inclusive

Figure 12a

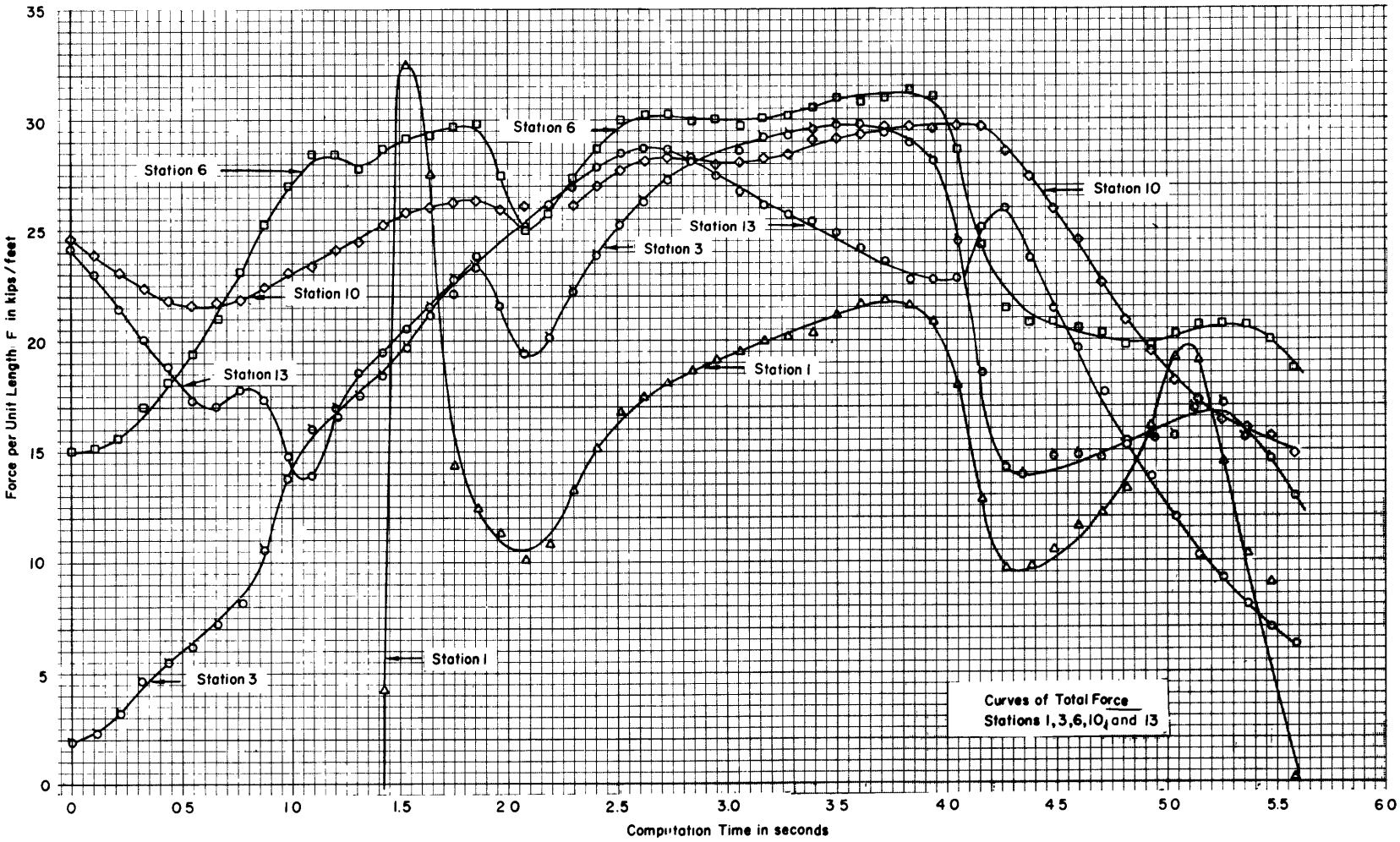

Figure 12b

Figure 12 – Time History of Total Force

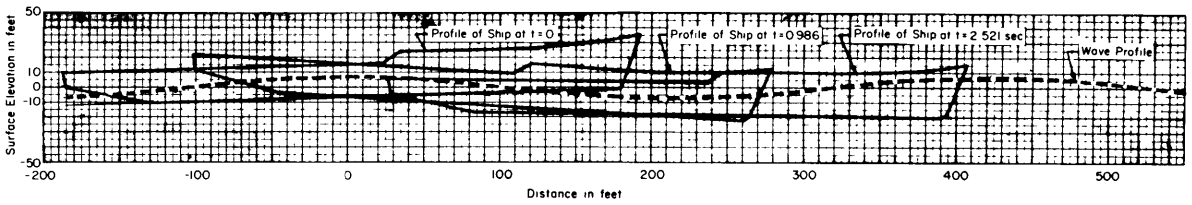

Figure 13 – Position of Ship on Wave at Several Instants

As an aid to visualization of the processes involved and evaluation of the results, the position of the ship on the wave is shown in Figure 13 for several instants including zero time, the time when the "unsteady force" is a maximum at Station 19, $t = 0.086$ sec, and the time when the total rigid-body force reaches a maximum at Station 15, $t = 2.521$ sec.

5.2 CALCULATION OF THE RESPONSE

The calculation of the transient elastic response of the ship to slam was made by the following procedure.[14] The total time-varying rigid-body plus elastic forces per unit length at all (20) ship stations,* and the ship's parameters[5] μ, $\frac{c}{\mu}$, $I_{\mu z}$, EI, and KAG (see Notation) evaluated for 20 or 21 sections of length Δx are tabulated in Table 4.** These data were used in the finite difference equations given in Appendix F, which is an *extension* of the method used in Reference 14.

Solutions of these equations by the IBM 704 digital computer were obtained for ψ, $\frac{dy}{dt}$ (angular velocity of a section about a horizontal axis), $\bar{y}$, y_ϵ, y_h, y_p, M (bending moment on hull), V (shearing force on hull), and other variables as functions of time at the stations or midstations (see Notation and Appendix F).† One of these solutions, the time history of the bending moment M at Station 10, is plotted in Figure 14.

---

*Forces at Stations 0, 2, 4, 5, 7, 8, 9, 11, 12, and 14 were obtained by interpolation of the forces computed for Stations 1, 3, 6, 10, 13, and 15 through 20 in Section 5.1. Forces at half stations were then obtained by straight line numerical interpolation. For purposes of computation on the IBM 704 digital computer, the final forces at each half station were obtained by subtracting the final forces at computation time 0 from the forces at succeeding times; thus at computation time $t = 0$ the force at each half station was taken as 0. This approach seemed reasonable because the recorded motions for the Dutch Destroyer indicate negligible oscillations at computation time 0. Hence, spurious impulsive forces incurred through the method of analysis, which may give rise to large oscillations, are eliminated. If, in a given problem, vibrations exist at time $t = 0$, this procedure can still be used but these vibrations should be superposed upon the calculated results.

**$\mu = \mu(x, t)$ is the sum of the time-varying added mass per unit length and the constant mass of the hull per unit length for a particular ship section of length Δx.

†$\bar{y} = y_\epsilon + y_h + y_p$ is the total displacement which includes a vibratory component y_ϵ as well as rigid-body components $y_h + y_p$; see Appendix F.

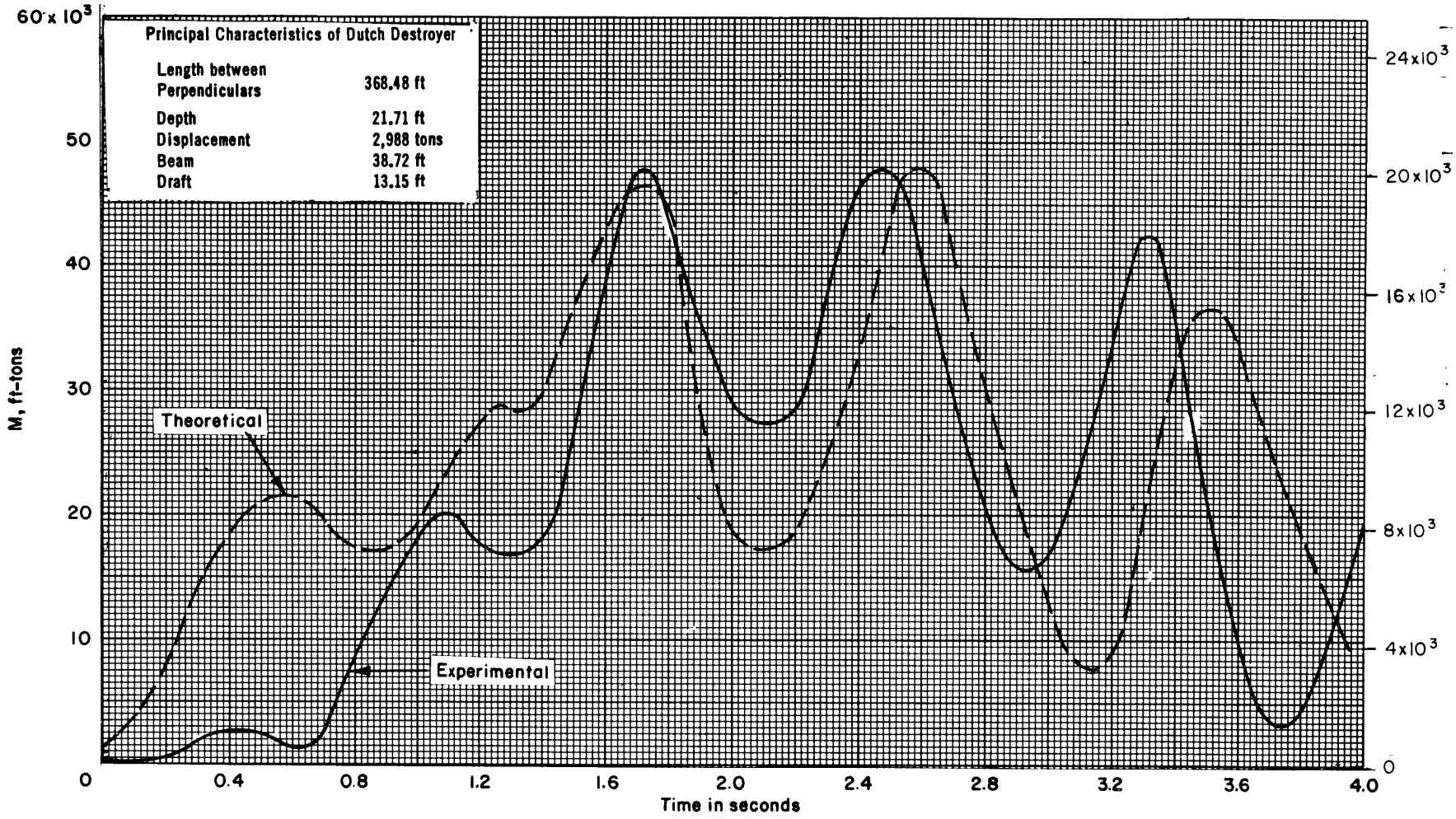

Figure 14b

Theoretical curve translated – 0.16 sec.

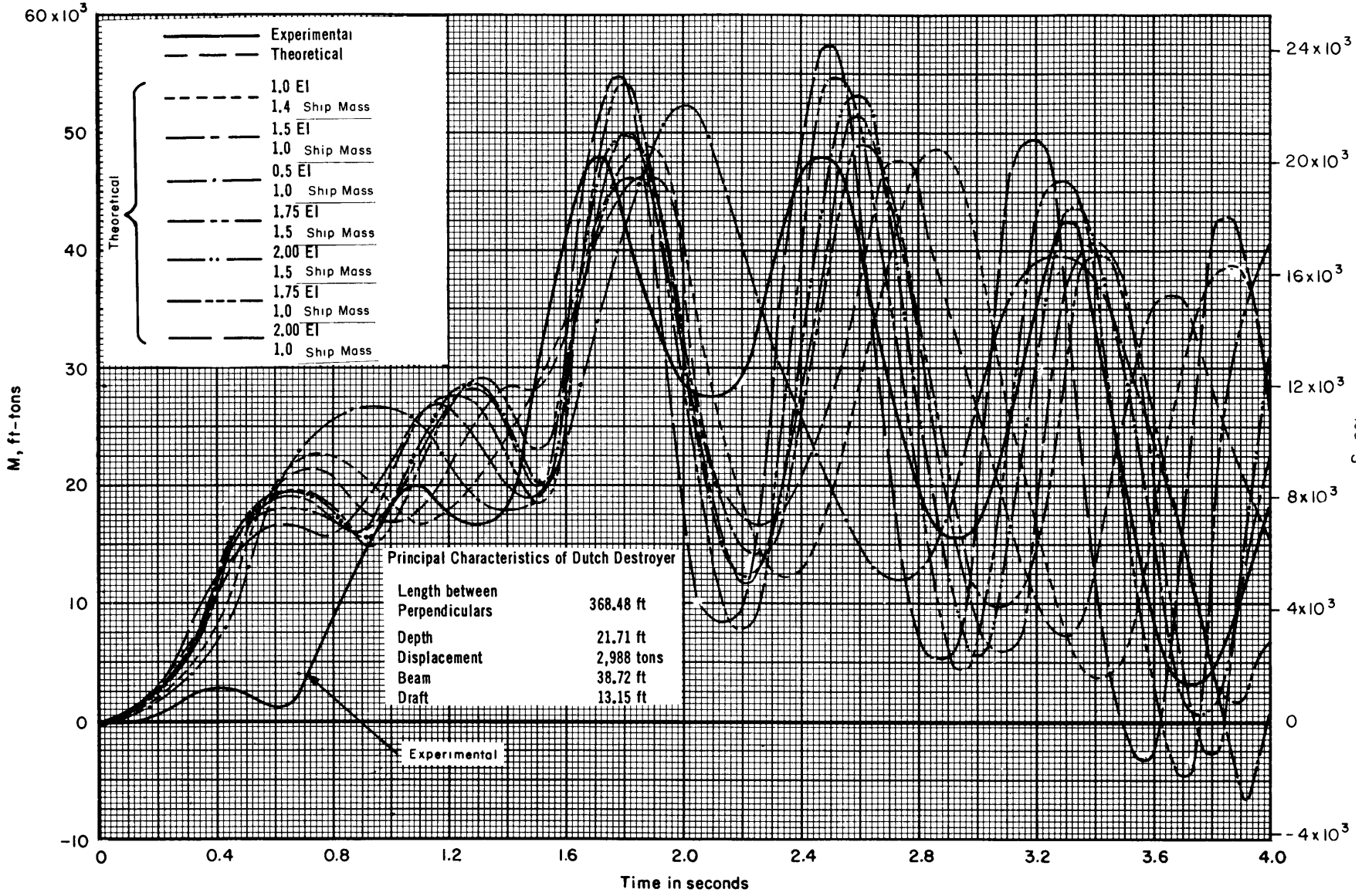

Figure 14c

Theoretical results are for several values of structural mass and EI.

A method of computing the forces on a ship by means of a digital computer rather than manually, as was done in this report, is also described in Appendix F.

6. COMPARISON OF DYNAMIC THEORETICAL AND EXPERIMENTAL STRESSES

The time history of the theoretical and experimental dynamic wave-induced stresses,* which are due to the combined elastic and rigid-body motions of the Dutch Destroyer, at the keel, amidships (i.e., Section 10), is shown in Figure 14a. The theoretical stress curve is a plot of the IBM 704 tabulations of solution data for the time-varying bending moment at Station 10 multiplied by the reciprocal of the section modulus $\frac{I}{C}$ = 64,116 in.^{3} at this station; see Appendix F. The experimental stress curve was obtained from a strain gage measurement, amidships, at the keel which is 10.88 ft below the neutral axis; this curve is a replot of the stress curve for the keel shown in Figure 4. Figure 14b shows the time histories for a −0.16-sec translation of the theoretical curve of Figure 14a. Figure 14c shows time histories corresponding to variations of the bending flexibilities EI and/or ship mass m_s.

7. DISCUSSION

Figures 14a and 14b show that the three largest theoretical and corresponding experimental peak stresses agree to about 3.0 percent, 1.0 percent, and 13.0 percent, respectively. The periods of the oscillatory portions of the curves are nearly the same, ranging from 0.8 sec to 1.0 sec.

The general character of the theoretical and experimental response curves of Figure 14 are similar with regard to the manner of variation, period, and peak magnitudes of whipping oscillation. The faster rise time of the computed curve and the difference in phase and peak-to-peak variation of the theoretical and experimental curves are due to the fact that the computed distributed forcing functions are somewhat in error. Consideration of the accuracy with which the basic data were obtained from the oscillographs and photographs (see Appendix C) yields the following estimates of the errors involved:**

a. Wave height estimate, ± 15 percent.

b. Longitudinal position of ship relative to wave crest, ± 5 percent.

c. Relative velocity of immersion near bow, ± 15 percent.

---

*The total stress at any section of the hull is the sum of the dynamic wave-induced stress plus the still-water stress. The latter stress is due to the difference between the buoyancy force when the immersion equals the draft and the lumped hull weights acting at the half stations of the ship. Note that, although the total buoyancy and weight forces are equal, they are not in equilibrium all along the hull.

**Use of a wave height recorder would lead to a more accurate time history of the wave profile and, therefore, of the immersion. Such a meter was not available at the time the records were obtained.

Thus the resultant error in force due to the error in wave height and relative velocity is $[(1.15)(1.15) - 1] \times 100$ percent = 32 percent. The error in longitudinal positioning would be reflected in part in a time difference between the computed and measured stress variation, i.e., 5 percent of the period of encounter.

The source of additional errors lies in the:

a. Method for determining the wave length and heaving and pitching displacements.

b. Method for determining the added mass.*

c. Assumption that the forcing functions used in the computation of the response are zero at computation time $t \leq 0$, whereas the actual forces are varying somewhat at computation time $t \leq 0$; hence the effects on the computed stresses of the time history of the forces prior to $t = 0$ are not included in the computation.** Although in this problem the initial conditions are known very approximately, a more realistic rise time subsequent to computation time $t = 0$ can be obtained by starting the computation at some suitable time $t < 0$. Impulsive effects at computation time $t = 0$ will not then enter the computations, while such effects at the moment of starting the actual computation (i.e., at $t < 0$) will have small effect at $t = 0$ because the limited memory of the vibrating system makes it less responsive to events farther away in time.

d. Omission of consideration of the effect of the hull's presence in altering the shape of the incident wave.

e. Various assumptions and approximations not mentioned above entering into the analysis and computation.

The study of the effect of the changes in mass and *EI* (Figure 14c) indicates that these changes are not sufficient to account for any significant part of "experiment-theory" discrepancies.

These considerations suggest that the differences between the measured and computed response could, for the greater part, be accounted for by the errors in the basic input data; a more accurate check on the theory requires a more accurate definition of the input data which can be obtained by controlled model tests. Thus comparison of calculation and experiment is considered to be good (at least within the range of accuracy of the basic data) in the main aspects of the response, although there are deviations in some details. It appears that good predictions, within 30 percent, can be made of whipping and wave frequency bending moment amplitudes.

Significantly, despite all the assumptions and approximations made in setting up and carrying out the computations, the results show that the mathematical representation of the physical mechanism assumed to be underlying the creation of the slamming forces is reasonably accurate.

---

*Determination of the added mass per unit length as a function of immersion may be achieved with greater accuracy if ellipses rather than flat plates (see Appendix B) are fitted to the wetted portions of the ship.[16, 17]

**The major stress at time $t < 0$ is due to the ordinary wave-induced stress associated with the heaving and pitching motions of the ship, the stress due to flexural vibrations, and the still-water bending moment.

If whipping were due to a step function load, the oscillatory bending moment would be the same for nearly all cases in Figure 14c, i.e., its magnitude would be the same but its periodicity would be that of the natural 2-noded mode. If the triplet phenomenon[18] were the major excitation, the magnitude of the whipping moment would be rather sensitive to the *natural period* of the 2-noded mode. Figure 14c indicates that the whipping moment is not very sensitive to the natural period. It is, therefore, concluded that the main excitation is associated with a fairly sudden change in the applied forces, the triplet contribution being small.

The procedure used in this report for computing the forces on the hull and the use of these forces to calculate the elastic response of the hull may be improved by resorting to the refinements shown as Method 2 in the following chart. The wave profile, ship parameters, and other input data are considered available.

Method	Quantity To Be Computed	Ship Motion Utilized in Calculation of Force or Response	Ship Motion Utilized in Calculating Virtual Mass at Each Station for Use in Force or Response Calculations
1 (Present Method)	Force on Hull	Rigid-Body Motion	Rigid-Body Motion*
	Response	Rigid- and Elastic-Body Motions	Rigid-Body Motion*
2 (Improved Method)	Force on Hull	Rigid- and Elastic-Body Motions**	Rigid-Body Motion or Rigid- and Elastic-Body Motions+
	Response	Rigid- and Elastic-Body Motions	Rigid-Body Motion or Rigid- and Elastic-Body Motions+

*Virtual mass varies with the instantaneous value of the rigid-body waterline.

**For this computation $(\dot{y}_r)_{\text{total}} = (\dot{y}_r)_{\text{rigid body}}$ + a component of velocity due to the elastic-body motion.

+For this computation $(m)_{\text{total}} = (m)_{\text{rigid body}}$ + a component of mass due to the elastic-body motion; similarly for $(\mu)_{\text{total}}$.

If the theory of slamming and the method of computation of slamming forces (and stresses) are verified for similar computations on other ships, and if for a given sea state the rigid-body motion can be predicted,[18]* then for an assumed sea state the girder stresses for any section of the ship still in the design stage can be predicted. This prediction would lead to an improvement in ship forms designed for high speed.

*See, Andrews, John N., "A Method for Computing the Response of a Ship to a Transient Load," David Taylor Model Basin Report 1544 (in preparation).

8. ANALOG AND DIGITAL METHOD OF SOLUTION FOR PREDICTING FORCES ON AND RESPONSE OF A SHIP DUE TO WAVE MOTION

It is desirable to reduce the complexity, expense, and time required in making numerical computations* for predicting the forces on and the dynamic (elastic- and rigid-body) response of a ship girder, i.e., bending moments, shearing forces, vibrations, heaving, and pitching moments. This can be accomplished by an analog or high-speed digital computer which uses basic input data.

One particular analog scheme, devised by the author, for performing the mathematical operations is discussed in Appendix G.

Another analog network, devised and constructed by Dr. R.H. MacNeal, was used for obtaining solutions of the bow slamming problem for ESSEX; see Reference 18 and Appendix G. The equations used in devising this analog are reformulations of the equations given in Reference 19 for convenience of electrical simulation.

A digital computer (IBM 7090) is presently being coded at the Applied Mathematics Laboratory of the David Taylor Model Basin to give solutions for the excitation forces and response when certain basic data are furnished; see Appendix F.

9. CONCLUSIONS

The following conclusions may be drawn from the analysis given in this report:

a. The girder stress in any section of the destroyer under study can be calculated from the ship's rigid-body motions in a heavy sea by utilizing integrated slamming loads per cross section which are derived as hydrodynamic and Smith-corrected buoyancy forces; specifically the theoretical and experimental time-varying girder stress midships show good agreement.

b. The bow flare immersion in heavy seas is a significant source of large stresses in the hull girder which may lead to hull girder damage.

c. The computed hydrodynamic and Smith-corrected buoyancy forces may be used to evaluate the transient response of the ship girder in heavy head-on seas, that is, moments, girder stresses, shearing forces, and angular rotation for any section of the ship.

d. There are many indications that, if the rigid-body motion can be predicted, the method used in this report will permit, for an assumed head-on sea state, the calculation of girder stresses for any section of a ship still in the design stage.

---

*Note that the computation of the forces in this report was manual. This computation can be performed automatically by an analog or a digital computer.

10. RECOMMENDATIONS

1. The approach described in this report and previous studies on ESSEX* resulted in good agreement between calculated and observed hull girder stresses. This method therefore offers promise for evaluating various hull shapes in the early design stages. It is therefore desirable to:

a. Extend the confidence limits for the method by checking observed and predicted girder response for several ship types of drastically different hull form.

b. Establish a reliable method for predicting the rigid-body motion of a ship in a head-on sea.

2. Examples of specific recommended studies are:

a. Theoretical and experimental virtual mass (forces) for large motions of the bow and for large and small deadrise angles of a ship section.

b. Effects of changes in bow flare and of bulbous bows upon the forces on and response of a ship.

c. Determination of significance of higher order effects in the theoretical treatment in order to simplify, where possible, the theory for a particular class of a ship.

3. Slamming studies of ships operating in oblique and confused seas and of local impact type hull damage are necessary supplements to the recommended extension of previous work.

11. ACKNOWLEDGMENTS

Mr. E. Hoyt, under contract to the David Taylor Model Basin assisted the author in developing the detailed procedure for and calculation of the wave forces. In the Structural Mechanics Laboratory, Mr. T. Dowd gave valuable assistance to the author on various phases of this project, Mr. J. Andrews assisted in making independent computations, and Mrs. B.H. Gesswein assisted in tabulating the data for the digital computer. Dr. Elizabeth Cuthill and Mr. Edward Osten of the Applied Mathematics Laboratory of the David Taylor Model Basin established and coded the finite difference equations given in Appendix F. Miss Susan Strand of the latter laboratory assisted in devising a method for computing the hydrodynamic force by means of the digital computer (Appendix F).

*See footnote on previous page.

APPENDIX A

COMPUTATION OF FORCES DUE TO MOTION OF A SHIP IN WAVES

The computation of the hydrodynamic forces due to the motion of a ship in waves is based on the cross-flow hypothesis.[8-11] In applying this hypothesis, the hydrodynamic force per unit length at any cross section is considered the same as that experienced by an infinitely long cylindrical ship having an identical cross section. The basic statement of this hypothesis given by Fay is:[11]

"Consider a thin sheet of fluid in a plane normal to the direction of motion of the vessel, which is pierced by the vessel as it moves forward. The flow of fluid in such a plane is assumed to be the same as the transient two-dimensional motion which would result from a cylindrical surface (with generator normal to the plane) which moves in time such that it occupies at each instant the same position as does the perimeter of the ship cross section lying in the plane in question at the same instant."

To justify and show the limitations of the cross-flow hypothesis, Fay considers an oscillating ship on a free surface whose length $l > D$, its draft, and whose draft $D \sim B$, its breadth; i.e., the ship is considered as a slender body. He shows that, on or near the ship, two-dimensional solution of Laplace's equation

$$\frac{\partial^2 \phi}{\partial y^2} + \frac{\partial^2 \phi}{\partial z^2}$$

gives the pressure distribution correct to order D/l, justifying the cross-flow hypothesis to this extent. If $\left(\frac{2\pi D}{\lambda}\right)^2 < 1$, the flow in any plane will be two-dimensional, and the transverse exciting forces are obtained in the same way as the pressures. *Thus, due to the presence of the ship, the perturbation of the original waveform is predominantly transverse* despite the fact that the undisturbed wave-particle motion is in the x-y plane; see Appendix D.

The cross-flow assumption is shown by Fay to be applicable when

$$U + V_w > \frac{\lambda}{l} |U|$$

where U is the velocity of the ship in feet per second,

V_w is the wave velocity in feet per second,

λ is the wave length in feet, and

l is the length of the ship in feet.

Note that U is negative in following seas.

We now formulate the problem of finding the hydrodynamic forces acting on a ship moving with uniform velocity U, at a heading θ_s, to the normal to the wave crests; see Figure 1. Since the waveform is assumed to be cylindrical, it is sufficient to locate a point on the ship by its coordinate x, measured from wave crest 1.

The force acting at a transverse section, or station, of the ship, whose distance forward of amidship is ξ, is equal and opposite to that exerted by the ship on a fluid lamina of differential thickness $d\xi$ instantaneously coincident with the section of the ship.

The lamina considered will consist always of the same fluid particles. In reality, such a lamina can be neither plane nor fixed in space. This is the case because the fluid particles describe circular paths about fixed centers with uniform angular velocity and the radii of these orbits decrease exponentially as depth increases (see Appendix D); the particles which were originally in some vertical plane sway to and fro with the passage of the wave. Consequently, a lamina consisting of the particles between two such originally plane surfaces separated by an infinitesimal distance $d\xi$ will also oscillate and become nonplanar. However, to avoid excessive computational detail, the effect of the exponential decay of the particle velocity with depth is ignored (i.e., the fluid motion at all depths is considered to be uniform), and the planes defining the lamina are taken to be vertical. Thus, the lamina or flow plane oscillates horizontally and always contains the same fluid particles at the surface.

Let $\bar{\eta}_w(x)$ denote the velocity vector of a particle at the surface whose position with respect to the ship, flow lamina, and wave crests is shown in Figure 1. The vector $\bar{\eta}_w(x)$ is directed at an angle to the x-y plane equal to the slope of the particle path in the x-z plane for any corresponding value of t and x. The horizontal and vertical components of $\bar{\eta}_w(x)$ are u and v, respectively; see Appendix D. The velocity components normal to and in the flow plane are $u \cos \theta_s$ and $u \sin \theta_s$, respectively. The latter component will be ignored, since its effect on the vertical forces is expected to be insignificant.

The components of fluid velocity are also shown in Figure 2, which is a view of the ship's center plane. The figure also shows the components of immersion D, y_w, y_h, and y_p of the cross section of the ship at the flow lamina.

The velocity of all points on the ship *in the flow plane* are nearly the same, differing only by a small normal component due to pitching, which may be ignored. The velocity of one point is taken as representative and designated as $\bar{\eta}_s(\xi)$, since it varies for different sections. The horizontal component of $\bar{\eta}_s(\xi)$ is U; the ship's forward velocity and the vertical component are the sum of the heaving and pitching components of velocity $\dot{y}_h + \dot{y}_p$.

To compute the transverse hydrodynamic forces on the ship, we consider the motion of points on a ship which penetrate the fluid plane relative to the motion of the fluid in this plane. These motions are:

a. The relative horizontal velocity $U - u \cos \theta_s$.

b. The relative vertical velocity (positive upward) $\dot{y}_h + \dot{y}_p - v$ plus a component generated by the velocity of advance $(d\xi/dt)_{s-f}$ of the ship through the flow plane when the ship is

pitching at an angle ψ. (Subscript $s-f$ means ship relative to the fluid.) This latter component of relative vertical velocity $-\psi\,(d\xi/dt)_{s-f}$ (positive upward, illustrated in Figure 15a, is seen to be equal to $\psi\,[-(U-u\cos\theta_s)]$, since the velocity of advance $(d\xi/dt)_{s-f}$ is also the relative horizontal velocity of the point at which the keel pierces the flow plane, i.e., $(U-u\cos\theta_s)$.

A vector representation of the velocities $\bar{q}_s$, V_{fluid}, and the relative ship-fluid velocity $(\bar{q}_s(\xi)-V_{\text{fluid}})$ and their horizontal and vertical components are shown in Figure 15b. It is desirable, however, to resolve the relative velocity vector into a vertical component $\dot{y}_r$ plus a vector $\dfrac{U-u\cos\theta_s}{\cos\psi} \approx U-u\cos\theta_s$ *along an oblique axis lying along the pitching keel.* Then we can ignore this oblique component, since the transverse force resulting from the variation with time of the velocity along the keel is considered to be negligible* (i.e., the velocity component parallel to the keel produces no change in momentum in the flow plane).

In accordance with the cross-flow hypothesis, we consider, therefore, the flow which would be produced in a flow plane by the motion of a cylinder whose shape at every instant is that of the cross section of the ship, with *downward* relative velocity

$$\dot{y}_r = v - \dot{y}_h - \dot{y}_p + (U-u\cos\theta_s)\,\psi$$

into fluid moving upward with velocity v. It is assumed that the relative flow, at any instant, can be described by the impulse $m\dot{y}_r$ necessary to establish that flow instantaneously from rest by impulsive pressure.[20] Here m is the hydrodynamic added mass per unit length associated with the motion of the body.

Now we show that the downward force on the fluid and, hence, the upward force on the body in such a flow is

$$\frac{dF}{d\xi} \approx \frac{d}{dt}\,(m\dot{y}_r) + (g+\dot{v})\,\rho A$$

per unit of length ξ along the keel, where

$\dfrac{dF}{d\xi}$ is force per unit length,

m is added mass per unit length,

$\dot{y}_r$ is downward relative velocity of the body with respect to the undisturbed fluid (i.e., undisturbed by ship, not the wave),

---

*The motion of the keel through the water at constant immersion and with velocity U causes a small change of trim with respect to the trim of the ship at rest. As a steady-state phenomenon, it is not of interest in the slamming problem. The additional forces along the keel resulting from the variation with time of the immersion and velocity along the keel are also neglected.

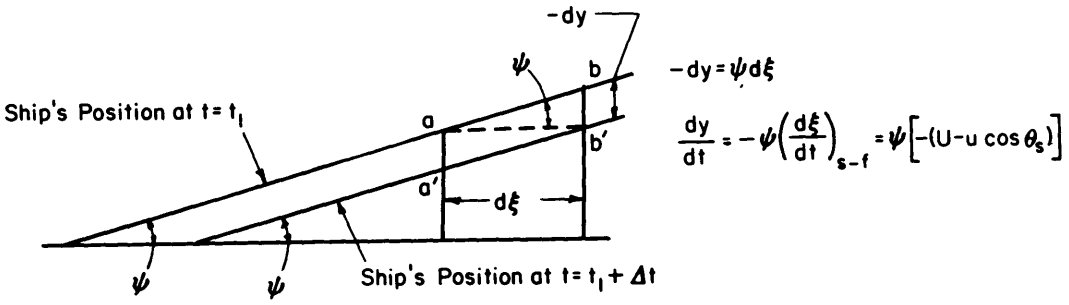

Figure 15a – Velocity Component Due to Forward Motion of Pitched Ship

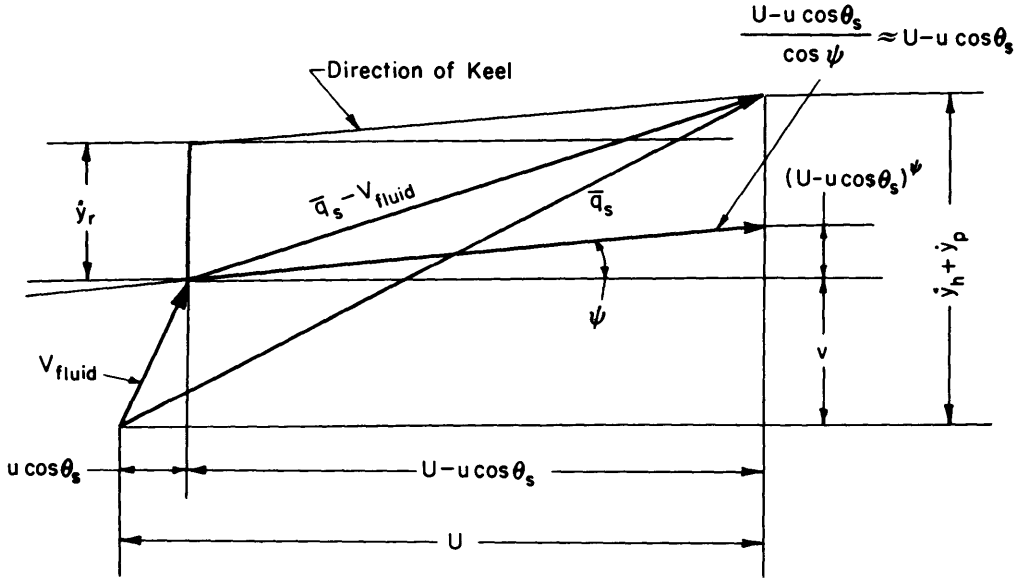

Figure 15b – Vector Relationships

Figure 15 – Components of Relative Velocity

Note: In time Δt all points on ship have been translated an amount $d\xi$ with respect to the fluid, and the point "a" at which the keel pierces the flow plane has moved downward an amount $-dy$ to point "a′"; similarly "b" has moved downward to "b'" the same amount.

g is the acceleration of gravity,

v is the vertical velocity of the undisturbed fluid,

ρ is the density, and

A is the area of the cross section.

The Smith-corrected buoyancy force term, $F_b = (g+\dot{v})\rho A$, due to the motion of the fluid particles vibrating under the action of gravity g can be derived by applying Newton's laws to an element of fluid;[21] *the ship is, for the present, considered stationary.* The dimensions of the small fluid element are Δx, Δy, and Δz; see Figure 16. Let u, v, and w be the components of velocity parallel, respectively, to the x-, y-, and z-axes of a fluid particle of mass m per unit length at point $P(x,y,z,t)$ of the element. $p(x,y,z,t)$ is the pressure at P at time t. Then the equation of motion of this particle is as Δx, Δy, and Δz all approach zero:[22]

$$m\frac{dv}{dt} = \rho\,dx\,dy\,dz\left(\frac{\partial v}{\partial t} + u\frac{\partial v}{\partial x} + v\frac{\partial v}{\partial y} + \frac{w\partial v}{\partial z}\right) = -p\,dx\,dz + \left(p - \frac{\partial p}{\partial y}\,dy\right)dx\,dz - \rho g\,dx\,dy\,dz$$

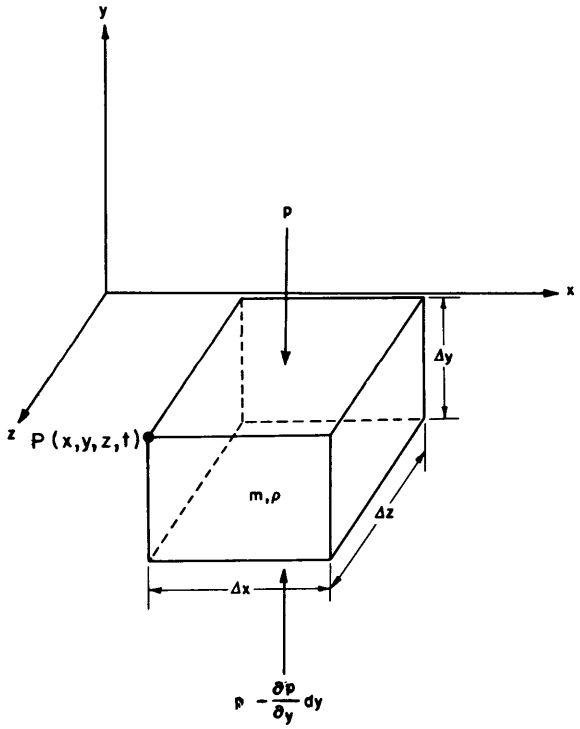

Figure 16 – Element of Fluid in Vertical Equilibrium

x, y, z are positive along directions shown, and forces are taken as positive upward.

or

$$\frac{\partial v}{\partial t} + u\frac{\partial v}{\partial x} + v\frac{\partial v}{\partial y} + w\frac{\partial v}{\partial z} = -\frac{1}{\rho}\frac{\partial p}{\partial y} - g$$

Since $\frac{\partial v}{\partial x}$, $\frac{\partial v}{\partial y}$, $\frac{\partial v}{\partial z}$ are known to be relatively small, the equation simplifies to

$$p \approx -\rho\int\frac{\partial v}{\partial t}\,dy - \rho g\int dy + C$$

But $\frac{\partial v}{\partial y} \approx 0$ so that $v \neq f(y)$; hence, $\dot{v} = \frac{\partial v}{\partial t} \neq f(y)$, and $p = -(\dot{v}+g)\rho y + C$. At the surface $y = 0$, $p = 0$; therefore $C = 0$. Also, the downward force on the fluid is

$$F_{\text{fluid}} = \iint p\,dx\,dz = -(\dot{v}+g)\,\rho\iint y\,dz\,dx = -(\dot{v}+g)\,\rho A\int dx$$

Therefore the downward force per unit length on the fluid is

$$\frac{dF_{\text{fluid}}}{dx} = \frac{dF_{\text{fluid}}}{d\xi} = -(\dot{v} + g)\,\rho A$$

The Smith-corrected buoyancy force F_b per unit length acting upward on the body is

$$F_b = -\frac{dF_{\text{fluid}}}{d\xi} = (\dot{v} + g)\,\rho A$$

Now let the ship move down with a velocity $\dot{y}_r$ relative to the fluid. Then the force per unit length on the fluid due to this motion is $-\frac{d}{dt}(m\dot{y}_r)$, and the corresponding reaction force per unit length on the ship is $\frac{d}{dt}(m\dot{y}_r)$. The sum of this force and F_b is the total force per unit length $\frac{dF}{d\xi}$ acting on the ship.

The derivative is to be taken with respect to the flow plane. The force is wanted, however, at stations fixed in the ship and it is most convenient to tabulate $m\dot{y}_r$ for such stations. Hence the impulse $m\dot{y}_r$ in the flow plane is expressed as a function of the time t and the position of the station along the keel. That is,

$$m\dot{y}_r = f(\xi, t)$$

and

$$\frac{d}{dt}(m\dot{y}_r) = \frac{\partial}{\partial t}\bigg|_{\xi}(m\dot{y}_r) + \frac{d\xi}{dt}\;\frac{\partial}{\partial \xi}\bigg|_{t}(m\dot{y}_r)$$

where

$$\frac{d\xi}{dt} = \left(\frac{d\xi}{dt}\right)_{f-s} = -(U - u\cos\theta_s)$$

so that finally

$$\frac{dF}{d\xi} = \frac{\partial}{\partial t}(m\dot{y}_r) - (U - u\cos\theta_s)\,\frac{\partial}{\partial \xi}(m\dot{y}_r) + (g + \dot{v})\rho A$$

where the term $\rho g A$ is the buoyancy force in still water and $\dot{v}\rho A$ represents the Smith correction* (at the mean waterline) induced by the vertical acceleration of the undisturbed fluid in the lamina.

---

*See Appendix D for a more accurate expression for the Smith correction.

APPENDIX B

METHOD FOR DETERMINATION OF ADDED (VIRTUAL) MASS PER UNIT LENGTH AS A FUNCTION OF IMMERSION*

The method used to determine the added mass per unit length m can be described by reference to Figure 17. This figure shows one section of the ship immersed to a depth y below

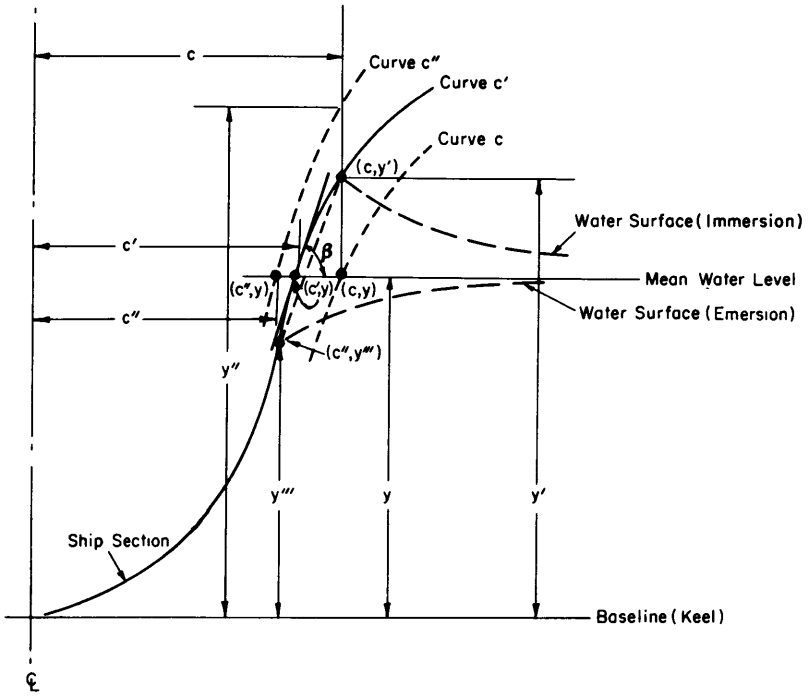

Figure 17 – Immersed Ship Section during Impact

Water surface (immersion) refers to elevation of water surface near ship due to increasing immersion. Water surface (emersion) refers to depression of water surface near ship due to decreasing immersion.

the surface of the water in the flow lamina undisturbed by the presence of the ship. The half breadth at this immersion is designated by c'.

When the immersion is increasing, the fluid flow results in an elevation of the water surface near the ship. The water surface then meets the ship at a height y' above the baseline,** where the half breadth is c. Conversely, when the immersion is decreasing, the surface near the ship is depressed to a point where the height is y''' and the half breadth is

*Alternative methods have been suggested in Section 7.

**The baseline lies along the keel of the midship section; see Figure 17.

c''. The problem is to first compute the half breadth corresponding to the immersion* and then to compute the virtual mass which varies as the square of the half breadth.

The amount of elevation can be estimated on the assumption that the half beam of the ship is increased during immersion in the same ratio as that of a wedge of slope equal to that of the point on the ship section profile at immersion y. This estimate is based upon the following equations given by Szebehely[12] for *large* deadrise angles β.

$$\frac{c}{c'} = \frac{\pi}{2} \frac{\tan \beta}{\beta} \cdot K \qquad [B1]$$

$$K = \frac{\Gamma\left(\frac{1}{2} + \frac{\beta}{\pi}\right) \Gamma\left(1 - \frac{\beta}{\pi}\right) \cos \beta}{\sqrt{\pi}} \qquad [B2]$$

where, in accordance with the assumption, tan β is the slope of the tangent at y; similarly, when the immersion is decreasing, the half breadth decreases in the ratio

$$\frac{c'}{c''} = \frac{c}{c'} \qquad [B3]$$

Equations [B1] and [B2] show that c/c' is a function of β only. A curve of c/c' versus β is plotted in Figure 18 for values of β ranging from 0 deg to 90 deg.

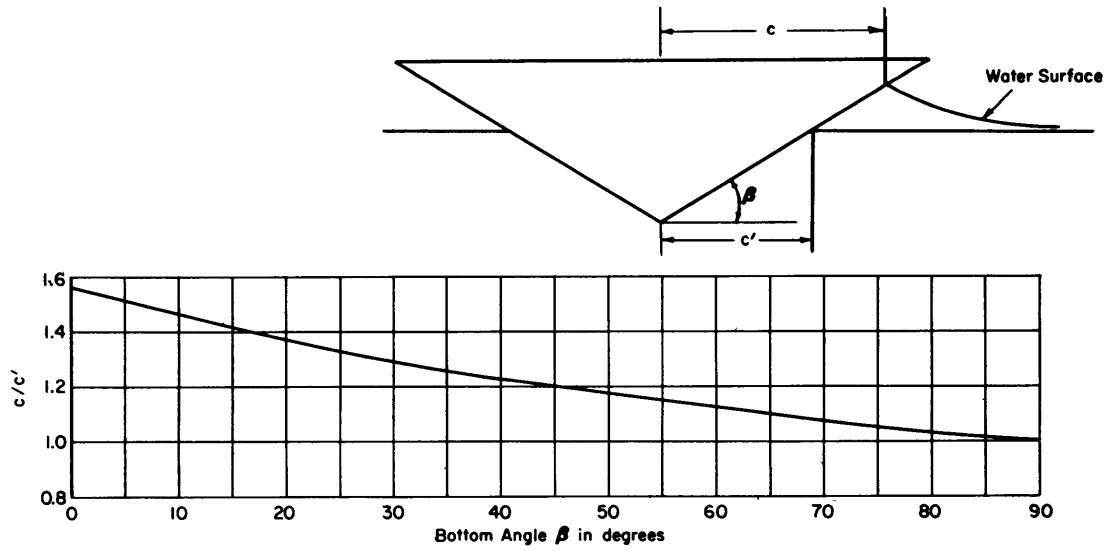

Figure 18 – Curve of c/c' as a Function of Deadrise Angle β

*That is, for increasing and decreasing immersion.

From the body plans of the ship the values of c' were obtained at regularly spaced drafts y and corresponding angles β. The value of c corresponding to these values of c' was computed from Figure 18. Finally, c'', corresponding to the values of c' and c, was computed by means of Equation [B3]. The values c', c, and c'' evaluated for regularly spaced drafts y are tabulated in Table 5. Curves c and c'' versus y may now be constructed; see dotted curves in Figure 17.

TABLE 5

Data for Computation of Added Mass at Station 20

Values of β corresponding to immersion are not tabulated here; however, these values were obtained and used in the computation of c and c''.

Immersion ft		c'	$\frac{c}{c'} = \frac{c'}{c''}$	c	y'	$\frac{2c}{y'-6} = \frac{B}{d}$	η	$[c_v]_{y'-6}$	m
y	y''	ft		ft	ft				slugs/ft
8		0							
12		0.2	1.02	0.204	12.0	0.068	0.5	0.735	0.1
16		0.6	1.025	0.615	16.0	0.123		0.735	0.9
20	20.45	1.11	1.035	1.15	20.15	0.1625		0.74	3.06
22	22.6	1.48	1.04	1.54	22.30	0.189		0.74	5.5
24	25.0	1.92	1.06	2.04	24.40	0.222		0.74	9.4
26	27.15	2.50	1.07	2.68	26.50	0.262		0.74	16.6
28	29.5	3.25	1.085	3.53	28.66	0.316		0.745	29.0
30	31.9	4.20	1.115	4.68	30.80	0.378		0.745	50.9
32		5.48	1.15	6.30	33.02	0.466		0.745	92.3

For a *particular* draft y and corresponding value c the elevation of the water surface near the ship for increasing immersion is then obtained by projecting a line vertically upward through the point (c,y) until it intersects the ship profile at point (c,y'), as shown in Figure 17. Similarly, the depression of the wave surface due to decreasing immersion is obtained by projecting a line vertically downward through the point (c'',y) until it intersects the ship profile at point (c'', y'''). In general, the elevation and depression of the water surface may be so obtained for all drafts y.

To simplify the computation of the added mass per unit length, use was made of the fact that the point (c,y') corresponds both to the *elevation* of the water surface when the

draft is y and to the *depression* of the water surface when the draft is y''. That is, in Figure 17, y and y'' are corresponding particular values on the c and c'' curves, respectively. Therefore, the added masses per unit length at draft y for increasing immersion and at draft y'' for decreasing immersion (i.e., for $c'' = c$ at draft y) were simultaneously evaluated by considering the immersion to be at y'. For example, at Station 19 of Figure 9, the *same value of mass per* unit length, 200 slugs/ft, was computed for a draft of 25.4 ft when the immersion was increasing and for a draft of 29.2 ft when the immersion was decreasing.

The added mass per unit length at any section was evaluated by a procedure suggested by Prohaska.[13] In particular, for hollow sections, i.e., sections of marked concavity, and for a particular draft y, a line is drawn from the point (c,y') tangent to the profile below, as shown in Figure 17. The added mass coefficient $(C_V)_{y'}$ corresponding to the proper value of η and $2c/y'$ is then read from Figure 19.* $(C_V)_{y'}$ is called the virtual mass coefficient and depends on the form of the section. In Figure 19 the section area coefficient η of the section is the ratio of the area A of the underwater section to $2cy'$. These values are tabulated in Table 5,** along with the added mass per unit length, computed by Szebehely's (and also Prohaska's) formulas[12,13] as:

$$m = \frac{\pi}{2} \rho c^2 C_V \qquad [B4]$$

In general, $c = c$ or c''.

The resulting values of m for Station 20 are plotted in Figure 9 against both y and y''.

Thus m was first calculated and plotted for various immersions. This stored graphical information was then available for use (i.e., was read out) in the dynamic problem.

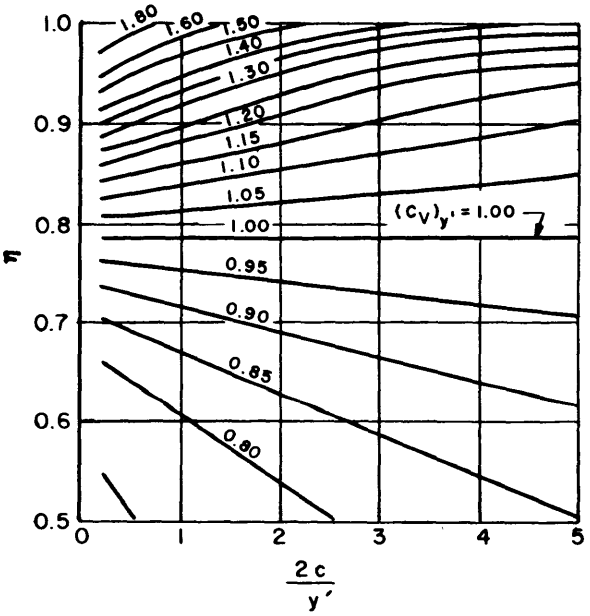

Figure 19 – Curves for Estimating Coefficient $(C_V)_{y'}$ for Use in Computation of Added Mass

*The curves of Figure 19 were taken from Figure 16 of Reference 13.

**Since the baseline lies 6 ft below the keel at Station 20, y' is replaced by $y' - 6$ for the computation at this station only.

APPENDIX C

PROCEDURE FOR OBTAINING WAVE PROFILE

The profile of the wave of encounter is determined from the photographs and data shown in Figures 3 and 4, respectively. Figure 3 shows a series of photographs of a destroyer in rough seas taken at known time intervals from two other ships steaming abreast, one to port and one to starboard. Figure 4 consists of time histories of the destroyer's heave acceleration, pitch, roll angle, and other data which comprehend the time period of the series of photographs.

In attempting to obtain directly a wave profile from Figures 3 and 4, the following obstacles are encountered:

1. The two-dimensionality of any single photograph does not permit good spatial perception. This coupled with the very low background contrast for a wave profile makes it impossible to trace a complete wave profile from any single photograph.

2. The series of photographs was taken from a moving platform at variable time intervals. Therefore, the determination of a continuous wave profile from a series of photographs requires compensation for the pitch of the platform (errors due to the heave and roll of the platform are negligible).

3. The wave profile is obscured by spray.

4. The wave surface is distorted by the passage of the ship and introduces an error that is impossible to eliminate. Probably this distortion and the resulting error are a minimum at those points where spray is absent. In particular, the intersection of the stem with the water surface is probably most dependable in view of the fineness of the bow.

To make tractable the problem of finding the shape of the wave, in view of the above difficulties, it has been deemed feasible to base the procedure for obtaining the wave profile upon the following assumption: There is a time-stationary cylindrical water surface profile which is propagated without distortion and with constant velocity throughout the period of the series of photographs. Reference axes are then established; points on the wave profile of all the photographs may be measured relative to these axes. In each photograph, these reference axes lie in a vertical plane containing the side of the ship. The intersection of this vertical "trace" plane with points on the wave profile which are unobscured by spray may be discerned in each photograph and marked off. The wave profile is traced through these points.

Using this concept gives the following details of the actual procedure used in obtaining the profile of Figure 20:

1. A *reference point* is established *on the ship.* It is located at the point of intersection of the line of the *G* deck (extended aft) with a transverse plane tangent to the utmost extremity of the cap of the forward smokestack; see Figure 21. This point, marked on the photographs,

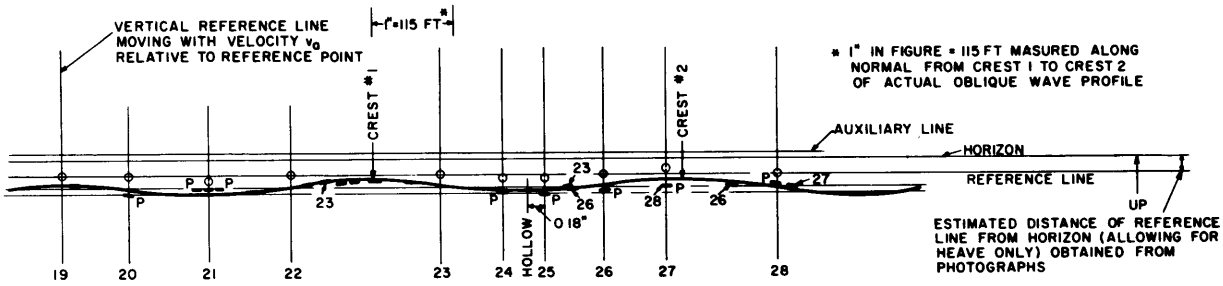

Figure 20 – Wave Surface 45-Degree Oblique Profile for Starboard Side

Scale: 1 in. = 115 ft
Crest 1 to Crest 2 = 3.6 in. on drawing = 414 ft
θ is the reference point
λ = 414 cos 45 deg = 293 ft (approximately 300 ft)

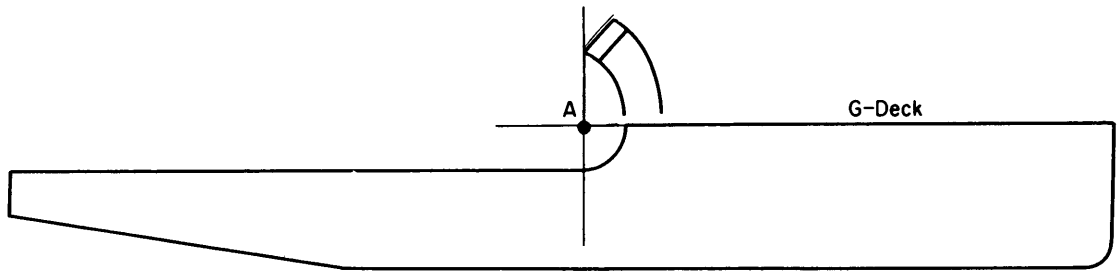

Figure 21 – Reference Point on Ship

Point *A* is intersection of vertical line tangent to aftmost point on smokestack and horizontal line which is an extension aft of *G*-deck.

is used to locate the horizontal and vertical reference lines in the trace plane of each photograph. These reference lines are necessary for "tracing" the whole wave profile.

The horizontal reference line passes through the reference point when the ship is on an even keel and at the position of zero heave. (The latter position is not absolutely determinable since no absolute reference is available. An arbitrary zero for heave is used.)

The vertical reference line is taken as the vertical line through the reference point on the ship in photograph 19 of Figure 3. This line is assumed to be moving with the wave profile.

2. Figure 1 shows that the apparent velocity of the ship along its heading with respect to the vertical reference line is

$$V_a = U + \frac{V_w}{\cos \theta_s}$$

where $V_w = \sqrt{\frac{g\lambda}{2\pi}}$ is the wave velocity in feet per second (see Equation [D16]),

λ is the wave length in feet,

U is the ship's speed in feet per second, and

$\theta_s = 45$ deg is the ship's heading in degrees.

From Figure 2 the period of encounter P is evidently

$$P = \frac{\lambda}{V_w + U \cos \theta_s} = \frac{\lambda}{\sqrt{\frac{g\lambda}{2\pi}} + U \cos \theta_s}$$

Hence

$$\lambda^2 - \left(\frac{P^2 g}{2\pi} + 2P\, U \cos \theta_s\right) \lambda + P^2 U^2 \cos \theta_s = 0$$

With $P = 5.25$ sec (estimated from the records of Figure 4),

$U = 28.71$ ft/sec,

$g = 32.2$ ft/sec^2, and

$\theta_s = 45$ deg,

the solution for λ of the above equation is $\lambda = 300$ ft (approximately). Then $V_w = 39.2$ ft/sec and $V_a = 84.14$ ft/sec.

3. The apparent velocity V_a and the time intervals between the photographs, which are read from the time scale of Figure 4, permit the longitudinal position of the reference point on the ship relative to the *moving* vertical reference line to be computed for each photograph. These positions were laid off on a *transparent overlay sheet*; see Figure 20. The *horizontal reference line* was also drawn, at arbitrary height, *on the overlay sheet.*

4. When the ship heaves, pitches, or rolls, the reference point on the ship will no longer lie on the horizontal reference line. The actual position of the reference point, relative to the horizontal reference line, is obtained by making corrections for the rigid-body motions; see Figure 20. The method for determining these corrections is now explained.

a. To correct for heave,* the heaving acceleration record is integrated twice. The resulting heaving velocity and displacement curves shown in Figures 7 and 5, respectively, require the determination of the:

(1) Line of zero acceleration. This is not marked on the record. An error results in the addition of a parabolic component to the heave displacement.

---

*By scaling the sketch of Figure 1 in Reference 23 and by using the plan of the shell and deck plating and inboard profile of the ship being analyzed, the heave meter was estimated to be 27.6 ft aft of the "reference point" used to determine the wave profile. From the plans, the reference point was found to be 15.91 ft forward of amidship.

(2) Line of zero velocity. This is an arbitrary constant of integration. An error results in a slope to the heave displacement curve.

(3) Line of zero heave displacement. This is an arbitrary constant of integration. An error is immaterial since it merely shifts the horizontal reference line up or down but does not affect the relative heights of the ship in the separate photographs.

To obtain the velocity and displacement curves of Figures 7 and 5, respectively, let us consider the curves of Figures 22a and 22b which show the final unfaired heave velocity and heave displacement curves and their corresponding baselines. These curves were obtained by first planimetering the original heave acceleration curve shown in Figure 4 and the resultant velocity curve about arbitrary baselines. The resultant heave displacement curve was then examined to determine the correction to be made to the acceleration and velocity baselines that would reduce the parabolic and slope components in the heave displacement curve. Several corrections and subsequent integrations were necessary before the heave displacement waveform was considered acceptable in the region for which the slamming forces were computed (t = 0–6 sec). In drawing the displacement curve, Figure 22b, no attempt was made to reproduce the high-frequency component associated with the whipping, since it is small in the second integral. For the same reason, it was decided to eliminate the whipping component of the heave velocity. This was done by recomputing the velocity by a numerical differentiation of the heave displacement. The results are shown in Figure 7. Figure 5 is identical with Figure 22b for computation time t = 0–6 sec.

b. To correct for pitch, the product of the distance from the accelerometer to the reference point on the ship (27.6 ft) and the pitch angle in radians is added to the uncorrected reference point, bow up pitch being taken as positive; see Figure 23. Note that the horizontal component of pitch displacement which corrects the horizontal position of the reference point is neglected. The value of this correction is negligible compared to the length of the wave along which it would correct.

c. The correction for roll is made on the assumption that the accelerometer is on the centerline of the ship. Reference points are taken port and starboard at one-half the beam off centerline. The height correction is computed as $\mp \frac{\text{beam}}{2}$ times the roll angle in radians, roll to starboard being taken as positive and the minus sign being used for the downward displacements of the reference point on the starboard side; see Figure 24.

The height of the reference point above or below the reference line, for each photograph time, is computed as the sum of the heave, pitch, and roll corrections.

5. The corrected height of the reference point on the ship for the time of each photograph is *laid off on the overlay sheet* along the appropriate vertical line. The overlay sheet is then superposed upon a photograph with its appropriate corrected "reference point" in coincidence with the corresponding one in the photograph. The horizontal reference line is then brought to the correct height by rotating the overlay sheet until the horizontal reference line is parallel to the horizon. This is accomplished with the aid of an auxiliary line drawn on the overlay sheet parallel to the horizontal reference line and at such a height above it as to fall nearly on the horizon.

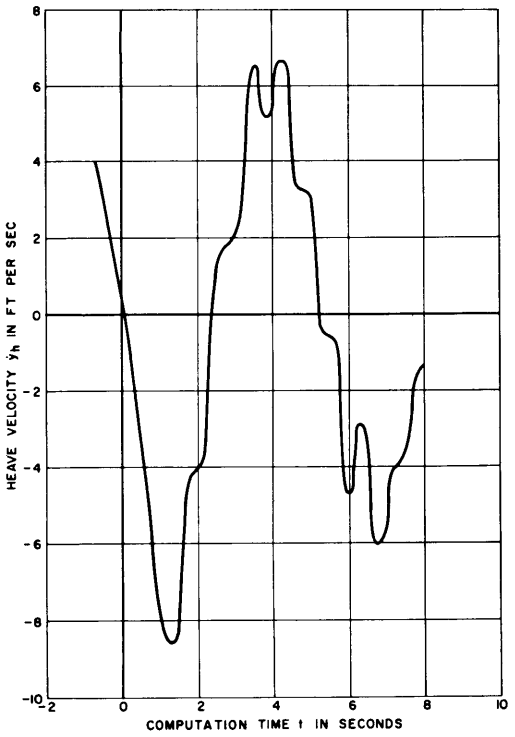

Figure 22a — Unfaired Heave Velocity Curve

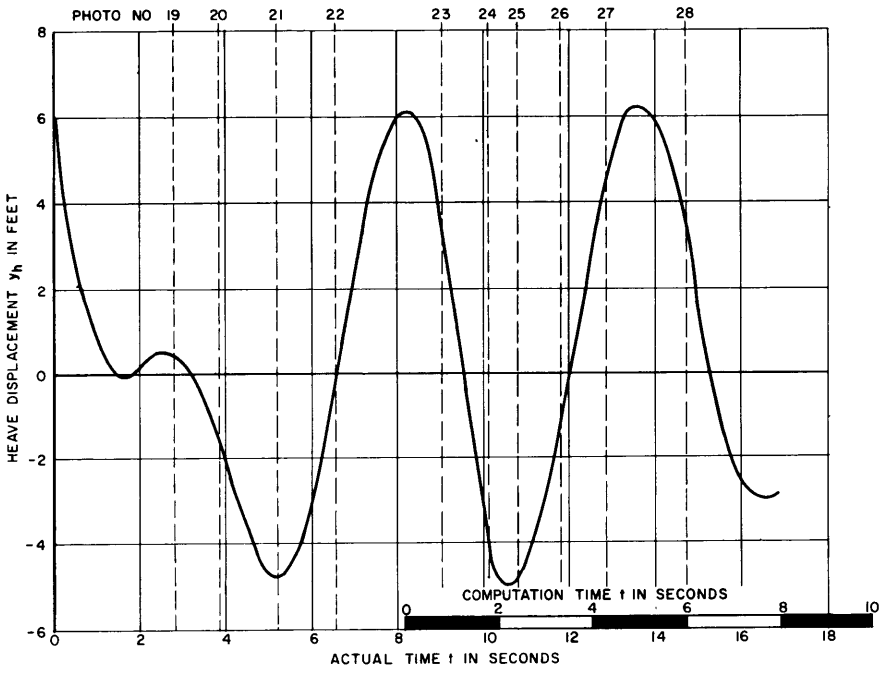

Figure 22b — Unfaired Heave Displacement Curve

Computation time zero seconds corresponds to 8.18 seconds of actual (recorded) time.

Figure 22 — Time History of Unfaired Heave Velocity and Displacement Curves

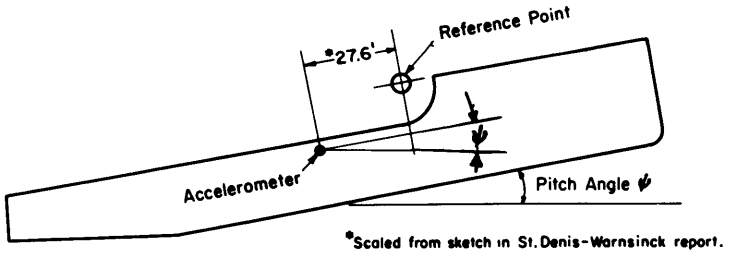

Figure 23a – Position of Reference Point and Accelerometer on Ship during Pitching Elevation of Bow

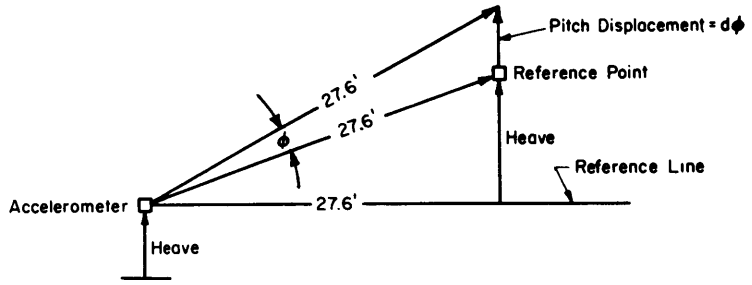

Figure 23b – Vector Relationships

Figure 23 – Pitched Ship and Vector Diagram Showing Correction for Pitch

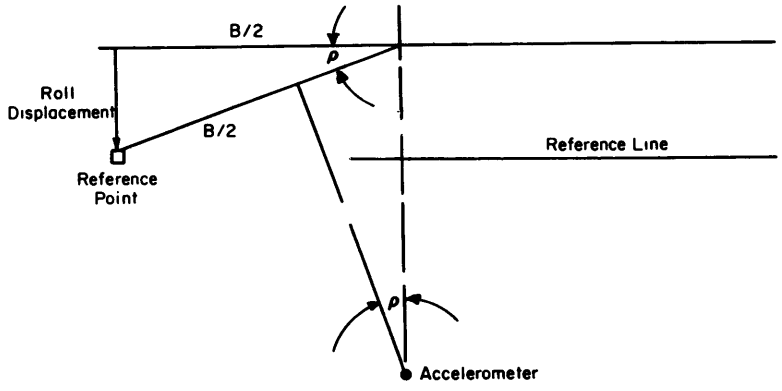

Figure 24 – Vector Diagram Showing Correction for Roll

$$\text{Roll displacement} = \mp \frac{B}{2} \rho$$

6. With the overlay sheet in position over a photograph, points of intersection of the ship's side with the wave profile that are truly discernible are marked off on the overlay sheet. The procedure is repeated for all the photographs, a separate overlay sheet being used for the port and starboard photographs because the scales are different. Points on the wave profile fall in their proper relative positions on the overlay, and the continuous wave profile may be drawn on the overlay by fairing through these various points. The wave profile traced for the starboard side is shown in Figure 20. From Figure 20, the length of the ship, the relative velocity, and the position of the reference point relative to the midship position, it was established that the water crest is amidship at $t = 8.18$ sec on the scale of time of the trial records (Figure 4). This time was then taken to be the zero of "computation" time.

7. The construction of the wave profile is such that, if the assumptions are correct, all the points should lie on a fair and continuous curve which is an oblique (45 deg) profile of the time-stationary cylindrical wave surface. The results for the starboard side are quite good. From Figure 20 a wave length of approximately 300 ft and a wave height of 14 ft were obtained. The resulting trace shows that a satisfactory approximation can be made to the wave profile at the time of the significant slam (about $t = 8.6$ sec or just before Photograph 23) by taking a regular wave of 300-ft length and 14-ft height; see Figure 20.

The results for the port side are incomplete; the whole of the wave crest into which the ship is entering at the time of slam is missing. These results are not shown. The computations in this report are based upon the foregoing dimensions.

8. The relative phase may be obtained by noting, from the wave profile on the overlay sheet, that the reference point is at a node before a crest in Photograph 26.

APPENDIX D

KINEMATICS OF FLUID PARTICLE MOTION

For the case of plane gravity waves in deep water, appropriate equations for y_w, u, v, and $\frac{\dot{v}}{g}$ are now derived; they are based upon kinematic relationships between fluid particles. For ease in readability, some fundamental classical relationships are reproduced first.

Consider the behavior of an inviscid, incompressible fluid vibrating under the action of gravity. Since the motion is irrotational, a velocity potential ϕ exists which must satisfy the Laplace equation

$$\frac{\partial^2 \phi}{\partial x^2} + \frac{\partial^2 \phi}{\partial y^2} = 0 \qquad [D1]$$

throughout the interior of the fluid. For a plane cylindrical wave, ϕ depends only on two spatial coordinates x and y. In Figure 25, the axes are at the undisturbed surface of the fluid and y is positive upward. The time dependence can also be included in the definition of the velocity potential ϕ since Equation [D1] defines the spatial but not the temporal behavior of ϕ. Therefore, if we assume that the wave is periodic (i.e., a sinusoid with angular velocity ω) and if we express the time dependence for a wave moving to the left in the form $e^{i\omega t}$, then one *possible* solution of Equation [D1] is[24,25]

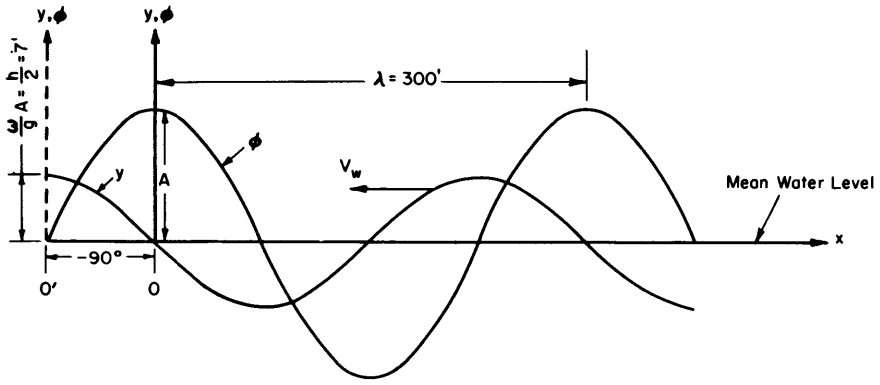

Figure 25 – Sign Convention for Sinusoidal Wave Propagating with Velocity V_w toward the Left

$$\phi(x, y, t) = \text{Re: } f(x - iy)\, e^{i\omega t} = \text{Re: } Ae^{K(ix+y)}\, e^{i\omega t} = \text{Re } Ae^{i(Kx+\omega t)}\, e^{+Ky} \qquad [D2]$$

where A, in general, is a complex quantity.

We note that the right member of Equation [D2] is also the solution in complex notation of the wave equation $\frac{\partial^2\phi}{\partial x^2} - \frac{1}{c^2}\frac{\partial^2\phi}{\partial t^2} = 0$, which has the same form as Equation [D1]. Therefore[24]

$$k = \frac{2\pi}{\lambda}\ ;\ \omega = \frac{2\pi}{\tau}$$

or

$$\frac{\omega}{k} = \frac{\lambda}{\tau} = V_w \qquad [D3]$$

where k is the wave number,

λ is the wave length,

τ is the period, and

V_w is the velocity of wave propagation.

If $-h'$ is the y-coordinate of the ground, then for infinitely deep water $ky = -\frac{2\pi h'}{\lambda} \to -\infty$, which satisfies Equation [D2].*

The equation of the surface profile can now be derived from Equation [D2] and the *generalization of Bernoulli's equation for* nonsteady motions, which relates the pressure p and the potential ϕ. Bernoulli's equation is

$$\frac{-\partial\phi}{\partial t} + \frac{1}{2}(\nabla\phi)^2 + \frac{1}{\rho}(p + U') = c(t) \qquad [D4]$$

In Equation [D4] let the atmospheric pressure $p = 0$ define the condition for the free surface. The quadratic term $(\nabla\phi)^2$ can be neglected, since the velocity of the water particles is small (i.e., A is small) and the fluid density ρ is a constant because the fluid is incompressible. Also the gravity potential per unit of volume taken at the surface is $U' = \rho g y$, and the only function of time which will not destroy the periodicity and uniform advancement of the wave is $c(t) = 0$. With these conditions, Equation [D4] simplifies to

$$\frac{\partial\phi}{\partial t} = gy \qquad [D5]$$

*Another possible solution of Equation [D1] $\phi = \text{Re: } f(x+iy) = \text{Re: } Ae^{i(kx+\omega t)}\, e^{-ky}$ would not be usable, since an infinite value of ϕ would be obtained at the ground.

Let $y = y_w(x, t)$ be the equation of the surface profile. Then from Equation [D5] it is apparent that y_w will have the form of a progressive wave similar to the one set up for ϕ. That is,

$$y_w = ae^{i(kx+\omega t)} \qquad [D6]$$

where a is, in general, complex since it includes the amplitude and phase of the surface function. Like A it is a small quantity.

Substitution of Equations [D2] and [D6] into Equation [D5] yields

$$i\omega Ae^{ky_w} = ga \qquad [D7]$$

Upon expanding e^{ky_w} in powers of ky_w and neglecting Ay_w, Ay_w^2, etc., as small quantities of higher order, Equation [D7] becomes*

$$i\omega A = ga \qquad [D8]$$

which gives the relationship between A and a. If A is chosen real, then a is a pure imaginary. Now writing Equations [D2] and [D6] in real form we have

$$\phi = A \cos(kx+\omega t)\, e^{+ky} \qquad [D9]$$

$$y_w = -\frac{\omega}{g} A \sin(kx+\omega t) \qquad [D10]$$

Where for mathematical convenience y and y_w are used interchangeably.

It is evident that A determines the amplitude of the wave for $y = 0$ and that both A and the circular frequency ω depend upon the particular form of the excitation. In Equations [D9] and [D10] the wave number k is related to ω (so far) only by the ratio given in Equation [D3]. Since λ is unknown, $V_w = \sqrt{\frac{g\lambda}{2\pi}}$ is unknown. Therefore, a direct relation between k and ω is desired. It can be obtained by stipulating a further kinematic condition that *the motion of the surface must coincide with the motion of those fluid particles that happen to be at the surface at this time*. Then the normal component $(V_s)_n$ of the velocity of the surface V_s is equal to the normal component v_n of the particle velocity v at the surface; that is,

*That is, the exponential variation of the wave form with depth is ignored.

$$(V_s)_n = v_n = -\frac{\partial \phi}{\partial n} \qquad [D11]$$

But for a wave sufficiently flat (i.e., A small), $\frac{\partial \phi}{\partial n} \approx \frac{\partial \phi}{\partial y}$ and $(V_s)_n \approx \frac{\partial (y_w)}{\partial t}$, the "sinking speed" of the surface. With these approximations, Equation [D11] becomes

$$\frac{\partial (y_w)}{\partial t} = -\frac{\partial \phi}{\partial y} \qquad [D12]$$

Substituting Equations [D6] and [D1] into Equation [D12], we obtain (ignoring products Ay_w, Ay_w^2, etc., after the differentiation $-\frac{\partial \phi}{\partial y}$ is performed)

$$-i\omega a = kA \qquad [D13]$$

Equations [D8] and [D13] yield the relation between k and ω, namely

$$\frac{A}{a} = \frac{g}{i\omega} = -\frac{i\omega}{k} \qquad [D14]$$

or

$$\omega^2 = gk \qquad [D15]$$

Also

$$V_w^2 = \frac{\omega^2}{k^2} = \frac{g}{k} = \frac{g\lambda}{2\pi} \; ; \; V_w = \sqrt{\frac{g\lambda}{2\pi}} \qquad [D16]$$

Now let the reference frame defined by the coordinate axes x-y move with the wave so that the origin is always a crest. This second reference frame, with origin at $0'$ is obtained by translating the original y-axis 90 deg to the left; see Figure 25. Since now Equations [D9] and [D10] are no longer time-dependent, the velocity potential and surface profile become

$$\phi = Ae^{ky} \cos (kx - 90°) = Ae^{ky} \sin kx \qquad [D17]$$

$$y_w = -\frac{\omega}{g} A \sin (kx - 90°) = \frac{\omega}{g} A \cos kx \qquad [D18]$$

but

$$A = -\frac{ia\omega}{k} = -iaV_w; \; \frac{\omega A}{g} = \frac{k}{\omega} A = -ia = \frac{h}{2} \; ; \; k = \frac{2\pi}{\lambda}$$

where h is the wave height.

Therefore

$$\phi = \frac{h}{2} V_w e^{\frac{2\pi y}{\lambda}} \sin \frac{2\pi x}{\lambda} \qquad [D19]$$

$$y_w = \frac{h}{2} \cos \frac{2\pi x}{\lambda} \qquad [D20]$$

The fluid particle velocity components u and v in the x- and y-directions are obtained with respect to a *new (third) reference frame fixed in space** which is coincident with the above moving x-y coordinate system at a particular instant $t = 0$. These components are

$$u = -\frac{\partial \phi}{\partial x} = -\frac{h}{2} \cdot \frac{2\pi}{\lambda} V_w e^{\frac{2\pi}{\lambda} y} \cos \frac{2\pi x}{\lambda} \qquad [D21]$$

$$v = -\frac{\partial \phi}{\partial y} = -\frac{h}{2} \cdot \frac{2\pi}{\lambda} V_w e^{\frac{2\pi}{\lambda} y} \sin \frac{2\pi x}{\lambda} \qquad [D22]$$

If the exponential variation of u and v with respect to depth is ignored, i.e., u and v are considered independent of depth,

$$u = -\frac{h}{2} \cdot \frac{2\pi}{\lambda} V_w \cos \frac{2\pi x}{\lambda} \qquad [D23]$$

$$v = -\frac{h}{2} \cdot \frac{2\pi}{\lambda} V_w \sin \frac{2\pi x}{\lambda} \qquad [D24]$$

We now designate $t = 0$ as the time that a particular particle is under the crest of the wave which lies above the origin. The horizontal displacement of that particle at any time t with respect to the third reference frame fixed in space is $x = V_w t$. Hence, from Equation [D24] the vertical velocity of that particle which is also the velocity of any point on the surface profile is

$$v = \dot{y}_w = -\frac{h}{2} \cdot \frac{2\pi}{\lambda} V_w \sin \frac{2\pi}{\lambda} V_w t \qquad [D25]$$

*The fixed reference axes will also be designated by x- and y-coordinates for convenience.

The vertical acceleration is*

$$\dot{v} = -\frac{h}{2}\left(\frac{2\pi}{\lambda} V_w\right)^2 \cos\frac{2\pi x}{\lambda} \qquad [D26]$$

since

$$\lambda = 300 \text{ ft}$$
$$h = 14 \text{ ft}$$

then

$$V_w = \sqrt{\frac{g\lambda}{2\pi}} = 39.209 \text{ ft/sec}$$

and

$$\frac{h}{2} \cdot \frac{2\pi}{\lambda} V_w = \frac{h}{2}\sqrt{\frac{2\pi g}{\lambda}} = 5.74 \text{ ft/sec}$$

and

$$\frac{1}{g} \cdot \frac{h}{2}\left(\frac{2\pi}{\lambda} V_w\right)^2 = \frac{h}{2} \cdot \frac{2\pi}{\lambda} = 0.1466$$

---

*More accurate computations for $\dot{v}$ are obtained if its derivation is based upon the equations for u and v which include an exponential variation of these variables with depth. The expressions for u and v including time dependence are then (see Equations [D21] and [D22]:)

$$u = -\frac{\partial\phi}{\partial x} = -\frac{h}{2} k V_w e^{ky} \cos(kx+\omega t)$$

$$v = -\frac{\partial\phi}{\partial y} = -\frac{h}{2} k V_w e^{ky} \sin(kx+\omega t)$$

where

$$k = \frac{2\pi}{\lambda} = \frac{\omega}{V_w}$$

since

$$v = v(x, y, t)$$

$$\dot{v} = \frac{dv}{dt} = \frac{\partial v}{\partial t} + u\frac{\partial v}{\partial x} + v\frac{\partial v}{\partial y}$$

Substitution of the equations for u and v and its partial time and two-dimensional space derivatives into the latter equation yields

$$\dot{v} = -\frac{h}{2}(kV_w)^2 e^{ky}\left[\cos(kx+\omega t) - \frac{h}{2} k e^{ky}\right]$$

and at the mean waterline, ignoring time variations,

$$(\dot{v})_{y=0} = -\frac{h}{2}(kV_w)^2\left[\cos kx - \frac{hk}{2}\right] = -0.1466\, g\,[\cos\theta - 0.1466]$$

Actually $\dot{v}$, at all points at which particles are in contact with hull, should be used, but the additional computational complexity does not warrant the relatively small increase in accuracy of the complete expression for buoyancy force.

For convenience write $\theta = \frac{2\pi x}{\lambda} = kx$

The results obtained for y_w, u, v, and $\frac{\dot{v}}{g}$ are

$$y_w = 7 \cos \theta, \text{ ft} \qquad [D27]$$

$$u = -5.74 \cos \theta, \text{ ft/sec} \qquad [D28]$$

$$v = -5.74 \sin \theta, \text{ ft/sec} \qquad [D29]$$

$$\frac{\dot{v}}{g} = -0.1466 \cos \theta \qquad [D30]$$

For use in Appendix A, it is convenient at this point to find the path of a particular particle disturbed by wave motion. Let η and ξ now represent the vertical and horizontal displacements, respectively, from the rest position of a particle at arbitrary depth y. Then for an x-y coordinate system *fixed in space* with y positive upward

$$\xi = x' - x; \; \eta = y' - y \qquad [D31]$$

where x and y are the particle coordinates of the particle at rest and x' and y', the particle coordinates of the particle disturbed by wave motion. The components of the particle velocity obtained by differentiating Equation [D9] with respect to x and y, respectively, are*

$$u = \dot{\xi} = -\frac{\partial \phi}{\partial x} = +Ak \sin (kx + \omega t) \cdot e^{ky} \qquad [D32]$$

$$v = \dot{\eta} = -\frac{\partial \phi}{\partial y} = -Ak \cos (kx + \omega t) \cdot e^{ky} \qquad [D33]$$

Integration of these equations with respect to t gives

$$\xi = -\frac{AK}{\omega} e^{ky} \cos (kx + \omega t) \qquad [D34]$$

*More exactly, ϕ should be differentiated with respect to the variable coordinates x' and y'; also Equations [D32] and [D33] should contain $x' = x + \xi$, $y' = y + \eta$ rather than x, and y. However, the difference would be of second order in ξ, η and is therefore neglected.

$$\eta = -\frac{AK}{\omega} e^{ky} \sin(kx + \omega t) \qquad [D35]$$

Hence, we obtain

$$\xi^2 + \eta^2 = \left[\frac{Ak}{\omega} e^{\frac{2\pi}{\lambda} y}\right]^2 = \left[\frac{h}{2} e^{\frac{2\pi}{\lambda} y}\right]^2 \qquad [D36]$$

Equation [D36] defines the path of any particle at depth y as a circle with a radius $\frac{h}{2} e^{\frac{2\pi}{\lambda} y}$;

The radii of the circles decrease rapidly and in an exponential manner as the depth increases. Note also that

$$u^2 + v^2 = (Ak)^2 = \left(\frac{h}{2} \omega\right)^2 \qquad [D37]$$

where h = 14 ft and $\omega \approx \frac{2\pi}{0.9}$ = 6.98 radians/sec (see Section 7, first paragraph).

APPENDIX E

METHOD FOR LOCATING EACH STATION ON THE WAVE AT REGULAR TIME INTERVALS

To reduce the number of computations, a formula for $\theta = kx = \frac{2\pi x}{\lambda}$ is derived which makes the computed and tabulated values of θ at any station, as a function of time, repeat themselves at all other stations but at later or earlier times. For example, Table 6 shows that the tabulated values of θ for Stations 19 and 20, which were calculated from the formula for θ derived below, are the same but are displaced in time an amount $2\Delta t = 0.2192$ sec, where $\Delta t = 0.1096$ sec is a regularly spaced time interval.

From Section 5, the zero of "computation" time is taken at the instant when the wave crest is amidships. Therefore, consider an x-y axis invariant with respect to the wave, and Station 10, corresponding to $\xi = 0$, to be at the crest of the wave, where $x = 0$ at time $t = 0$.* To locate the nth station on the wave,** we first note that the velocity of Station 10 in the x-direction relative to the y-axis is $(V_w + U \cos \theta_s)$. Then the x-coordinate of Station 10 at any time t is

$$x_{10} = (V_w + U \cos \theta_s)\, t$$

and for the nth station

$$x_n = (V_w + U \cos \theta_s)\, t + \xi_n \cos \theta_s$$

From Appendix D, $\theta_n = \frac{2\pi x_n}{\lambda}$ thus

$$\theta_n = \frac{2\pi}{\lambda} [(V_w + U \cos \theta_s)\, t + \xi_n \cos \theta_s]$$

The station designation measured with respect to Station 10 is $n - 10$; $\frac{l}{20}$ is the distance between stations equal to the section length Δx. Therefore the distance from Station 10 to Station n is

$$\xi_n = \frac{l}{20}(n - 10)$$

---

*Thus Crest 1 in Figure 1 is located at the centerline of the ship ($\xi = 0$) at $t = 0$.

**n = 0, 10, 20 at the after, midship, and forward perpendiculars, respectively.

TABLE 6

Tabulation of θ for Stations 19 and 20

t sec	θ_{20}	θ_{19}	t sec	θ_{20}	θ_{19}
0	2.7320	2.4588	3.2880	6.8300	6.5568
0.1096	2.8686	2.5954	3.3976	6.9666	6.6934
0.2192	3.0052	2.7320	3.5072	7.1032	6.8300
0.3288	3.1418	2.8686	3.6188	7.2398	6.9666
0.4384	3.2784	3.0052	3.7264	7.3764	7.1032
0.5480	3.4150	3.1418	3.8360	7.5130	7.2398
0.6576	3.5516	3.2784	3.9456	7.6496	7.3764
0.7672	3.6882	3.4150	4.0552	7.7862	7.5130
0.8768	3.8248	3.5516	4.1648	7.9228	7.6496
0.9864	3.9614	3.6882	4.2744	8.0594	7.7862
1.0960	4.0980	3.8248	4.3840	8.1960	7.9228
1.2056	4.2346	3.9614	4.4936	8.3326	8.0594
1.3152	4.3712	4.0980	4.6032	8.4692	8.1960
1.4248	4.5076	4.2346	4.7128	8.6058	8.3326
1.5344	4.6444	4.3712	4.8224	8.7424	8.4692
1.6440	4.7810	4.5076	4.9320	8.8790	8.6058
1.7536	4.9176	4.6444	5.0416	9.0156	8.7424
1.8632	5.0542	4.7810	5.1512	9.1522	8.8790
1.9728	5.1908	4.9176	5.2608	9.2888	9.0156
2.0824	5.3274	5.0542	5.3704	9.4254	9.1522
2.1920	5.4640	5.1908	5.4800	9.5620	9.2888
2.3016	5.6006	5.3274	5.5896	9.6986	9.4254
2.4112	5.7372	5.4640			
2.5208	5.8738	5.6006			
2.6304	6.0104	5.7372			
2.7400	6.1470	5.8738			
2.8496	6.2836	6.0104			
2.9592	6.4202	6.1470			
3.0688	6.5568	6.2836			
3.1784	6.6934	6.4202			

Since the computations are made for regularly spaced stations on the ship designated by numbers $n = 0, 1, 2 \ldots 20$ from the after perpendicular, it is convenient to write

$$\theta_n = \frac{2\pi}{\lambda}\left[(V_w + U\cos\theta_s)\,t + \frac{l}{20}(n-10)\cos\theta_s\right]$$

It is convenient to make computations of θ for regular time intervals Δt and to make the values of θ for any station n at regular times t_1, $2t_1$, $3t_1$ ... repeat themselves at adjacent stations at succeeding regular times $t_1 + K\Delta t$; $2t_1 + K\Delta t$; $3t_1 + K\Delta t$ (see table 6); here $K = \frac{t}{\Delta t}$ is the number of regular time intervals which separate the repetitive values of θ at any two stations. To achieve this let

$$(V_w + U\cos\theta_s)t + \frac{l}{20}(n-10)\cos\theta_s = (V_w + U\cos\theta_s)(t + K\Delta t) + \frac{l}{20}[(n-1)-10]\cos\theta_s$$

from which

$$\Delta t = \frac{\frac{l}{20}\cos\theta_s}{K(V_w + U\cos\theta_s)}$$

In this problem

$$\begin{aligned}\theta_s &= 45 \text{ deg}\\ l &= 369 \text{ ft}\\ V_w &= 39.21 \text{ ft/sec}\\ U &= 28.71 \text{ ft/sec}\end{aligned}$$

and $K = 2$ was arbitrarily chosen since the value

$$\Delta t = \frac{369 \times 0.70711}{40\,(39.21 + 28.71 \times 0.70711)} = 0.1096 \text{ sec}$$

was found to be a satisfactory interval for use in the calculation.

The formula for θ_n then becomes

$$\theta_n = 0.1366\,\frac{t}{0.1096} + 0.2732\,n - 2.732$$

θ_n is tabulated in column 3 of Table 1 and Column 1 of Table 3 for increments of 0.1096 sec.

APPENDIX F

DIFFERENTIAL AND FINITE-DIFFERENCE EQUATIONS FOR OBTAINING RESPONSE OF SHIP TO SLAMMING FORCES

The differential and finite-difference equations used to obtain the transient response of a ship to slamming forces are derived in this appendix, and a method for computing the forces on a ship by means of a digital computer, rather than manually as was done in this report, is described. This method is presently being coded by the Applied Mathematics Laboratory of the David Taylor Model Basin. For further details on the differential and finite-difference equations and the method for evaluating the parameters used in these equations, see Reference 5.

F1. DIFFERENTIAL EQUATIONS

The damped vertical response of a ship's hull of length l, i.e., $0 \leq x \leq l$, assumed to act like a free-free nonuniform beam, to transient forces can be calculated by solving the following system of partial differential equations:[14,26]

$$\mu \frac{\partial^2 \bar{y}}{\partial t} + c \frac{\partial \bar{y}}{\partial t} + \frac{\partial V}{\partial x} = \bar{P}(x,t) \qquad [F1]$$

$$M = EI \frac{\partial \gamma}{\partial x} \qquad [F2]$$

$$I_{\mu z} \frac{\partial^2 \gamma}{\partial t^2} + V - \frac{\partial M}{\partial x} = 0 \qquad [F3]$$

$$V = (KAG)\gamma - (KAG) \frac{\partial \bar{y}}{\partial x} \qquad [F4]$$

where for present and future use we define:*

t Time; sec

x Distance coordinate along longitudinal centerline axis of ship's hull; the independent variable x as used in the equations lies along the same axis as ξ, hence $dx = d\xi$ and $\frac{\partial}{\partial x} = \frac{\partial}{\partial \xi}$. Note, however, that this is not the same x used in Figure 1 and other parts of the text where x is normal to the wavefront; ft

*For more complete definitions, see Reference 5.

$\bar{y}$ Total vertical displacement of point of beam (hull) initially on x-axis, i.e., displacement of point from equilibrium position in still water; ft

y_ϵ Elastic (flexural) component of $\bar{y}$; ft

γ Rotation of transverse section of hull about an axis through the section normal to the x-y plane; radians

M Bending moment; ft-tons

V Net shear force in y-direction; tons

μ Apparent mass per unit length including allowance for virtual mass of surrounding water; $\frac{\text{ton-sec}^2}{\text{ft}^2}$

c Damping force per unit velocity per unit length; $\frac{\text{ton-sec}}{\text{ft}^2}$

$\bar{P}$ Total force per unit length acting upon ship's hull; tons/ft

$I_{\mu z}$ Mass moment of inertia of hull per unit length with respect to an axis normal to the x-y plane; ton-sec^2

EI Bending rigidity; ton-ft^2

KAG Shear rigidity; tons

y Vertical component of displacement of point on hull due to flexure; ft

$W = m_s g$ Gravity load per unit length where m_s is the ship mass per unit length; tons/ft

For convenience in solving for the variables, these partial differential equations are rewritten as*

---

*To include the elastic (i.e., flexural) component of the hydrodynamic force in a manner convenient for computation by a digital computer, Equation [F1] was modified to Equation [F6] by means of the following derivation:

Newton's law for a differential section of the ship yields $m_s \frac{\partial^2 \bar{y}}{\partial t^2}$ = sum of rigid-body and flexural hydrodynamic forces on hull section $-\frac{\partial V}{\partial x} - c\frac{\partial \bar{y}}{\partial t} - W = \frac{d}{dt}\left[m\left(\dot{y}_v - \frac{\partial y_\epsilon}{\partial t}\right)\right] + (g+\dot{v})\rho A - \frac{\partial V}{\partial x} - c\frac{\partial \bar{y}}{\partial t} - W$. Substituting $\bar{y} = y_h + y_p + y_\epsilon$ gives: $m_s \frac{\partial \dot{y}_\epsilon}{\partial t} + \frac{d}{dt}(m\dot{y}_\epsilon) = -m_s\left(\frac{\partial \dot{y}_h}{\partial t} + \frac{\partial \dot{y}_p}{\partial t}\right) + \frac{d}{dt}(m\dot{y}_r) + (g+\dot{v})\rho A - \frac{\partial V}{\partial x} - c\frac{\partial}{\partial t}(y_\epsilon + y_p + y_h) - W.$

When the total derivative is written in terms of partial derivatives, the left member becomes

$$m_s \frac{\partial \dot{y}_\epsilon}{\partial t} + m\frac{\partial \dot{y}_\epsilon}{\partial t} + \left[\dot{y}_\epsilon \frac{\partial m}{\partial t} + \frac{\partial}{\partial x}(m\dot{y}_\epsilon)\frac{dx}{dt}\right]$$

hence,

$$(m_s+m)\frac{\partial \dot{y}_\epsilon}{\partial t} = -\left[\dot{y}_\epsilon \frac{\partial m}{\partial t} + m\frac{\partial \dot{y}_\epsilon}{\partial x}\frac{dx}{dt} + \dot{y}_\epsilon \frac{\partial m}{\partial x}\frac{dx}{dt}\right] - m_s\left(\frac{\partial \dot{y}_h}{\partial t} + \frac{\partial \dot{y}_p}{\partial t}\right)$$
$$+ \frac{d}{dt}(m\dot{y}_r) + (g+\dot{v})\rho A - \frac{\partial V}{\partial x} - c\frac{\partial y_\epsilon}{\partial t} - c\left(\frac{\partial y_h}{\partial t} + \frac{\partial y_p}{\partial t}\right) - W$$

[Footnote continued on bottom of page 67]

$$\frac{\partial y_\epsilon}{\partial t} = \dot{y}_\epsilon \qquad \text{[F5]}$$

$$\mu \frac{\partial \dot{y}_\epsilon}{\partial t} + \bar{c}\, \dot{y}_\epsilon + m \frac{dx}{dt} \frac{\partial \dot{y}_\epsilon}{\partial x} + \frac{\partial V}{\partial x} = \bar{P} \qquad \text{[F6]}$$

$$\frac{1}{EI} \frac{\partial m}{\partial t} - \frac{\partial \dot{\gamma}}{\partial x} = 0 \qquad \text{[F7]}$$

$$I_{\mu z} \frac{\partial \gamma}{\partial t} - \frac{\partial m}{\partial x} + V = 0 \qquad \text{[F8]}$$

$$\frac{1}{KAG} \frac{\partial V}{\partial t} + \frac{\partial \dot{\bar{y}}}{\partial x} - \dot{\gamma} = 0 \qquad \text{[F9]}$$

Since

$$\dot{\bar{y}} = \dot{y}_\epsilon + \dot{y}_h + \dot{y}_p$$

then

$$\frac{\partial \dot{\bar{y}}}{\partial x} = \frac{\partial \dot{y}_\epsilon}{\partial x} + \frac{\partial \dot{y}_h}{\partial x} + \frac{\partial \dot{y}_p}{\partial x}$$

and since

$$\frac{\partial \dot{y}_p}{\partial x} = \dot{\psi}; \quad \frac{\partial \dot{y}_h}{\partial x} = 0$$

Equation [F9] can be rewritten as

$$\frac{1}{KAG} \frac{\partial V}{\partial t} + \frac{\partial \dot{y}_\epsilon}{\partial x} - \dot{\gamma} = -\dot{\psi} \qquad \text{[F9]}'$$

Moreover, the rigid-body motions $\dot{y}_p$, $\dot{y}_h$, and $\dot{\psi}$ can be determined by means of the

---

[Footnote continued]

Defining

$$\mu = m_s(x, t) + m(x)$$

$$\bar{c} = c + \frac{\partial m}{\partial t} + \frac{\partial m}{\partial x} \frac{dx}{dt}$$

$$\bar{P}_e(x, t) = \frac{d}{dt}(m\dot{y}_r) + (g + \dot{v})\rho A - W$$

$$\bar{P} = \bar{P}_e(x, t) - m_s \left(\frac{\partial y_h}{\partial t} + \frac{\partial y_p}{\partial t} \right) - c \left(\frac{\partial y_h}{\partial t} + \frac{\partial y_p}{\partial t} \right)$$

gives Equation [F6]. Equation]F7] is obtained by differentiating Equation [F2]

following equations if $m_s(x)$, $\bar{P}_e(x, t)$, $\dot{y}_h(0)$, and $\dot{\psi}(0)$ are known.*

$$x_{c.g.} = \frac{\int_0^l m_s x dx}{\int_0^l m_s dx} \qquad [F10]$$

$$\dot{y}_p(x, t) = \dot{\psi}(x - x_{c.g.}) \qquad [F11a]$$

where

$$\frac{\partial \dot{y}_p(x, t)}{\partial t} = \ddot{\psi}(x - x_{c.g.}) \qquad [F11b]$$

$$\dot{y}_h(t) = \int_0^t \ddot{y}_h(t)\, dt + \dot{y}_h(0) \qquad [F12a]$$

where

$$\frac{d\dot{y}_h(t)}{dt} = \frac{\int_0^l \bar{P}_e\, dx}{\int_0^l m_s\, dx} \qquad [F12b]$$

$$\dot{\psi}(t) = \int_0^t \ddot{\psi}(t)\, dt + \dot{\psi}(0) \qquad [F13a]$$

where

$$\ddot{\psi}(t) = \frac{\int_0^l \bar{P}_e (x - x_{c.g.})\, dx}{\int_0^l m_s (x - x_{c.g.})^2\, dx} \qquad [F13b]$$

Thus given c, m, $\frac{dx}{dt}$, and $\bar{P}_e$ as functions of x and t, and m_s as a function of x, as well as $\dot{\psi}(0)$, $\dot{y}_h(0)$, we can compute $\bar{P}(x, t)$ and $\bar{c}(x, t)$; note that $\bar{P}_e$ constitutes numerical terms which are entirely predetermined from the analyses of the *oscillograph*, whereas the remaining terms in $\bar{P}(x, t)$ associated with rigid-body motions, as well as other variables, are determined by the differential equations, as will be explained presently.

---

*For the present problem $x_{c.g.} = \frac{l}{2} - 11.69$ (the position of the heave meter being 11.69 ft aft of the midship position). Hence $x_{c.g.} = (18.439)(10) - 11.69 = 172.7$ ft.

In working with Equation [F6], it proves convenient to eliminate $\frac{\partial \dot{y}_{\epsilon}}{\partial x}$ by using Equation [F9]'. Thus the system of equations to be actually solved will have the form:

$$\frac{\partial y_{\epsilon}(x,t)}{\partial t} = \dot{y}_{\epsilon}(x,t) \qquad \text{[F14]}$$

$$\mu(x,t)\frac{\partial \dot{y}_{\epsilon}(x,t)}{\partial t} + \bar{c}(x,t)\dot{y}_{\epsilon}(x,t) + m(x,t)\frac{dx(x,t)}{dt}\left[\dot{\gamma}(x,t) - \frac{1}{KAG(x)}\frac{\partial V(x,t)}{\partial t}\right]$$

$$+ \frac{\partial V(x,t)}{\partial x} = \bar{P}(x,t) + m(x,t)\frac{dx(x,t)}{dt}\dot{\psi}(t) \qquad \text{[F15]}$$

$$\frac{1}{EI(x)}\frac{\partial M(x,t)}{\partial t} - \frac{\partial \dot{\gamma}(x,t)}{\partial x} = 0 \qquad \text{[F16]}$$

$$I_{\mu z}(x)\frac{\partial \dot{\gamma}(x,t)}{\partial t} - \frac{\partial M(x,t)}{\partial x} + V(x,t) = 0 \qquad \text{[F17]}$$

$$\frac{1}{KAG}\frac{\partial V(x,t)}{\partial t} + \frac{\partial \dot{y}_{\epsilon}(x,t)}{\partial x} - \dot{\gamma}(x,t) = -\dot{\psi}(t) \qquad \text{[F18]}$$

In these equations, the following restrictions are imposed:

$$I_{\mu z}(x) \geq 0$$

$$\frac{1}{KAG(x)} \geq 0$$

$$\mu(x,t) > 0$$

$$\frac{1}{EI(x)} > 0$$

The ship is assumed to have free ends. Therefore, the end (boundary) conditions imposed for *all times t* are:

$$V(0,t) \equiv V(l,t) \equiv M(0,t) \equiv M(l,t) \equiv 0 \qquad \text{[F19]}$$

This is equivalent to $V = \frac{d\dot{\gamma}}{dx} = 0$ at $x = 0$, and $x = l$ for all times.

The initial conditions required are:

$$y_\epsilon(x,0);\ \dot{y}_\epsilon(x,0);\ \dot{\gamma}(x,0);\ M(x,0);\ V(x,0)$$

The initial conditions actually supplied are

$$y_\epsilon(x,0);\ \dot{y}_\epsilon(x,0);\ \gamma(x,0);\ \dot{\gamma}(x,0)$$

Then the required $M(x, 0)$ and $V(x, 0)$ are obtained by using

$$M(x,0) = EI(x)\ \frac{\partial \gamma(x,0)}{\partial x} \qquad \text{[F20]}$$

$$V(x,0) \approx \frac{\partial M(x,0)}{\partial x} \qquad \text{[F21]}$$

In addition to end conditions and initial conditions, the following quantities are supplied:

$$m(x,t);\ c(x,t);\ \frac{dx(x,t)}{dt};\ P_e(x,t) = \frac{d}{dt}(m\dot{y}_r) + (g+\dot{v})\rho A;\ m_s(x);\ \frac{1}{KAG(x)};\ \frac{1}{EI(x)};\ I_{\mu z}(x);$$

$$\dot{\psi}(0);\ \dot{y}_h(0)$$

These quantities furnish all the coefficients required in Equations [F16] and [F17] directly. In addition to coefficients given directly by these quantities, Equation [F18] has a quantity $\dot{\psi}(t)$, while Equation [F15] has coefficients $\mu(x, t)$, $\bar{c}(x, t)$, and $\bar{P}(x, t)$ as well as a quantity $\dot{\psi}(t)$. These can all be computed by using the above quantities and the relations just given. First, $\mu(x, t)$ and $\bar{c}(x, t)$ are given by

$$\mu(x,t) = m(x,t) + m_s(x)$$

$$\bar{c}(x,t) = c(x,t) + \frac{\partial m(x,t)}{\partial t} + \frac{\partial m(x,t)}{\partial x}\ \frac{\partial x(x,t)}{\partial t}$$

Then $\dot{\psi}(t)$ is obtained by using Equations [F10], [F13], and

$$\bar{P}_e(x,t) = P_e(x,t) - g m_s(x)$$

where

$$P_e(x, t) = \frac{d}{dt}(m\dot{y}_r) + (g+\dot{v})\,\rho A$$

$$\bar{P}(x, t) = \bar{P}_e(x, t) - m_s\left(\frac{\partial y_p(x, t)}{\partial t} + \frac{d\dot{y}_h(t)}{dt}\right) - c(x, t)\left[\dot{y}_p(x, t) + \dot{y}_h(x, t)\right]$$

where, in addition to Equations [F10] and [F13], we use Equations [F11] and [F12].

Thus Equations [F14] to [F18] are solved subject to end conditions [F19], using as input values supplied for initial conditions listed below Equation [F19] as well as the quantities listed after Equation [F21]. Equations [F20] and [F21] are used to compute initial values of M and V. Then, as explained in the preceding paragraph, the coefficients and quantity $\dot{\psi}(t)$ appearing in Equation [F15] are computed from input quantities. The quantities computable as output, then, are

$$y_\epsilon(x, t);\ \dot{y}_\epsilon(x, t);\ \gamma(x, t);\ \dot{\gamma}(x, t);\ \psi(t);\ \dot{\psi}(t);\ M(x, t);\ V(x, t)$$

and the displacement

$$\bar{y}(x, t) = y_\epsilon(x, t) + y_h(x, t) + y_p(x, t)$$

and each of its rigid-body components and their derivatives.

F2. FINITE-DIFFERENCE EQUATIONS

The set of equations, [F14] to [F18] specifying the equations of motion used for the ship hull together with initial conditions and end conditions, are incorporated into the set of implicit finite-difference equations which follows. Thus we are now dealing with discrete rather than distributed parameters and variables; see Figure 26. The solutions to these equations have been programmed and carried out on the IBM 704 at the Applied Mathematics Laboratory, David Taylor Model Basin. The final results are a set of printed tables giving for each station or midstation[5] the value of the variables (y_ϵ, V, M, etc.) subsequent to the initiation of the transient excitation.

The interval $0 \le x \le l$ is subdivided into N subintervals* of lengths $(\Delta x)_{1/2}$, $(\Delta x)_{3/2}$, ..., $(\Delta x)_{N-1/2}$, respectively, by the coordinates (stations) $x_0, x_1, \ldots, x_N = l$; see Figure 27. The following notation is used:**

$$x_{n+1/2} = \frac{1}{2}(x_n + x_{n+1})$$

*$N = 20$ is usual although $N = 40$ gives somewhat more accurate results.[5]

**This notation is in accord with the Jasper-Theilheimer representation of a beam.[5]

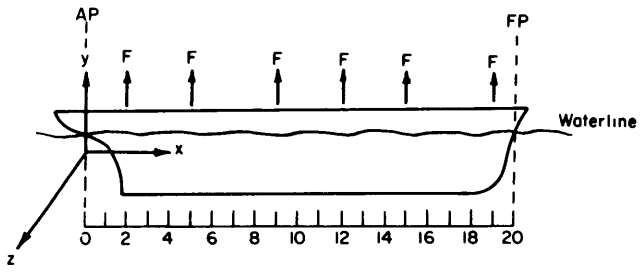

Figure 26a – Ship Hull Showing Excitation Forces; $F = F(x, t)$

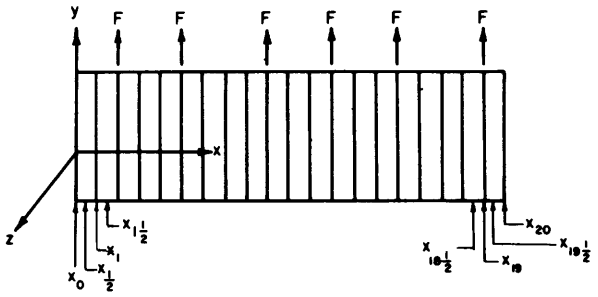

Figure 26b – Equivalent Nonuniform Beam Divided into 20 Sections

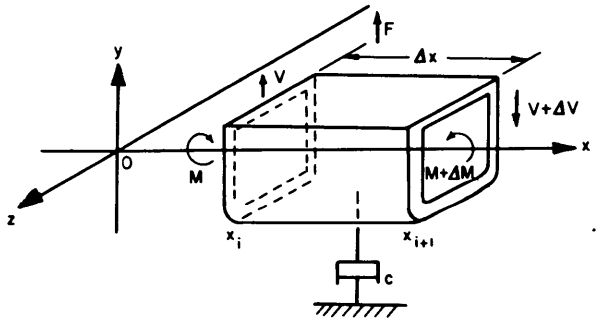

Figure 26c – Free Body Diagram of Ship Section of Length Δx
Subject to Forces and Moments during Transient Vibrations

Figure 26 – Representation of Ship Hull by Nonuniform Beam Divided into 20 Sections

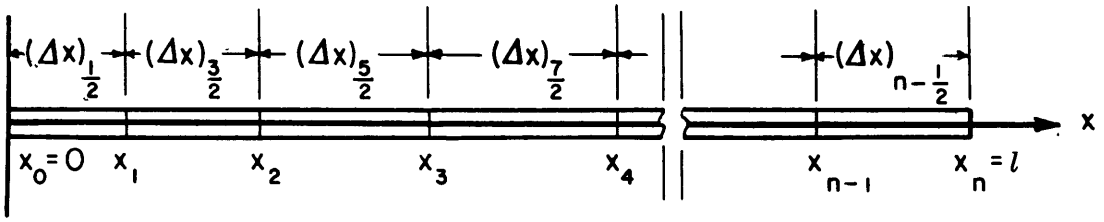

Figure 27 – Subdivision of the Interval $(0, l)$

for $n = 0, 1, \ldots, N-1$. In addition, definitions

$$x_{-\frac{1}{2}} = x_0$$

and

$$x_{N+\frac{1}{2}} = x_N$$

are made so that for $n = 0, 1, 2, \ldots, N$

$$(\Delta x)_n = x_{n+\frac{1}{2}} - x_{n-\frac{1}{2}}$$

can be used.

In the set of difference equations which follows, each approximation to a function of space and time, say $f(x, t)$ at position $x = x_n$ and time $t = t^{(m)}$ is represented by $f_n^{(m)}$, i.e., subscripts, in general, refer to station indexes and superscripts to time indexes.

We approximate Equation [F14] for the nth section and mth time interval by approximating the following equation:

$$\int_{x_n}^{x_{n+1}} \int_{t^{(m)}}^{t^{(m+1)}} \left[\frac{\partial y_\epsilon(x,t)}{\partial t} - \dot{y}_\epsilon(x,t) \right] dt\, dx = 0$$

using

$$(y_{\epsilon,n+\frac{1}{2}}^{(m+1)} - y_{\epsilon,n+\frac{1}{2}}^{(m)})(\Delta x)_{n+\frac{1}{2}} - (\dot{y}_{\epsilon,n+\frac{1}{2}}^{(m)} + \dot{y}_{\epsilon,n+\frac{1}{2}}^{(m+1)}) \left[\frac{(\Delta t)(\Delta x)_{n+\frac{1}{2}}}{2} \right] = 0$$

For convenience, we rewrite this equation as

$$y_{\epsilon,n+\frac{1}{2}}^{(m+1)} - \alpha \dot{y}_{\epsilon,n+\frac{1}{2}}^{(m+1)} = y_{\epsilon,n+\frac{1}{2}}^{(m)} + \alpha \dot{y}_{\epsilon,n+\frac{1}{2}}^{(m)} \qquad [F22]$$

for $n = 0, 1, \ldots, N-1$, with

$$\alpha = \frac{\Delta t}{2} \qquad [F23]$$

Next, the following equation derived from Equation [F15] is approximated:

$$\int_{x_n}^{x_{n+1}} \int_{t^{(m)}}^{t^{(m+1)}} \left\{ \mu(x,t) \frac{\partial \dot{y}_\epsilon(x,t)}{\partial t} + \bar{c}(x,t)\, \dot{y}_\epsilon(x,t) + m(x,t) \frac{dx(x,t)}{dt} \dot{\gamma}(x,t) \right.$$

$$\left. - \frac{m(x,t)}{KAC(x)} \frac{dx(x,t)}{dt} \frac{\partial V(x,t)}{\partial t} + \frac{\partial V(x,t)}{\partial x} - \bar{P}(x,t) - m(x,t) \frac{dx(x,t)}{dt} \dot{\psi}(t) \right\} \cdot dx\, dt = 0 \qquad [F24]$$

The difference equation used to approximate this equation is of the form:

$$(\mu\Delta x)^{(m+\frac{1}{2})}_{n+\frac{1}{2}} (\dot{y}^{(m+1)}_{\epsilon,\, n+\frac{1}{2}} - \dot{y}^{(m)}_{\epsilon,\, n+\frac{1}{2}}) + (\bar{c}\Delta x)^{(m+\frac{1}{2})}_{n+\frac{1}{2}} (\dot{y}^{(m+1)}_{\epsilon,\, n+\frac{1}{2}} + \dot{y}^{(m)}_{\epsilon,\, n+\frac{1}{2}}) \frac{\Delta t}{2}$$

$$+ \frac{1}{2} \left(m \frac{dx}{dt} \right)^{(m+\frac{1}{2})}_{n+\frac{1}{2}} (\Delta x)_{n+\frac{1}{2}} (\dot{\gamma}^{(m+1)}_{n+1} + \dot{\gamma}^{(m+1)}_{n} + \dot{\gamma}^{(m)}_{n+1} + \dot{\gamma}^{(m)}_{n}) \frac{\Delta t}{2}$$

$$- \frac{1}{2} \left(m \frac{dx}{dt} \right)^{(m+\frac{1}{2})}_{n+\frac{1}{2}} \cdot \left[\left(\frac{\Delta x}{KAG} \right)_{n+1} (V^{(m+1)}_{n+1} - V^{(m)}_{n+1}) + \left(\frac{\Delta x}{KAG} \right)_{n} (V^{(m+1)}_{n} - V^{(m)}_{n}) \right]$$

$$+ (V^{(m+1)}_{n+1} - V^{(m+1)}_{n} + V^{(m)}_{n+1} - V^{(m)}_{n}) \frac{\Delta t}{2} - (\bar{P}\Delta x)^{(m+\frac{1}{2})}_{n+\frac{1}{2}} \Delta t - \left(m \frac{dx}{dt} \right)^{(m+\frac{1}{2})}_{n+\frac{1}{2}} (\Delta x)_{n+\frac{1}{2}} \dot{\psi}^{(m+\frac{1}{2})} \Delta t = 0 \qquad [F25]$$

for $n = 0, 1, \ldots, N-1$. For convenience, we rewrite this equation as follows:

$$\mathcal{F}^{(m+\frac{1}{2})}_{n+\frac{1}{2}} \dot{y}^{(m+1)}_{\epsilon,\, n+\frac{1}{2}} + \mathcal{K}^{(m+\frac{1}{2})}_{n+\frac{1}{2}} (\dot{\gamma}^{(m+1)}_{n+1} + \dot{\gamma}^{(m+1)}_{n}) + \mathcal{J}^{(m+\frac{1}{2})}_{n+\frac{1}{2}} V^{(m+1)}_{n+1} + \mathcal{K}^{(m+\frac{1}{2})}_{n+\frac{1}{2}} V^{(m+1)}_{n} =$$

$$\bar{\mathcal{P}}^{(m+\frac{1}{2})}_{n+\frac{1}{2}} + \bar{\mathcal{F}}^{(m+\frac{1}{2})}_{n+\frac{1}{2}} \dot{y}^{(m)}_{\epsilon,\, n+\frac{1}{2}} - \mathcal{K}^{(m+\frac{1}{2})}_{n+\frac{1}{2}} (\dot{\gamma}^{(m)}_{n+1} + \dot{\gamma}^{(m)}_{n}) + \bar{\mathcal{J}}^{(m+\frac{1}{2})}_{n+\frac{1}{2}} V^{(m)}_{n+1} + \bar{\mathcal{K}}^{(m+\frac{1}{2})}_{n+\frac{1}{2}} V^{(m)}_{n} \qquad [F26]$$

where

$$\mathcal{a} = \frac{1}{2} \Delta t \qquad [F27]$$

$$\mathcal{F}^{(m+\frac{1}{2})}_{n+\frac{1}{2}} = (\mu\Delta x)^{(m+\frac{1}{2})}_{n+\frac{1}{2}} + (\bar{c}\Delta x)^{(m+\frac{1}{2})}_{n+\frac{1}{2}} \mathcal{a} \qquad [F28]$$

$$\bar{\mathcal{F}}^{(m+\frac{1}{2})}_{n+\frac{1}{2}} = (\mu\Delta x)^{(m+\frac{1}{2})}_{n+\frac{1}{2}} - (\bar{c}\Delta x)^{(m+\frac{1}{2})}_{n+\frac{1}{2}} \mathcal{a} \qquad [F29]$$

$$\mathcal{K}^{(m+\frac{1}{2})}_{n+\frac{1}{2}} = \frac{1}{2} \left(m \frac{dx}{dt} \right)^{(m+\frac{1}{2})}_{n+\frac{1}{2}} (\Delta x)_{n+\frac{1}{2}} \mathcal{a} \qquad [F30]$$

$$\mathcal{J}^{(m+\frac{1}{2})}_{n+\frac{1}{2}} = -\frac{1}{2} \left(m \frac{dx}{dt} \right)^{(m+\frac{1}{2})}_{n+\frac{1}{2}} \left(\frac{\Delta x}{KAG} \right)_{n+1} + \mathcal{a} \qquad [F31]$$

$$\bar{\mathcal{J}}^{(m+\frac{1}{2})}_{n+\frac{1}{2}} = -\frac{1}{2} \left(m \frac{dx}{dt} \right)^{(m+\frac{1}{2})}_{n+\frac{1}{2}} \left(\frac{\Delta x}{KAG} \right)_{n+1} - \mathcal{a} \qquad [F32]$$

$$\mathcal{K}^{(m+\frac{1}{2})}_{n+\frac{1}{2}} = -\frac{1}{2} \left(m \frac{dx}{dt} \right)^{(m+\frac{1}{2})}_{n+\frac{1}{2}} \left(\frac{\Delta x}{KAG} \right)_{n} - \mathcal{a} \qquad [F33]$$

$$\bar{\mathcal{K}}_{n+\frac{1}{2}}^{(m+\frac{1}{2})} = -\frac{1}{2}\left(m\,\frac{dx}{dt}\right)_{n+\frac{1}{2}}^{(m+\frac{1}{2})}\left(\frac{\Delta x}{KAG}\right)_n + a \qquad \text{[F34]}$$

and

$$\bar{\varphi}_{n+\frac{1}{2}}^{(m+\frac{1}{2})} = \left[(\bar{P}\Delta x)_{n+\frac{1}{2}}^{(m+\frac{1}{2})} + \left(m\,\frac{dx}{dt}\right)_{n+\frac{1}{2}}^{(m+\frac{1}{2})}(\Delta x)_{n+\frac{1}{2}}\,\dot{\psi}^{(m+\frac{1}{2})}\right]\Delta t \qquad \text{[F35]}$$

where the values of $\left(\frac{\Delta x}{KAG}\right)_n$ are obtained from the input data, while values of

$$(\mu\Delta x)_{n+\frac{1}{2}}^{(m+\frac{1}{2})};\ (\bar{c}\Delta x)_{n+\frac{1}{2}}^{(m+\frac{1}{2})}a;\ \frac{1}{2}\left(m\,\frac{dx}{dt}\right)_{n+\frac{1}{2}}^{(m+\frac{1}{2})};\ \bar{\varphi}_{n+\frac{1}{2}}^{(m+\frac{1}{2})};\ \dot{\psi}^{(m+\frac{1}{2})};\ \dot{y}_h^{(m+\frac{1}{2})} \qquad \text{[F36]}$$

are obtained at the required times $t^{(m+\frac{1}{2})}$ by interpolation, using the set of three values obtained at the nearest times from a set of key values precomputed at a set of uniformly spaced times described as follows:

Each of the time-dependent input quantities

$$\left(\frac{dx}{dt}\right)_{n+\frac{1}{2}};\ m_{n+\frac{1}{2}};\ P_{e_{n+\frac{1}{2}}};\left(\frac{c}{\mu}\right)_{n+\frac{1}{2}}$$

can each be supplied at a different sequence of time intervals. These time intervals need not be uniform. The program first interpolates these input quantities to a key set of uniformly spaced times using three-point interpolation formulas. At each time $t^{(\nu)}$ of this key set, the quantities [F36] are computed by using the following set of equations:

$$\Delta t' = t^{(\nu+1)} - t^{(\nu)} \qquad \text{[F37]}$$

$$(\mu\Delta x)_{n+\frac{1}{2}}^{(\nu)} = (m\Delta x)_{n+\frac{1}{2}}^{(\nu)} + (m_s\Delta x)_{n+\frac{1}{2}} \qquad \text{[F38]}$$

$$(\bar{c}\Delta x)_{n+\frac{1}{2}}^{(\nu)}a = \left(\frac{c}{\mu}\right)_{n+\frac{1}{2}}^{(\nu)}(\mu\Delta x)_{n+\frac{1}{2}}\,a + \left[\frac{(m\Delta x)_{n+\frac{1}{2}}^{(\nu+1)} - (m\Delta x)_{n+\frac{1}{2}}^{(\nu-1)}}{2\Delta t'}\right]a$$

$$+\frac{(m)_{n+3/2}^{(\nu)} - (m)_{n-\frac{1}{2}}^{(\nu)}}{(\Delta x)_n + (\Delta x)_{n+1}}\left(\frac{dx}{dt}\right)_{n+\frac{1}{2}}^{(\nu)}a\,(\Delta x)_{n+\frac{1}{2}} \qquad \text{[F39]}$$

$$\frac{1}{2}\left(m\frac{dx}{dt}\right)^{(\nu)}_{n+\frac{1}{2}} = \frac{1}{2}\, m^{(\nu)}_{n+\frac{1}{2}} \cdot \left(\frac{dx}{dt}\right)^{(\nu)}_{n+\frac{1}{2}} \qquad [F40]$$

$$\bar{\varphi}^{(\nu)}_{n+\frac{1}{2}} = (\bar{P}\Delta x)^{(\nu)}_{n+\frac{1}{2}}\, \Delta t + \left(m\frac{dx}{dt}\right)^{(\nu)}_{n+\frac{1}{2}} (\Delta x)_{n+\frac{1}{2}}\, \dot{\psi}^{(\nu)}\, \Delta t \qquad [F41]$$

where

$$(\bar{P}\Delta x)^{(\nu)}_{n+\frac{1}{2}} = (P_e \Delta x)^{(\nu)}_{n+\frac{1}{2}} - g(m_s \Delta x)_{n+\frac{1}{2}} - (m_s \Delta x)_{n+\frac{1}{2}} [\ddot{\psi}^{(\nu)} (x_{n+\frac{1}{2}} - x_{c.g.}) + \ddot{y}^{(\nu)}_h]$$

$$- (c\Delta x)^{(\nu)}_{n+\frac{1}{2}} [\dot{\psi}^{(\nu)} (x_{n+\frac{1}{2}} - x_{cg}) + \dot{y}^{(\nu)}_h] \qquad [F42]$$

$$x_{c.g.} = \sum_{n=0}^{N-1} x_{n+\frac{1}{2}} (m_s \Delta x)_{n+\frac{1}{2}} \Bigg/ \sum_{n=0}^{N-1} (m_s \Delta x)_{n+\frac{1}{2}} \qquad [F43]$$

$$\ddot{\psi}^{(\nu)} = \frac{\sum_{n=0}^{N-1} [(P_e \Delta x)^{(\nu)}_{n+\frac{1}{2}} - g(m_s \Delta x)_{n+\frac{1}{2}}]\, (x_{n+\frac{1}{2}} - x_{c.g.})}{\sum_{n=0}^{N-1} (m_s \Delta x)_{n+\frac{1}{2}} (x_{n+\frac{1}{2}} - x_{c.g.})^2} \qquad [F44]$$

$$\dot{\psi}^{(\nu)} = \dot{\psi}^{(\nu-1)} + \frac{\Delta t'}{2} (\ddot{\psi}^{(\nu)} + \ddot{\psi}^{(\nu-1)}) \qquad [F45]$$

$$\ddot{y}^{(\nu)}_h = \frac{\sum_{n=0}^{N-1} [(P_e \Delta x)^{(\nu)}_{n+\frac{1}{2}} - g(m_s \Delta x)_{n+\frac{1}{2}}]}{\sum_{n=0}^{N-1} (m_s \Delta x)_{n+\frac{1}{2}}} \qquad [F46]$$

$$\dot{y}^{(\nu)}_h = \dot{y}^{(\nu-1)}_h + \frac{\Delta t'}{2} (\ddot{y}^{(\nu)} + \ddot{y}^{(\nu-1)}) \qquad [F47]$$

In addition to the time-dependent input quantities already described, the following set of time-independent input quantities is required for the calculations in Equations [F37] to [F47]:

$$(\Delta x)_{n+\frac{1}{2}};\ (m_s \Delta x)_{n+\frac{1}{2}};\ \dot{\psi}^{(0)};\ \text{and}\ \dot{y}_h^{(0)}$$

Returning now to obtain a finite-difference equation using [F16], we approximate

$$\int_{t^{(m)}}^{t^{(m+1)}} \int_{x_n}^{x_{n+1}} \left[\frac{1}{EI(x)} \frac{\partial M(x,t)}{\partial t} - \frac{\partial \dot{\gamma}(x,t)}{\partial x} \right] dt\, dx = 0 \qquad [F48]$$

using

$$\left(\frac{\Delta x}{EI} \right)_{n+\frac{1}{2}} (M_{n+\frac{1}{2}}^{(m+1)} - M_{n+\frac{1}{2}}^{(m)}) - (\dot{\gamma}_{n+1}^{(m+1)} - \dot{\gamma}_n^{(m+1)} + \dot{\gamma}_{n+1}^{(m)} - \dot{\gamma}_n^{(m)})\, \mathcal{A} = 0 \qquad [F49]$$

Rewriting this equation in a more convenient form, we obtain for $n = 0, 1, \ldots, N-1$:

$$\mathcal{E}_{n+\frac{1}{2}} M_{n+\frac{1}{2}}^{(m+1)} - \mathcal{A} (\dot{\gamma}_{n+1}^{(m+1)} - \dot{\gamma}_n^{(m+1)}) = \mathcal{E}_{n+\frac{1}{2}} M_{n+\frac{1}{2}}^{(m)} + \mathcal{A} (\dot{\gamma}_{n+1}^{(m)} - \dot{\gamma}_n^{(m)}) \qquad [F50]$$

where

$$\mathcal{E}_{n+\frac{1}{2}} = \left(\frac{\Delta x}{EI} \right)_{n+\frac{1}{2}} \qquad [F51]$$

which is supplied as input, directly.

Similarly, to replace Equation [F17], we approximate

$$\int_{t^{(m)}}^{t^{(m+1)}} \int_{x_{n-\frac{1}{2}}}^{x_{n+\frac{1}{2}}} \left[I_{\mu z}(x) \frac{\partial \dot{\gamma}(x,t)}{\partial t} - \frac{\partial M(x,t)}{\partial x} + V(x,t) \right] dx\, dt = 0$$

using

$$(I_{\mu z} \Delta x)_n (\dot{\gamma}_n^{(m+1)} - \dot{\gamma}_n^{(m)}) - (M_{n+\frac{1}{2}}^{(m+1)} - M_{n-\frac{1}{2}}^{(m+1)} + M_{n+\frac{1}{2}}^{(m)} - M_{n-\frac{1}{2}}^{(m)})\, \mathcal{A} + (V_n^{m+1} + V_n^m) \frac{(\Delta x)_n \Delta t}{2} = 0$$

This equation can be rewritten in the form:

$$\mathcal{D}_n \dot{\gamma}_n^{(m+1)} - \mathcal{A} (M_{n+\frac{1}{2}}^{(m+1)} - M_{n-\frac{1}{2}}^{(m+1)}) + \mathcal{B}_n V_n^{(m+1)} = \mathcal{D}_n \dot{\gamma}_n^{(m)} + \mathcal{A} (M_{n+\frac{1}{2}}^{(m)} - M_{n-\frac{1}{2}}^{(m)}) - \mathcal{B}_n V_n^{(m)} \qquad [F52]$$

where

$$\mathcal{D}_n = (I_{\mu z} \Delta x)_n \qquad [F53]$$

$$\mathcal{B}_n = (\Delta x)_n \frac{\Delta t}{2} \qquad [F54]$$

These quantities are available in the input data.

Finally, in a similar manner we obtain the following finite difference-equation to replace Equation [F18]:

$$\mathcal{E}_n V_n^{(m+1)} + \mathcal{A}(\dot{y}_{\mathcal{E},\, n+\frac{1}{2}}^{(m+1)} - \dot{y}_{\mathcal{E},\, n-\frac{1}{2}}^{(m+1)} - \mathcal{B}_n \dot{\gamma}_n^{(m+1)} \qquad [F55]$$

$$= \mathcal{Q}_n^{(m+\frac{1}{2})} + \mathcal{E}_n V_n^{(m)} - \mathcal{A}(\dot{y}_{\mathcal{E},\, n+\frac{1}{2}}^{(m)} - \dot{y}_{\mathcal{E},\, n-\frac{1}{2}}^{(m)} + \mathcal{B}_n \dot{\gamma}_n^{(m)}$$

where

$$\mathcal{E}_n = \left(\frac{\Delta x}{KAG}\right)_n \qquad [F56]$$

$$\mathcal{Q}_n^{(m+\frac{1}{2})} = -2\mathcal{B}_n \dot{\psi}^{(m+\frac{1}{2})} \qquad [F57]$$

with $\mathcal{B}_n$ given by Equation [F54] and $\dot{\psi}^{(m+\frac{1}{2})}$ by Equations [F43] to [F45].

The end conditions imposed will be

$$V_0^{(m)} = V_N^{(m)} = 0 \qquad [F58]$$

as well as

$$\dot{\gamma}_0^{(m)} = \dot{\gamma}_1^{(m)};\ \dot{\gamma}_N^{(m)} = \dot{\gamma}_{N-1}^{(m)} \qquad [F59]$$

for all m.

Equation [F59] is used to replace

$$M_0^{(m)} = M_N^{(m)} = 0 \qquad [F60]$$

since only $M_{n+\frac{1}{2}}$ for $n = 0, 1, \ldots, N-1$ will be available.

The initial conditions to be specified include values of

$$\gamma_n^{(0)};\ \dot{\gamma}_n^{(0)} \qquad \text{for } n = 0, 1, \ldots, N$$

and

$$y_{\mathcal{E},\, n+\frac{1}{2}}^{(0)};\ \dot{y}_{\mathcal{E},\, n+\frac{1}{2}}^{(0)} \text{ for } n = 0, 1, \ldots, N-1.$$

From these we compute (see Equations [F20] and [F21]

$$M^{(0)}_{n+\frac{1}{2}} = \frac{\gamma^{(0)}_{n+1} - \gamma^{(0)}_{n}}{\ell_{n+\frac{1}{2}}} \qquad \text{for } n = 0, 1, \ldots, N-1 \qquad [F61]$$

and

$$V^{(0)}_{n} = \frac{M^{(0)}_{n+\frac{1}{2}} - M^{(0)}_{n-\frac{1}{2}}}{(\Delta x)_n} \qquad \text{for } n = 1, 2, \ldots, N-1 \qquad [F62]$$

The conditions [F58], [F59], [F61], [F62], together with initial values for γ_n, $\dot{\gamma}_n$, $y_{\ell,n+\frac{1}{2}}$, $\dot{y}_{\ell,n+\frac{1}{2}}$, and Equations [F22], [F26], [F50], [F52]; and [F55] will be used to determine the state of the system at a specified set of times beyond the initial time.

For further details on the coding, refer to the Applied Mathematics Laboratory of the David Taylor Model Basin.

F3. COMPUTATION OF HYDRODYNAMIC (SLAMMING) FORCES BY DIGITAL COMPUTER

To reduce the labor and expense involved in computing the response of a ship to slamming forces, it is desirable to compute the *forces* by means of a digital computer. A method is now described for carrying out such computations on a computer, currently being used to establish a code for the IBM 7090 by the Applied Mathematics Laboratory.

In this new coding, Equations [F14] through [F21] are again used to describe the motion of a ship. To solve these equations, the following data are to be supplied (as input):

$\frac{c}{\mu(x, t)}$, where c is damping constant; $EI(x)$; $I_{\mu z}(x)$; $KAG(x)$; $m_s(x)$ initial values; end conditions; time intervals; and quantities, described below, necessary to compute P_e. *Now, however, the digital computer will calculate* P_e.

Recall that

$$P_e = \frac{d}{dt}(m\dot{y}_r) + (g + \dot{v})\rho A$$

is a part of the force

$$\overline{P} = P_e - m_s g - m_s \left(\frac{\partial \dot{y}_p}{\partial t} + \frac{\partial \dot{y}_h}{\partial t} \right) - c\,(\dot{y}_p + \dot{y}_h)$$

here* m_- = added mass per unit length = $\frac{\pi}{2}\rho c^2 C_V$

$\dot{y}_r$ = downward relative velocity = $v - \dot{y}_h - \dot{y}_p + (U - u\cos\theta_s)\psi$

g = acceleration due to gravity

*In the equation for $\dot{y}_r$, ψ is in radians, whereas in the equation for γ_p which follows, ψ is in degrees.

$\dot{v}$ = fluid particle vertical acceleration $= -\frac{h}{2}\left(\frac{2\pi}{\lambda} V_w\right)^2 \cos\frac{2\pi x}{\lambda}$

V_w = wave velocity = $\sqrt{\frac{g\lambda}{2\pi}}$

ρ = density of fluid

A = cross-sectional area

λ = wave length

h = wave height

For the digital computer to calculate the needed P_e, the following quantities must be supplied in numerical form:

$$\rho,\ V,\ \theta_s,\ g,\ \zeta \text{ or } k,\ \lambda,\ h,\ c(x) \text{ (half-breadth)},\ \dot{\psi}(t),\ \dot{y}_h(t)$$

and the number of sections or stations to be used in solving the finite difference-equations.

Using these data, the computer calculates

$$v = -\frac{h}{2}\frac{2\pi}{\lambda} V_w \sin\frac{2\pi x}{\lambda}$$

$$u = -\frac{h}{2}\frac{2\pi}{\lambda} V_w \cos\frac{2\pi x}{\lambda}$$

$$\dot{y}_p = \frac{\pi}{180}\zeta\dot{\psi}$$

$$y_p = \frac{\pi}{180}\zeta\psi$$

where $\zeta = \xi + k$ = distance from heave meter located at center of gravity to any ship section, k being the distance from the heave meter to the midship section; see Figure 2.

From Appendix E,

$$\theta = \frac{2\pi x}{\lambda} = \frac{2\pi}{\lambda}\left[(V_w + V\cos\theta_s)t + \xi\cos\theta_s\right]$$

The quantities $c(x, t)$, $C_V(x, t)$, and $m(x, t)$ are determined by the computer using the following procedure:

a. The Applied Mathematics Laboratory is supplied with a description of each ship section in the form of a *finite* number of breadths $c'(x)$ at regularly spaced drafts $y(x)$;* see Appendix B

*It is important to note that $c'(x)$ rather than $c'(x, t)$ (a time-dependent quantity) is being furnished here. The latter quantity is to be determined by the computer for corresponding input immersion data $y(x, t)$, using the data stored in accordance with this procedure.

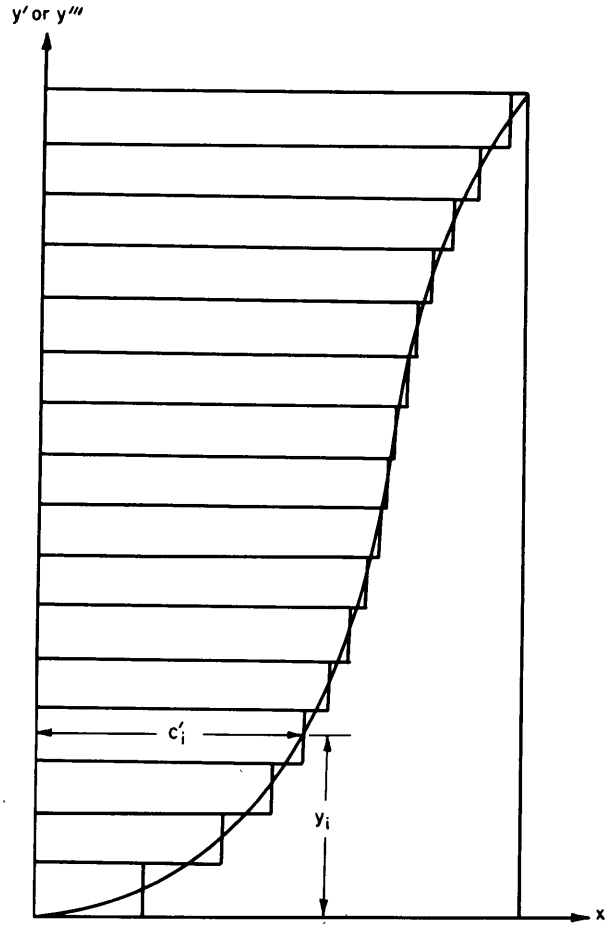

Figure 28 – Hypothetical Ship Section Profile

$i = 1, 2, \ldots, N$

and Figure 17. This would actually describe a polygon similar in form to Figure 28. However, intermediate values of $c'(x)$ and the corresponding $y(x)$ can be found by interpolation, which is a part of the coding. Thus, although the data is stored at a discrete number of values, an approximate value for $c'(x)$ can be calculated for *any* x supplied.* More accuracy in the determination of $m(x)$ may be expected if more $c'(x)$'s are provided and/or if the slope (or angle β) of the ship line at each $c'(x)$ is given. If β is not given, it can be computed; see Item b.

b. For each value of $c'(x)$ and corresponding $y(x)$, the half-breadths $c(x)$ and $c''(x)$ corresponding to the immersion y' and the emersion y''', respectively, *which would occur in the dynamic case*,** are determined from the coded Equations [B1] to [B3]; see Appendix B and Figure 17. The quantity β, used in these equations, at any point $(c'(x), y)$ on the ship section

*That is, $c'(x)$ is effectively or practically (though not actually) a continuous function of $y(x)$.

**That is, when slamming occurs and there is a time-varying half-breadth, immersion, and virtual mass.

profile is precomputed from the coded equation $\frac{y_j - y_i}{c'_j - c'_i}$ (c'_j, y_j, and c'_i, y_i being values at predetermined points, on the profile, above and below the point in question); as explained in Item a., continuous values of c' as a function of y are available. Where required, Newton's method of interpolation rather than linear interpolation will be used to find β.

c. For each value of $c(x)$ and its corresponding immersion $y'(x)$, the code permits the determination of:

$$\frac{c(x)}{y'(x)}$$

the ratio of half-breadth to draft, and

$$\eta = \frac{A(x)}{2c(x)\,y'(x)} = \frac{2\sum_{i=0}^{n} c_i y_i}{2c(x)\,y'(x)}$$

the section area coefficient. Here η corresponds to the section with immersion $y'(x)$.

Similar quantities are found for $c''(x)$ corresponding to the emersion $y'''(x)$.

d. For any value of (c, y') or (c'', y'''), C_V is then obtained from *Prohaska's equation* given in Reference 13 (French version) which is coded for the computer. Note that the functional relationship between C_V and the quantities in Item c. supersedes *Prohaska's curves* hitherto used to find C_V; see Figure 19.

e. The coded equation $m = \frac{\pi}{2} \rho c^2 C_V$ is then used to determine the virtual mass for any value of c (or c'). Hence an added mass at each draft for immersion and emersion can be calculated. It is possible that the immersion level y' at one draft y will equal the emersion level y''' at *another* draft y; see Appendix B and Figure 9.

Thus the calculation of $c(x)$, $c''(x)$, $C_V(x)$, and m for any value of immersion and emersion can be carried out in a separate routine on the computer, and the resulting values of m (two for each draft; see Appendix B) can be stored for use (and interpolation) in a problem of a dynamic nature; i.e., when time-varying immersion $y(x, t)$ is fed into the computer as input data.

Note that the equation

$$\frac{d\xi}{dt} = \frac{dx}{dt} = -(U - u\cos\theta_s)$$

is also coded for the computer, the equation for computing u being given on page 80.

APPENDIX G

ANALOG METHOD OF SOLUTION FOR PREDICTING FORCES ON AND RESPONSE OF A SHIP DUE TO WAVE MOTION

G1. GENERAL

It is desirable to reduce the complexity, expense, and time required to make numerical computations for predicting the forces on and dynamic (elastic and rigid-body) response of a ship; i.e., bending moments, shearing forces, vibrations, and heaving and pitching motions.* This can be accomplished by an analog computer called the "Seaworthiness Computer and Predictor,"** illustrated in schematic and block diagram form in Figure 29 for *one section* of a ship.

This computer has been designed by the author to satisfy the equations used hitherto. *It is stressed that the analog shown in Figure 29 represents one particular scheme for performing the mathematical operations giving the forces and response—it is not the only nor necessarily the desirable method.* Moreover, even if the concept of a computer as shown in Figure 29 were adopted for development it is likely that many modifications of the details would be made for practical reasons. Some design considerations and the basis for design are discussed in G3.

Finally, we note that such a computer has utility for:

1. The prediction of the response of a given ship in a given seaway.
2. The calculation of the bending moments and shearing forces, both static and dynamic, leading to the evaluation of the suitability of a given ship design as to the (a) structural strength of the ship in waves and (b) severity of response of the ship due to slamming. †
3. The prediction of the motion of the flight deck of an aircraft carrier several seconds ahead of time. This information would be extremely valuable when applied to the automatic landing of aircraft.

G2. DESCRIPTION

The analog computer generates the current equivalent of the forces acting upon each section of a ship's hull, due to the relative motion of the ship with respect to the waves, and gives the response of the ship to this motion. The computer represents, as will be shown,

---

*Static forces due to the weight of the hull are also included in the computations. Static buoyancy forces are already included in the Smith-corrected buoyancy force term.

**Dr. N.H. Jasper originated the conception of such a computer and, upon completion of the theoretical analysis and computer design given in this report, established an additional computer design feasibility study;[19] this study involved the reformulation of the theory for the purpose of simplicity and economy of components. Finally, upon recommendation by the author, Dr. R.H. MacNeal of Computer Engineering Associates, Incorporated, Pasadena, California, was given a contract requiring the further reformulation of the problem for the purpose of devising a practical analog for ESSEX.[18] The author acted as liaison for the David Taylor Model Basin on this contract.

†Figure 29 does not give static results. These results can, however, be obtained on a passive analog computer and superposed on the dynamic results.

the differential and finite difference equations used previously for the numerical computation of the forces on and response of a ship moving through a specified seaway (train of waves).

The ship, considered as a beam, is divided into $n = N$ sections (or $n = N + 1$ stations) and its mechanical properties are represented by lumped electrical parameters.*[5, 27] In Figure 29 the immersion of the ship at any station is represented by the distance from the mean water line on Plate P_2 to the base of the template drawn on Plate P_1. The total immersion $(y_t)_{n-\frac{1}{2}}$ of P_2 is a function of the response (displacement) of the ship, the draft, and wave elevation; see Equations [G1], [G4], and [G5] which follow.** A time-varying virtual mass at any station corresponding to the immersion and direction of immersion at that station may then be generated;† the details of generation are shown in Figure 29. The time (partial) derivative of the product of this mass and the generated ship to wave velocity (including the vibratory component) is then obtained for that station. This term plus the generated transport momentum term,†† Smith-corrected byoyancy force term, and hull weight force term are then injected as the *current equivalent of the force* into the beam analog[5] at the appropriate station; see Equations [G9] and [G10]. Clearly, then, a feedback system has been devised which represents the *interaction* of the ship and the fluid medium.

The method of electromechanically generating the virtual mass as a function of the breadth, area, total immersion, and direction of the velocity of immersion of a section of a ship will now be explained.

For each of the N sections a plate, P_1, is made on which the cross section of the ship is drawn; see Figure 29. The base of this cross section represents the keel. The area A within the cross section is made transparent and the remainder of the plate is made opaque. A similar Plate P_2 is constructed, the upper half (portion above the still water line) of which is opaque and the lower half of which is transparent. The two plates are set side by side

---

*N = 20 to 40, depending upon the accuracy desired.[5] In Figure 29 $(\dot{\bar{y}})'_{n-\frac{1}{2}}$ and $(\dot{\gamma})'_n$ are voltages representing the linear velocity at Station $n - \frac{1}{2}$ and the angular velocity at Station n, respectively; $(V)'_{n-1}$ and $(M)'_{n-\frac{1}{2}}$ are currents representing the shear force at Station $n - 1$ and bending moment at Station $n - \frac{1}{2}$, respectively; currents injected at Station $n - \frac{1}{2}$ represent forces acting at that station $(m_s)'_{n-\frac{1}{2}}$, $\left(\frac{\Delta x}{KAG}\right)'_{n-\frac{1}{2}}$, $\left(\frac{\Delta x}{EI}\right)'_{n-\frac{1}{2}}$, and $(I_{mz})'_n$ represent respectively, the total mass of the section of the beam between $n - 1$ and n, the mean value of the reciprocal of the shear rigidity or $\frac{1}{KAG}$ between $n - \frac{1}{2}$ and $n + \frac{1}{2}$ multiplied by Δx, the mean value of the bending compliance $\left(\frac{1}{EI}\right)$ between points $n - 1$ and n multiplied by Δx, and the effective mass between $n - \frac{1}{2}$ and $n + \frac{1}{2}$ multiplied by the square of the radius of gyration of the cross section at n.

**In Figure 29, $(y_t)_{n-\frac{1}{2}}$ is a distance, whereas $(y_t)'_{n-\frac{1}{2}}$ is a voltage.

†Generation here means electrical generation corresponding to equivalent mechanical quantities.

†† This is the product of the space derivative of momentum and the relative horizontal ship to wave velocity term.

into a movable carrier and Plate P_2 (or P_1) is adjusted so that initially the immersion equals the draft. A voltage proportional to the instantaneous immersion less the draft drives a motor and its gear train which displaces the mid or still water line position of P_2 with respect to the keel a proportional distance. A light source located behind P_2 transmits light uniformly through the time-varying area $A_{n-\frac{1}{2}}$ of Plate P_1 which is below the still water line. This light is collected by a photocell, located on the near side of P_1, which generates a current (or voltage) proportional to the amount of light (lumens) transmitted through $A_{n-\frac{1}{2}}$ and therefore to the area $A_{n-\frac{1}{2}}$ at any time.* Thus we have obtained $[y_t(t)]'_{n-\frac{1}{2}}$ and $[A(t)]'_{n-\frac{1}{2}}$. The breadth

$$[2c'(t)]_{n-\frac{1}{2}} = \left[\frac{dA}{dy_t}\right]_{n-\frac{1}{2}} = \frac{\left[\frac{dA}{dt}\right]_{n-\frac{1}{2}}}{\left[\frac{dy_t}{dt}\right]_{n-\frac{1}{2}}}$$

may be obtained by means of differentiating and function divider circuits as shown in Figure 29. The terms $\left[\frac{A}{2cy_t}\right]'_{n-\frac{1}{2}}$ and $\left[\frac{2c}{y_t}\right]'_{n-\frac{1}{2}}$ are then electrically generated and the corresponding term $[C_V(t)]'_{n-\frac{1}{2}}$ is also generated as a function of these two terms variables; see Figure 29. A suitable generator of a function of two variables can be purchased from Mid-Century Instrumatic Corporation. To take into account the *rise of water* due to *increasing immersion*, the area A and breadth $2c$ can be modified in accordance with the theory previously presented; see Appendix B. A similar transparent area A_1 modified to take into account the *depressed surface* due to *decreasing immersion* can be drawn on P_1 next to A. The virtual mass at any time is then generated as a function of either $A_{n-\frac{1}{2}}$, etc., or $(A_1)_{n-\frac{1}{2}}$, etc., depending upon the direction of the velocity of immersion as shown schematically in Figure 29 by dotted and undotted arrows and phototubes; area $(A_1)_{n-\frac{1}{2}}$ is not shown in the figure.

The current (voltage) equivalent of the Area A (or A_1) is also used in obtaining the Smith-corrected byoyancy force.

Examination of Figure 29 shows that the computer design satisfies the following system of differential and algebraic equations used previously (at least in equivalent form) in making the numerical computations:**

$$(\bar{y})'_{n-\frac{1}{2}} = (y_\epsilon)'_{n-\frac{1}{2}} + (y_p)'_{n-\frac{1}{2}} + (y_h)'_{n-\frac{1}{2}} \qquad [G1]$$

---

*Because of the large inertia of the servo system, in practice a vertically deflected field of uniform light (obtained say from a scanning cathode ray oscilloscope (CRO) or a vidicon tube) could replace P_2 and the light source behind P_2; a template of $A_{n-\frac{1}{2}}$ can be pasted on the CRO. A photoformer or diode function generator could also be used to generate the virtual mass.

**Here the primes denote electrical quantities; note that $v = v_{\text{surface}} = \dot{y}_w$; see Equation [D25].

Differentiation gives

$$(\dot{\bar{y}})'_{n-\frac{1}{2}} = (\dot{y}_\epsilon)'_{n-\frac{1}{2}} + (\dot{y}_p)'_{n-\frac{1}{2}} + (\dot{y}_h)'_{n-\frac{1}{2}} \qquad [G2]$$

or

$$(\dot{y}_\epsilon)'_{n-\frac{1}{2}} = (\dot{\bar{y}})'_{n-\frac{1}{2}} - (\dot{y}_p)'_{n-\frac{1}{2}} - (\dot{y}_h)'_{n-\frac{1}{2}} \qquad [G3]$$

The total immersion $(y_t)'_{n-\frac{1}{2}}$ is

$$(y_t)'_{n-\frac{1}{2}} = (y)'_{n-\frac{1}{2}} - (y_\epsilon)'_{n-\frac{1}{2}} = (D)'_{n-\frac{1}{2}} + (y_w)'_{n-\frac{1}{2}} - (y_h)'_{n-\frac{1}{2}} - (y_p)'_{n-\frac{1}{2}} - (y_\epsilon)'_{n-\frac{1}{2}}$$

$$= (D)'_{n-\frac{1}{2}} + (y_w)'_{n-\frac{1}{2}} - (\bar{y})'_{n-\frac{1}{2}} \qquad [G4]$$

Differentiation gives

$$(\dot{y}_t)'_{n-\frac{1}{2}} = (\dot{y})'_{n-\frac{1}{2}} - (\dot{y}_\epsilon)'_{n-\frac{1}{2}} = (\dot{y}_w)'_{n-\frac{1}{2}} - (\dot{y}_h)'_{n-\frac{1}{2}} - (\dot{y}_p)'_{n-\frac{1}{2}} - (\dot{y}_\epsilon)'_{n-\frac{1}{2}} = (\dot{y}_w)'_{n-\frac{1}{2}} - (\dot{\bar{y}})'_{n-\frac{1}{2}} \qquad [G5]$$

Also

$$(\dot{y}_r)'_{n-\frac{1}{2}} - (\dot{y}_\epsilon)'_{n-\frac{1}{2}} = (v)'_{n-\frac{1}{2}} - (\dot{y}_h)'_{n-\frac{1}{2}} - (\dot{y}_p)'_{n-\frac{1}{2}} + [(U - u\cos\theta_s)\psi]'_{n-\frac{1}{2}} - (\dot{y}_\epsilon)'_{n-\frac{1}{2}}$$

$$= (\dot{y})'_{n-\frac{1}{2}} + [(U - u\cos\theta_s)\psi]'_{n-\frac{1}{2}} - (\dot{y}_\epsilon)'_{n-\frac{1}{2}} = (\dot{y}_t)'_{n-\frac{1}{2}} + [(U - u\cos\theta_s)\psi]'_{n-\frac{1}{2}} \qquad [G6]$$

Addition of Equation [G2] and [G6] gives

$$(\dot{\bar{y}})'_{n-\frac{1}{2}} + (\dot{y}_r' - \dot{y}_\epsilon')_{n-\frac{1}{2}} = (v)'_{n-\frac{1}{2}} + [(U - u\cos\theta_s)\psi]'_{n-\frac{1}{2}} \qquad [G7]$$

or

$$(\dot{\bar{y}})'_{n-\frac{1}{2}} = -(\dot{y}_r' - \dot{y}_\epsilon')_{n-\frac{1}{2}} + (v)'_{n-\frac{1}{2}} + [(U - u\cos\theta_s)\psi]'_{n-\frac{1}{2}} \qquad [G8]$$

Finally

$$\left[m_s \Delta x \frac{\partial^2 \bar{y}}{\partial t^2}\right]_{n-\frac{1}{2}} = \left\{\left(\frac{d}{dt}\left[m\left(\dot{y}_r - \frac{\partial y_\epsilon}{\partial t}\right)\right]_{n-\frac{1}{2}} + [(g+\dot{v})\rho A]_{n-\frac{1}{2}} - \left(\frac{\partial v}{\partial x}\right)_{n-\frac{1}{2}} - \left(\frac{c\partial\bar{y}}{\partial t}\right)_{n-\frac{1}{2}} - (m_s g)_{n-\frac{1}{2}}\right)\Delta x\right\}' \qquad [G9]$$

where $m_s g$ is the static force due to the mass of the ship
and

$$\frac{d}{dt}\left[m\left(\dot{y}_r - \frac{\partial y_\epsilon}{\partial t}\right)\right]'_{n-\frac{1}{2}} = \frac{\partial}{\partial t}\left[m\left(\dot{y}_r - \frac{\partial y_\epsilon}{\partial t}\right)\right]'_{n-\frac{1}{2}} + \frac{\partial}{\partial \xi}\left[m\left(\dot{y}_r - \frac{\partial y_\epsilon}{\partial t}\right)\right]'_{n-\frac{1}{2}} \left(\frac{\partial \xi}{\partial t}\right)'_{n-\frac{1}{2}} \quad [G10]$$

where $\frac{\partial}{\partial \xi} = \frac{\partial}{\partial x}$ and $d\xi = dx$.

For the purpose of illustration, y_w is assumed to be a sinusoidal waveform. Treatment of y_w as a complex waveform should involve only slight modifications in the computer design.

In Figure 29, the tape recorder output $(y_w)'$ is a voltage which may be obtained from an instantaneous wave height measurement, by a wave meter at the bow (Station 20) of a ship, i.e., a voltage proportional to wave height is stored on tape. Assuming that the wave does not change shape as it propagates the length of the ship, delay lines can be incorporated in the computer to give the values of y_w at all other stations.

The pitch angle ψ may also be the voltage output of a measured and stored signal.

Sprung bodies may also be included in the computer, using the methods of Reference 5.

G3. BASIS FOR DESIGN

Some important technical considerations in the details of and general procedure for the final circuit design of this computer are discussed.

The proper functioning of the computer requires that a time (or frequency) scale be devised to yield practical values for the electrical parameters[5, 27] of the beam and, at the same time, permit the servo or an equivalent electronic system to operate effectively.

Damping in the ship can be simulated by either inserting resistances in the beam analog, the values of which may be developed by test data, or by injecting currents proportional to the damping forces at the appropriate terminals; see dotted current arrow and component in Figure 29. If resistances are used, the inherent dissipation in the other electrical elements of the beam analog has to be considered.

Since the signal output of an electronic differentiator is directly proportional to the frequency of the input signal, this device tends to amplify the relatively high-frequency noise which may develop in the circuits or contacts or gears etc., out of proportion to the desired signal output. Thus the noise may mask the desired signal. Further, special precautions may be required to prevent high-frequency oscillations in the computer due to the inherently high frequency response of the differentiator. However, satisfactory results may be obtained by using an approximate differentiating circuit whose output signal can be made to approach as arbitrarily close to a true derivative as the noise level and stability requirements will permit. Alternatively, since integration is a smoothing process which tends to iron out irregularities caused by high frequency noise, it may be preferable to rewrite the set of

differential equations so that integrating circuits rather than differentiating circuits are used in the computer.

The accuracy and dynamic range of the computer must be specified if good results are to be obtained.

Prior to the design of the computer, the performance requirements of the computer must be clearly specified. The computer should then be dynamically synthesized according to accepted procedures in computer engineering.* Then a detailed mathematical analysis of the synthesized computer should be made to demonstrate that the final design not only meets specifications but also gives optimum performance; i.e., sinusoidal and transient response curves describing the performance and stability conditions of the computer should be given.[28, 29, 30] Investigation of these curves is sufficient to supply all the required information indicating whether or not the specifications are satisfied by this design. The computer developed in accordance with this design should then be tested to show that the actual operating performance approximates the design performance and meets the specifications.**

*The use of purely cut-and-try procedures as a basis for the design and development of the computer is inadequate.

**The selection and design of the components performing the mathematical operations requires careful consideration.

REFERENCES

1. Jasper, N.H. and Birmingham, J.T., "Strains and Motions of USS ESSEX (CVA 9) during Storms near Cape Horn," David Taylor Model Basin Report 1216 (Aug 1958).

2. Reed Research Report, "Calculation of Forces due to Wave Encounter," Contract NObs 72736 with David Taylor Model Basin (Oct 1958).

3. Reed Research Report, "Computation of Forces due to Motion of a Ship in Waves," Contract NObs 72376, T.O. 6 with David Taylor Model Basin (Dec 1958); also Amendment 1 (Mar 1959).

4. Rossell, H.E. and Chapman, L.B., Editors, "Principles of Naval Architecture," Vol. 2, The Society of Naval Architects and Marine Engineers, New York (1939).

5. Leibowitz, R.C. and Kennard, E.H., "Theory of Freely Vibrating Nonuniform Beams, Including Methods of Solution and Application to Ships," Section 2.43, David Taylor Model Basin Report 1317 (May 1961).

6. Csupor, D., "Methods for Calculating the Free Vibrations of a Ship's Hull (Methoden zur Berechnung der Freien Schwingungen des Schiffskörpers)," Jahrb. d. STG, Vol. 50 (1956). David Taylor Model Basin Translation 288 (May 1959).

7. Wendel, K., "Hydrodynamic Masses and Hydrodynamic Moments of Inertia (Hydrodynamische Massen und Hydrodynamische Massentragheitsmomente)," Jahrb. d. STG, Vol. 44 (1950). David Taylor Model Basin Translation 260 (Jul 1956).

8. Munk, M.M., "The Aerodynamic Forces on Airship Hulls," National Advisory Committee for Aeronautics Report 184 (1923).

9. Mayo, W.L., "Analysis and Modification of Theory for Impact of Seaplanes on Water," National Advisory Committee for Aeronautics Report 810 (1945).

10. Korvin-Kroukovsky, B.V., "Investigation of Ship Motions in Regular Waves," Trans. The Society of Naval Architects and Marine Engineers, Vol. 63 (1955) pp. 386–435.

11. Fay, J.A., "The Motion and Internal Reactions of a Vessel in Regular Waves," Journal of Ship Research, Vol. 1, No. 4 (Mar 1958).

12. Szebehely, V.G., "Hydrodynamics of Slamming of Ships," David Taylor Model Basin Report 823 (Jul 1952).

13. Prohaska, C.W., "The Vertical Vibration of Ships," The Shipbuilder and Marine Engine Builder, Vol. 54 (Oct, Nov 1947); see also "Vibrations Verticales Du Navire," Bulletin de L'Association Technique Maritime et Aéronautique," No. 46 (1947); see Annexe II.

14. Polachek, H., "Calculation of Transient Excitation of Ship Hulls by Finite Difference Methods," Mathematical Tables and Other Aids to Computation, Vol. XIII, No. 66 (Apr 1959) or David Taylor Model Basin Report 1120 (Jul 1957).

15. Scarborough, J.B., "Numerical Mathematical Analysis," Johns Hopkins Press, Baltimore (1930).

16. Fabula, A.G., "Ellipse-Fitting Approximation of Two-Dimensional Normal Symmetric Impact of Rigid Bodies on Water," Fifth Midwestern Conference on Fluid Mechanics Held at University of Michigan (Apr 1 and 2, 1957).

17. Ochi, K. and Bledsoe, M.D., "Theoretical Consideration of Impact Pressure during Ship Slamming," David Taylor Model Basin Report 1321 (Nov 1960).

18. MacNeal R.H., "Analog Computer Analyses of the Bow Slamming Problem for the USS ESSEX, Part I: Method of Analysis (Dec 1960), Part II: Results of the Analysis (Jan 1961), Computer Engineering Associates, Inc., Pasadena, California.

19. Reed Research Report, "Simulation of the Sea and Analog Computation of the Forces on a Ship in Waves," Contract NObs 72736, T.O. 9 with David Taylor Model Basin (Nov 1959).

20. Milne-Thomson, L.M., "Theoretical Hydrodynamics," Second Edition, MacMillan Co., New York (1950), p. 467.

21. Vennard, J.K., "Elementary Fluid Mechanics," John Wiley and Sons, Inc., New York (1940), p. 41.

22. Lamb, H., "Hydrodynamics," Dover Publications, New York (1945).

23. Warnsinck, W.H. and St. Denis, M., "Destroyer Seakeeping Trials," Proceedings of Symposium on the Behavior of Ships in a Seaway, H. Veenman and Zoenen, Wageningen, Holland (1957), p. 441.

24. Sommerfeld, A., "Mechanics of Deformable Bodies," Vol. II, Academic Press, Inc., New York (1950).

25. Margenau, H. and Murphy, G.M., "The Mathematics of Physics and Chemistry," D. Van Nostrand Co., Inc. (1943).

26. McGoldrick, R.T., "Calculation of the Response of a Ship Hull to a Transient Load by a Digital Process," David Taylor Model Basin Report 1119 (Mar 1957).

27. Kenney, J.H. and Leibowitz, R.C., "Design Details and Operating Procedure for the TMB Network Analyzer," David Taylor Model Basin Report 1272 (Apr 1959).

28. Leibowitz, R.C. and Kant, S., "The Design of an Electromechanical Servomechanism with Photoelectric Detection," NavOrd Report 5526, U.S. Naval Gun Factory Technical Report N.G.F.-T-42-57 (Jan 1958).

29. Brown and Campbell, "Principles of Servomechanisms," John Wiley and Sons, Inc., New York (1948).

30. Ahrendt and Taplin, "Automatic Feedback Control," McGraw-Hill Book Company, Inc., New York (1951).

BIBLIOGRAPHY

Bledsoe, M.D., "Series Investigation of Slamming Pressures," David Taylor Model Basin Report 1043 (Dec 1956).

Borg, S.F., "The Analysis of Ship Structures Subjected to Slamming Loads," Journal of Ship Research, Vol. 4, No. 3 (Dec 1960).

Chu, W.H., "On the Development of a More Accurate Method for Calculating Body-Water Impact Pressures," Southwest Research Institute Technical Report 2, Contract Nonr 2729(00) (Sep 1960).

Chu, W.H. and Abramson, H.N., "Hydrodynamic Theories of Ship Slamming – Review and Extension," Journal of Ship Research, Vol. 4. No. 4 (Mar 1961).

Chu, W.H. and Abramson, H.N., "Hydrodynamic Theories of Ship Slamming – Review and Extension," Southwest Research Institute Technical Report 1, Contract Nonr 2729(00) (Nov 1959).

Chu, W.H. and Abramson, H.N., "A Preliminary Analysis of Nonlinear Coupled Pitching and Heaving Motions and Slamming Conditions for a Ship in Regular Waves," Southwest Research Institute Technical Report 3, Contract Nonr 2729(00) (Sep 1960).

Chu, W.H. and Abramson, H.N., "Application of the Generalized Phase-Plane–Method to Multi-Degree-of-Freedom Vibrating Systems," Southwest Research Institute Technical Report 4, Contract Nonr 2729(00) (Jun 1961).

Convair, "The Application of an Analogue Computer–Slender Body Technique to the Loads and Motions of Surface Ships in Waves," Convair Hydromechanic Laboratory, Convair Proposal Report 250 (Apr 1958).

Cummins, W.E., "On Ship Model Testing for the Prediction of Extreme Conditions in Confused Seas," David Taylor Model Basin Report 1410 (Aug 1960).

Durand, W.F., Editor in Chief, "Aerodynamic Theory," Vol. III, Divisions F-I (1934).

Hunt, J.N., "A Note on Gravity Waves of Finite Amplitude," Quarterly Journal of Mechanics and Applied Mathematics Vol. VI (1953).

"International Ship Structures Congress. Report of the Committee on Response to Wave Loads," David Taylor Model Basin Report 1537 (Jun 1961).

Jacobs, W.R., "The Analytical Calculation of Ship Bending Moments in Regular Waves," Journal of Ship Research, Vol. 2, No. 1 (Jun 1958).

Kaplan, P., "Application of Slender Body Theory to Forces Acting on Submerged Bodies and Surface Ships in Regular Waves," Journal of Ship Research, Vol. 1, No. 3 (Nov 1957).

Kaplan, P. and Hu, P.N., "The Forces Acting on Slender Submerged Bodies and Body-Appendage Combinations in Oblique Waves," Proceedings of 3rd U.S. National Congress of Applied Mechanics (1958).

Kaplan, P. and Hu, P.N., "Virtual Mass and Slender Body Theory for Bodies in Waves," Proceedings of Sixth Midwestern Conference on Fluid Mechanics (Sep 1959).

Kennard, E. H., "Generation of Surface Waves by a Moving Partition," Quarterly of Applied Mathematics, Vol. 7 (1949).

Korvin-Kroukovsky, B.V., "Ships at Sea (Seakeeping Monograph);" "Hydrodynamic Forces" (Chapter II), "Ship Motions" (Chapter III), Stevens Institute of Technology (Sep 1957).

Korvin-Kroukovsky, B.V., "Ships at Sea (Seakeeping Monograph)," Chapter V, "Loads Acting on a Ship and the Elastic Response of a Ship," Stevens Institute of Technology (Jan 1958).

Kudosauljevic, LJ. B., "On the Smith Effect," International Shipbuilding Progress, No. 4 (1957).

LeMehaute, B. and Brebner, A., "An Introduction to the Mathematical Theories of Two-Dimensional Periodic Progressive Gravity Waves," Civil Engineering Department, Queen's Univ, Kingston, Ontario, C.E. Research Report 11 (Jul 1960).

Lewis, E.V. and Dalzell, J.F., "Motion, Bending Moment and Shear Measurements on a Destroyer Model in Waves," Stevens Institute of Technology Report 656 (Apr 1958).

Lewis, E.V. and Gerard, G., "A Long-Range Research Program in Ship Structural Design," Stevens Institute of Technology E.T.T. Report 703 (Dec 1958).

Lewis, E.V. and Numata, E., "Ship Model Tests in Regular and Irregular Seas," Stevens Institute of Technology Report 567 (Sep 1956).

Martin, M., "Preliminary Study of Free Surface Effects on Water-to-Air Exit of Slender Bodies," Stevens Institute of Technology TM-125 (Feb 1960).

Neumann, G., "On Wind Generated Ocean Waves with Special Reference to the Problem of Wave Forecasting," New York University, Contract Nonr 285(05) (May 1952).

Nienartowicz, K., "Obliczanie kołysań wzdłużnych i zanurzeniowych statku znajdującego się na fali (Calculations on Pitching and Immersion of Ships in Waves)," Prace Morskiego Instytutu Technicznego 195-, pp. 45–49, David Taylor Model Basin Translation 274 (Jul 1957).

Ochi, K., "The Effect of Slamming Impact on a Ship Hull Structure," Stevens Institute of Technology, D.L. Project 2067, Note 497 (Sep 1958).

Schmitz, G., "Querkraft und Moment infolge Schräganströmung von Schiffsrudern, Schiffskörpern und Gleitflächen (Transverse Force and Moment Due to the Oblique Flow against Ship Rudders, Hulls and Planing Surfaces)," Schiffbautechnik, Vol. 9 (Oct 1959).

Schnitzer, E., "Theory and Procedure for Determining Loads and Motions in Chine-Immersed Hydrodynamic Impacts of Prismatic Bodies," National Advisory Committee for Aeronautics Report 1152 (1953).

Smith, W.E., "Hogging and Sagging Strains in a Sea Way as Influenced by Wave Structure," Transactions of the Institution of Naval Architects, Vol. XXIV (1883).

Szebehely, V.G., "Hydrodynamic Impact," Applied Mechanics Reviews, Vol. 12, No. 5 (May 1959).

Szebehely, V.G. and Todd, M.A., "Ship Slamming in Head Seas," David Taylor Model Basin Report 913 (Feb 1955).

Ward, L.W., "Method for Estimating Impact Forces on Ships," Stevens Institute of Technology Report 616 (Dec 1956).

Weinblum, G. and St. Denis, M., "On the Motions of Ships at Sea," Society of Naval Architects and Marine Engineers (Nov 1950).

INITIAL DISTRIBUTION

Copies

12 CHBUSHIPS
- 3 Ship Noise, Meas, & Red (Code 345)
- 1 Lab Mgt (Code 320)
- 1 Appl Res (Code 340)
- 3 Tech Info (Code 335)
- 1 Prelim Des (Code 420)
- 1 Hull Des (Code 440)
- 1 Sci & Res (Code 442)
- 1 Struc (Code 443)

3 CHONR
- 1 Math Sci (Code 430)
- 1 Fluid Dyn (Code 439)

1 CO & DIR, USNEES

1 CO & DIR, USNMDL

1 CHBUWEPS

1 CO, USNOL, White Oak

1 CO, USNOS

1 CDR, USNOTS, China Lake

1 CDR, USNOTS, Pasadena

1 DIR, USNRL

1 CDR, USNROTC & NAVADMINU MIT

1 O in C, PGSCOL, Webb

2 COMDT, USCG
- 1 Secy, Ship Struc Comm

1 NAVSHIPYD LBEACH

1 NAVSHIPYD PEARL

1 NAVSHIPYD SFRAN

1 NAVSHIPYD PUG

1 NAVSHIPYD NORVA

1 NAVSHIPYD PHILA

1 NAVSHIPYD BSN

3 NAVSHIPYD NYK
- 1 Des Supt (Code 240)
- 1 MATLAB (Code 912b)

1 DIR, WHOI

1 DIR, NATBUSTAND

1 St Anthony Falls Hydraulic Lab
Univ of Minn

1 MARAD

1 ABS

2 NAS
- 1 Ship Struc Comm

Copies

2 Computer Engineering Assoc

1 NNS & DD Co, Attn: Mr. Montgomery

1 Genl Dyn Corp, Electric Boat Div, Groton

1 SW Res Inst

1 Dept NAME, MIT

2 New York Univ
- 1 Dept of Meteorology
- 1 Fluid Mech

1 Webb Inst

1 Univ of Iowa, Inst of Hydrau Res

1 Catholic Univ, Sch of Engin & Arch

1 DIR, ORL Penn State

1 Univ of Calif, Inst of Engin Res

1 DIR, DL, SIT, Hoboken

2 Univ of Mich
- 1 Experl Naval Tank
- 1 Dept of Engin Mech

1 Columbia Univ, Hudson Lab

1 Univ of Notre Dame,
Attn: Prof. A. Strandhagen, Head,
Dept of Eng Mech

1 John Hopkins Univ, APL

10 CDR, ASTIA

2 SNAME
- 1 Hull Struc Comm

1 Engin Index, New York

2 SIT

David Taylor Model Basin. Report 1511.
COMPARISON OF THEORY AND EXPERIMENT FOR SLAMMING OF A DUTCH DESTROYER, by Ralph C. Leibowitz. Jun 1962. ix, 95p. illus., graphs, diagrs., refs. UNCLASSIFIED

This report presents a theoretical analysis and computation of the "slamming" (hydrodynamic) forces acting on a ship, based upon an experimental knowledge of the ship's rigid-body motions relative to the wave. These forces are considered to be due to the time rate of change of fluid momentum and to buoyancy forces incident to immersion of the hull. In addition, a computation is made of the transient elastic response and associated hull girder stresses of the ship due to the total force exerted by the fluid on the ship. A comparison between the theoretical and measured stresses shows good agreement.

1. Destroyers--Vibration--Mathematical analysis
2. Ship hulls--Impact--Measurement
3. Ship hulls--Slamming--Mathematical analysis
4. Ship hulls--Rigid body motions--Mathematical analysis
5. Ship hulls--Transients--Mathematical analysis
6. Ship hulls--Transients--Theory
7. Ship hulls--Vibration--Mathematical analysis

David Taylor Model Basin. Report 1511.
COMPARISON OF THEORY AND EXPERIMENT FOR SLAMMING OF A DUTCH DESTROYER, by Ralph C. Leibowitz. Jun 1962. ix, 95p. illus., graphs, diagrs., refs. UNCLASSIFIED

This report presents a theoretical analysis and computation of the "slamming" (hydrodynamic) forces acting on a ship, based upon an experimental knowledge of the ship's rigid-body motions relative to the wave. These forces are considered to be due to the time rate of change of fluid momentum and to buoyancy forces incident to immersion of the hull. In addition, a computation is made of the transient elastic response and associated hull girder stresses of the ship due to the total force exerted by the fluid on the ship. A comparison between the theoretical and measured stresses shows good agreement.

1. Destroyers--Vibration--Mathematical analysis
2. Ship hulls--Impact--Measurement
3. Ship hulls--Slamming--Mathematical analysis
4. Ship hulls--Rigid body motions--Mathematical analysis
5. Ship hulls--Transients--Mathematical analysis
6. Ship hulls--Transients--Theory
7. Ship hulls--Vibration--Mathematical analysis

David Taylor Model Basin. Report 1511.
COMPARISON OF THEORY AND EXPERIMENT FOR SLAMMING OF A DUTCH DESTROYER, by Ralph C. Leibowitz. Jun 1962. ix, 95p. illus., graphs, diagrs., refs. UNCLASSIFIED

This report presents a theoretical analysis and computation of the "slamming" (hydrodynamic) forces acting on a ship, based upon an experimental knowledge of the ship's rigid-body motions relative to the wave. These forces are considered to be due to the time rate of change of fluid momentum and to buoyancy forces incident to immersion of the hull. In addition, a computation is made of the transient elastic response and associated hull girder stresses of the ship due to the total force exerted by the fluid on the ship. A comparison between the theoretical and measured stresses shows good agreement.

1. Destroyers--Vibration--Mathematical analysis
2. Ship hulls--Impact--Measurement
3. Ship hulls--Slamming--Mathematical analysis
4. Ship hulls--Rigid body motions--Mathematical analysis
5. Ship hulls--Transients--Mathematical analysis
6. Ship hulls--Transients--Theory
7. Ship hulls--Vibration--Mathematical analysis

David Taylor Model Basin. Report 1511.
COMPARISON OF THEORY AND EXPERIMENT FOR SLAMMING OF A DUTCH DESTROYER, by Ralph C. Leibowitz. Jun 1962. ix, 95p. illus., graphs, diagrs., refs. UNCLASSIFIED

This report presents a theoretical analysis and computation of the "slamming" (hydrodynamic) forces acting on a ship, based upon an experimental knowledge of the ship's rigid-body motions relative to the wave. These forces are considered to be due to the time rate of change of fluid momentum and to buoyancy forces incident to immersion of the hull. In addition, a computation is made of the transient elastic response and associated hull girder stresses of the ship due to the total force exerted by the fluid on the ship. A comparison between the theoretical and measured stresses shows good agreement.

1. Destroyers--Vibration--Mathematical analysis
2. Ship hulls--Impact--Measurement
3. Ship hulls--Slamming--Mathematical analysis
4. Ship hulls--Rigid body motions--Mathematical analysis
5. Ship hulls--Transients--Mathematical analysis
6. Ship hulls--Transients--Theory
7. Ship hulls--Vibration--Mathematical analysis

8. Ship hulls--Motion--Mathematical analysis
9. Ship hulls--Stresses--Mathematical analysis
10. Ship hulls--Whipping motion--Mathematical analysis
11. Analog computers--Applications
12. Digital computers--Applications
I. Leibowitz, Ralph C.

8. Ship hulls--Motion--Mathematical analysis
9. Ship hulls--Stresses--Mathematical analysis
10. Ship hulls--Whipping motion--Mathematical analysis
11. Analog computers--Applications
12. Digital computers--Applications
I. Leibowitz, Ralph C.

8. Ship hulls--Motion--Mathematical analysis
9. Ship hulls--Stresses--Mathematical analysis
10. Ship hulls--Whipping motion--Mathematical analysis
11. Analog computers--Applications
12. Digital computers--Applications
I. Leibowitz, Ralph C.

8. Ship hulls--Motion--Mathematical analysis
9. Ship hulls--Stresses--Mathematical analysis
10. Ship hulls--Whipping motion--Mathematical analysis
11. Analog computers--Applications
12. Digital computers--Applications
I. Leibowitz, Ralph C.

David Taylor Model Basin. Report 1511.
COMPARISON OF THEORY AND EXPERIMENT FOR SLAMMING OF A DUTCH DESTROYER, by Ralph C. Leibowitz. Jun 1962. ix, 95p. illus., graphs, diagrs., refs. UNCLASSIFIED

This report presents a theoretical analysis and computation of the "slamming" (hydrodynamic) forces acting on a ship, based upon an experimental knowledge of the ship's rigid-body motions relative to the wave. These forces are considered to be due to the time rate of change of fluid momentum and to buoyancy forces incident to immersion of the hull. In addition, a computation is made of the transient elastic response and associated hull girder stresses of the ship due to the total force exerted by the fluid on the ship. A comparison between the theoretical and measured stresses shows good agreement.

1. Destroyers--Vibration--Mathematical analysis
2. Ship hulls--Impact--Measurement
3. Ship hulls--Slamming--Mathematical analysis
4. Ship hulls--Rigid body motions--Mathematical analysis
5. Ship hulls--Transients--Mathematical analysis
6. Ship hulls--Transients--Theory
7. Ship hulls--Vibration--Mathematical analysis

David Taylor Model Basin. Report 1511.
COMPARISON OF THEORY AND EXPERIMENT FOR SLAMMING OF A DUTCH DESTROYER, by Ralph C. Leibowitz. Jun 1962. ix, 95p. illus., graphs, diagrs., refs. UNCLASSIFIED

This report presents a theoretical analysis and computation of the "slamming" (hydrodynamic) forces acting on a ship, based upon an experimental knowledge of the ship's rigid-body motions relative to the wave. These forces are considered to be due to the time rate of change of fluid momentum and to buoyancy forces incident to immersion of the hull. In addition, a computation is made of the transient elastic response and associated hull girder stresses of the ship due to the total force exerted by the fluid on the ship. A comparison between the theoretical and measured stresses shows good agreement.

1. Destroyers--Vibration--Mathematical analysis
2. Ship hulls--Impact--Measurement
3. Ship hulls--Slamming--Mathematical analysis
4. Ship hulls--Rigid body motions--Mathematical analysis
5. Ship hulls--Transients--Mathematical analysis
6. Ship hulls--Transients--Theory
7. Ship hulls--Vibration--Mathematical analysis

David Taylor Model Basin. Report 1511.
COMPARISON OF THEORY AND EXPERIMENT FOR SLAMMING OF A DUTCH DESTROYER, by Ralph C. Leibowitz. Jun 1962. ix, 95p. illus., graphs, diagrs., refs. UNCLASSIFIED

This report presents a theoretical analysis and computation of the "slamming" (hydrodynamic) forces acting on a ship, based upon an experimental knowledge of the ship's rigid-body motions relative to the wave. These forces are considered to be due to the time rate of change of fluid momentum and to buoyancy forces incident to immersion of the hull. In addition, a computation is made of the transient elastic response and associated hull girder stresses of the ship due to the total force exerted by the fluid on the ship. A comparison between the theoretical and measured stresses shows good agreement.

1. Destroyers--Vibration--Mathematical analysis
2. Ship hulls--Impact--Measurement
3. Ship hulls--Slamming--Mathematical analysis
4. Ship hulls--Rigid body motions--Mathematical analysis
5. Ship hulls--Transients--Mathematical analysis
6. Ship hulls--Transients--Theory
7. Ship hulls--Vibration--Mathematical analysis

David Taylor Model Basin. Report 1511.
COMPARISON OF THEORY AND EXPERIMENT FOR SLAMMING OF A DUTCH DESTROYER, by Ralph C. Leibowitz. Jun 1962. ix, 95p. illus., graphs, diagrs., refs. UNCLASSIFIED

This report presents a theoretical analysis and computation of the "slamming" (hydrodynamic) forces acting on a ship, based upon an experimental knowledge of the ship's rigid-body motions relative to the wave. These forces are considered to be due to the time rate of change of fluid momentum and to buoyancy forces incident to immersion of the hull. In addition, a computation is made of the transient elastic response and associated hull girder stresses of the ship due to the total force exerted by the fluid on the ship. A comparison between the theoretical and measured stresses shows good agreement.

1. Destroyers--Vibration--Mathematical analysis
2. Ship hulls--Impact--Measurement
3. Ship hulls--Slamming--Mathematical analysis
4. Ship hulls--Rigid body motions--Mathematical analysis
5. Ship hulls--Transients--Mathematical analysis
6. Ship hulls--Transients--Theory
7. Ship hulls--Vibration--Mathematical analysis

8. Ship hulls--Motion--Mathematical analysis
9. Ship hulls--Stresses--Mathematical analysis
10. Ship hulls--Whipping motion--Mathematical analysis
11. Analog computers--Applications
12. Digital computers--Applications

I. Leibowitz, Ralph C.

8. Ship hulls--Motion--Mathematical analysis
9. Ship hulls--Stresses--Mathematical analysis
10. Ship hulls--Whipping motion--Mathematical analysis
11. Analog computers--Applications
12. Digital computers--Applications

I. Leibowitz, Ralph C.

8. Ship hulls--Motion--Mathematical analysis
9. Ship hulls--Stresses--Mathematical analysis
10. Ship hulls--Whipping motion--Mathematical analysis
11. Analog computers--Applications
12. Digital computers--Applications

I. Leibowitz, Ralph C.

8. Ship hulls--Motion--Mathematical analysis
9. Ship hulls--Stresses--Mathematical analysis
10. Ship hulls--Whipping motion--Mathematical analysis
11. Analog computers--Applications
12. Digital computers--Applications

I. Leibowitz, Ralph C.

David Taylor Model Basin. Report 1511.
COMPARISON OF THEORY AND EXPERIMENT FOR SLAMMING OF A DUTCH DESTROYER, by Ralph C. Leibowitz. Jun 1962. ix, 95p. illus., graphs, diagrs., refs. UNCLASSIFIED

This report presents a theoretical analysis and computation of the "slamming" (hydrodynamic) forces acting on a ship, based upon an experimental knowledge of the ship's rigid-body motions relative to the wave. These forces are considered to be due to the time rate of change of fluid momentum and to buoyancy forces incident to immersion of the hull. In addition, a computation is made of the transient elastic response and associated hull girder stresses of the ship due to the total force exerted by the fluid on the ship. A comparison between the theoretical and measured stresses shows good agreement.

1. Destroyers--Vibration--Mathematical analysis
2. Ship hulls--Impact--Measurement
3. Ship hulls--Slamming--Mathematical analysis
4. Ship hulls--Rigid body motions--Mathematical analysis
5. Ship hulls--Transients--Mathematical analysis
6. Ship hulls--Transients--Theory
7. Ship hulls--Vibration--Mathematical analysis

David Taylor Model Basin. Report 1511.
COMPARISON OF THEORY AND EXPERIMENT FOR SLAMMING OF A DUTCH DESTROYER, by Ralph C. Leibowitz. Jun 1962. ix, 95p. illus., graphs, diagrs., refs. UNCLASSIFIED

This report presents a theoretical analysis and computation of the "slamming" (hydrodynamic) forces acting on a ship, based upon an experimental knowledge of the ship's rigid-body motions relative to the wave. These forces are considered to be due to the time rate of change of fluid momentum and to buoyancy forces incident to immersion of the hull. In addition, a computation is made of the transient elastic response and associated hull girder stresses of the ship due to the total force exerted by the fluid on the ship. A comparison between the theoretical and measured stresses shows good agreement.

1. Destroyers--Vibration--Mathematical analysis
2. Ship hulls--Impact--Measurement
3. Ship hulls--Slamming--Mathematical analysis
4. Ship hulls--Rigid body motions--Mathematical analysis
5. Ship hulls--Transients--Mathematical analysis
6. Ship hulls--Transients--Theory
7. Ship hulls--Vibration--Mathematical analysis

David Taylor Model Basin. Report 1511.
COMPARISON OF THEORY AND EXPERIMENT FOR SLAMMING OF A DUTCH DESTROYER, by Ralph C. Leibowitz. Jun 1962. ix, 95p. illus., graphs, diagrs., refs. UNCLASSIFIED

This report presents a theoretical analysis and computation of the "slamming" (hydrodynamic) forces acting on a ship, based upon an experimental knowledge of the ship's rigid-body motions relative to the wave. These forces are considered to be due to the time rate of change of fluid momentum and to buoyancy forces incident to immersion of the hull. In addition, a computation is made of the transient elastic response and associated hull girder stresses of the ship due to the total force exerted by the fluid on the ship. A comparison between the theoretical and measured stresses shows good agreement.

1. Destroyers--Vibration--Mathematical analysis
2. Ship hulls--Impact--Measurement
3. Ship hulls--Slamming--Mathematical analysis
4. Ship hulls--Rigid body motions--Mathematical analysis
5. Ship hulls--Transients--Mathematical analysis
6. Ship hulls--Transients--Theory
7. Ship hulls--Vibration--Mathematical analysis

David Taylor Model Basin. Report 1511.
COMPARISON OF THEORY AND EXPERIMENT FOR SLAMMING OF A DUTCH DESTROYER, by Ralph C. Leibowitz. Jun 1962. ix, 95p. illus., graphs, diagrs., refs. UNCLASSIFIED

This report presents a theoretical analysis and computation of the "slamming" (hydrodynamic) forces acting on a ship, based upon an experimental knowledge of the ship's rigid-body motions relative to the wave. These forces are considered to be due to the time rate of change of fluid momentum and to buoyancy forces incident to immersion of the hull. In addition, a computation is made of the transient elastic response and associated hull girder stresses of the ship due to the total force exerted by the fluid on the ship. A comparison between the theoretical and measured stresses shows good agreement.

1. Destroyers--Vibration--Mathematical analysis
2. Ship hulls--Impact--Measurement
3. Ship hulls--Slamming--Mathematical analysis
4. Ship hulls--Rigid body motions--Mathematical analysis
5. Ship hulls--Transients--Mathematical analysis
6. Ship hulls--Transients--Theory
7. Ship hulls--Vibration--Mathematical analysis

8. Ship hulls--Motion--Mathematical analysis
9. Ship hulls--Stresses--Mathematical analysis
10. Ship hulls--Whipping motion--Mathematical analysis
11. Analog computers--Applications
12. Digital computers--Applications
I. Leibowitz, Ralph C.

8. Ship hulls--Motion--Mathematical analysis
9. Ship hulls--Stresses--Mathematical analysis
10. Ship hulls--Whipping motion--Mathematical analysis
11. Analog computers--Applications
12. Digital computers--Applications
I. Leibowitz, Ralph C.

8. Ship hulls--Motion--Mathematical analysis
9. Ship hulls--Stresses--Mathematical analysis
10. Ship hulls--Whipping motion--Mathematical analysis
11. Analog computers--Applications
12. Digital computers--Applications
I. Leibowitz, Ralph C.

8. Ship hulls--Motion--Mathematical analysis
9. Ship hulls--Stresses--Mathematical analysis
10. Ship hulls--Whipping motion--Mathematical analysis
11. Analog computers--Applications
12. Digital computers--Applications
I. Leibowitz, Ralph C.

David Taylor Model Basin. Report 1511.
COMPARISON OF THEORY AND EXPERIMENT FOR SLAMMING OF A DUTCH DESTROYER, by Ralph C. Leibowitz. Jun 1962. ix, 95p. illus., graphs, diagrs., refs. UNCLASSIFIED

This report presents a theoretical analysis and computation of the "slamming" (hydrodynamic) forces acting on a ship, based upon an experimental knowledge of the ship's rigid-body motions relative to the wave. These forces are considered to be due to the time rate of change of fluid momentum and to buoyancy forces incident to immersion of the hull. In addition, a computation is made of the transient elastic response and associated hull girder stresses of the ship due to the total force exerted by the fluid on the ship. A comparison between the theoretical and measured stresses shows good agreement.

1. Destroyers--Vibration--Mathematical analysis
2. Ship hulls--Impact--Measurement
3. Ship hulls--Slamming--Mathematical analysis
4. Ship hulls--Rigid body motions--Mathematical analysis
5. Ship hulls--Transients--Mathematical analysis
6. Ship hulls--Transients--Theory
7. Ship hulls--Vibration--Mathematical analysis

David Taylor Model Basin. Report 1511.
COMPARISON OF THEORY AND EXPERIMENT FOR SLAMMING OF A DUTCH DESTROYER, by Ralph C. Leibowitz. Jun 1962. ix, 95p. illus., graphs, diagrs., refs. UNCLASSIFIED

This report presents a theoretical analysis and computation of the "slamming" (hydrodynamic) forces acting on a ship, based upon an experimental knowledge of the ship's rigid-body motions relative to the wave. These forces are considered to be due to the time rate of change of fluid momentum and to buoyancy forces incident to immersion of the hull. In addition, a computation is made of the transient elastic response and associated hull girder stresses of the ship due to the total force exerted by the fluid on the ship. A comparison between the theoretical and measured stresses shows good agreement.

1. Destroyers--Vibration--Mathematical analysis
2. Ship hulls--Impact--Measurement
3. Ship hulls--Slamming--Mathematical analysis
4. Ship hulls--Rigid body motions--Mathematical analysis
5. Ship hulls--Transients--Mathematical analysis
6. Ship hulls--Transients--Theory
7. Ship hulls--Vibration--Mathematical analysis

David Taylor Model Basin. Report 1511.
COMPARISON OF THEORY AND EXPERIMENT FOR SLAMMING OF A DUTCH DESTROYER, by Ralph C. Leibowitz. Jun 1962. ix, 95p. illus., graphs, diagrs., refs. UNCLASSIFIED

This report presents a theoretical analysis and computation of the "slamming" (hydrodynamic) forces acting on a ship, based upon an experimental knowledge of the ship's rigid-body motions relative to the wave. These forces are considered to be due to the time rate of change of fluid momentum and to buoyancy forces incident to immersion of the hull. In addition, a computation is made of the transient elastic response and associated hull girder stresses of the ship due to the total force exerted by the fluid on the ship. A comparison between the theoretical and measured stresses shows good agreement.

1. Destroyers--Vibration--Mathematical analysis
2. Ship hulls--Impact--Measurement
3. Ship hulls--Slamming--Mathematical analysis
4. Ship hulls--Rigid body motions--Mathematical analysis
5. Ship hulls--Transients--Mathematical analysis
6. Ship hulls--Transients--Theory
7. Ship hulls--Vibration--Mathematical analysis

David Taylor Model Basin. Report 1511.
COMPARISON OF THEORY AND EXPERIMENT FOR SLAMMING OF A DUTCH DESTROYER, by Ralph C. Leibowitz. Jun 1962. ix, 95p. illus., graphs, diagrs., refs. UNCLASSIFIED

This report presents a theoretical analysis and computation of the "slamming" (hydrodynamic) forces acting on a ship, based upon an experimental knowledge of the ship's rigid-body motions relative to the wave. These forces are considered to be due to the time rate of change of fluid momentum and to buoyancy forces incident to immersion of the hull. In addition, a computation is made of the transient elastic response and associated hull girder stresses of the ship due to the total force exerted by the fluid on the ship. A comparison between the theoretical and measured stresses shows good agreement.

1. Destroyers--Vibration--Mathematical analysis
2. Ship hulls--Impact--Measurement
3. Ship hulls--Slamming--Mathematical analysis
4. Ship hulls--Rigid body motions--Mathematical analysis
5. Ship hulls--Transients--Mathematical analysis
6. Ship hulls--Transients--Theory
7. Ship hulls--Vibration--Mathematical analysis

8. Ship hulls--Motion--Mathematical analysis
9. Ship hulls--Stresses--Mathematical analysis
10. Ship hulls--Whipping motion--Mathematical analysis
11. Analog computers--Applications
12. Digital computers--Applications
I. Leibowitz, Ralph C.

8. Ship hulls--Motion--Mathematical analysis
9. Ship hulls--Stresses--Mathematical analysis
10. Ship hulls--Whipping motion--Mathematical analysis
11. Analog computers--Applications
12. Digital computers--Applications
I. Leibowitz, Ralph C.

8. Ship hulls--Motion--Mathematical analysis
9. Ship hulls--Stresses--Mathematical analysis
10. Ship hulls--Whipping motion--Mathematical analysis
11. Analog computers--Applications
12. Digital computers--Applications
I. Leibowitz, Ralph C.

8. Ship hulls--Motion--Mathematical analysis
9. Ship hulls--Stresses--Mathematical analysis
10. Ship hulls--Whipping motion--Mathematical analysis
11. Analog computers--Applications
12. Digital computers--Applications
I. Leibowitz, Ralph C.